3-24-2016

Analysis of a Modified Equivalent Circuit Model for Lithium-Ion Battery Modules in CubeSats

James J. Liu

ANALYSIS OF A MODIFIED EQUIVALENT CIRCUIT MODEL FOR LITHIUM-ION BATTERY MODULES IN CUBESATS

THESIS

James J. Liu, 2d Lt, USAF

AFIT-ENY-MS-16-M-224

DEPARTMENT OF THE AIR FORCE
AIR UNIVERSITY

AIR FORCE INSTITUTE OF TECHNOLOGY

Wright-Patterson Air Force Base, Ohio

AFIT-ENY-MS-16-M-224

ANALYSIS OF A MODIFIED EQUIVALENT CIRCUIT MODEL FOR LITHIUM-ION BATTERY MODULES IN CUBESATS

THESIS

Presented to the Faculty

Department of Aeronautics and Astronautics

Graduate School of Engineering and Management

Air Force Institute of Technology

Air University

Air Education and Training Command

In Partial Fulfillment of the Requirements for the

Degree of Master of Science in Astronautical Engineering

James J. Liu, BS

2d Lt, USAF

March 2016

AFIT-ENY-MS-16-M-224

ANALYSIS OF A MODIFIED EQUIVALENT CIRCUIT MODEL FOR LITHIUM-ION BATTERY MODULES IN CUBESATS

James J. Liu, BS

2d Lt, USAF

Committee Membership:

Dr. Swenson
Chair

Dr. Hartsfield
Member

Professor Hart
Member

Abstract

Failure of the electrical power system (EPS) to meet mission requirements is a common problem in nano-size satellites commonly referred to as CubeSats. The motivation for this research stems from the desire to prevent EPS failure through a process of testing and space qualification of components. Utilizing models to predict the behavior of an EPS before it is designed, built, and tested for space can provide critical insight in areas of limitation in performance and survivability. Modeling an entire EPS system is challenging because it requires extensive knowledge of all components and their behavior. This research focuses specifically on the storage component of the EPS often referred to as secondary batteries. The secondary batteries, such as Li-Ion battery cells, are modeled to predict the performance of the storage component in the space environment. Experimental test data is collected under a simulated space environment through the use of a Thermal Vacuum Chamber (TVAC). Data collected from battery testing in the space environment is used to validate a modified Thevenin Equivalent Circuit model. The experimental test data and battery model are compared and evaluated resulting in a promising model that can reasonably predict performance of a battery pack in a two-series two-parallel configuration.

To Joy and a Vampire

Acknowledgments

I would like to extend my appreciation out to the staff at AFIT. This research would not have been possible without the help of Sean Miller, Chris Sheffield and Jorge Urena. These individuals provided valuable assistance in answering the many questions I had on electronics, testing, and setup. Without their help, the harnesses used to test the battery would not have been made possible. I would also like to thank my advisor, Dr. Eric Swenson, for providing valuable guidance and expertise in steering me in the right direction.

Lastly, I would like to thank FritoLayChips, TheMule, AstronautX, Jimmy2, CaptainMorgan, MoonGirl14, BeachGirlMonica, and MasterOfComet for joining my party and spending many nights raiding with me in the dungeon.

James J. Liu

Table of Contents

Page

List of Figures

Page

List of Tables

Page

List of Acronyms

A Ampere

AFIT Air Force Institute of Technology

Ah Ampere Hour

Cal Poly California Polytechnic State University, San Luis Obispo

COTS Commercial-Off-The-Shelf

DoD Department of Defense

DOD Depth of Discharge

EMF Electromotive Force

EPS Electrical power subsystem

Km Kilometer

LEO low Earth orbit

Li-Ion Lithium-Ion

LCO Lithium-Cobalt

mV Millivolt

NASA National Aeronautics and Space Administration

NCA Nickle Cobalt Aluminum

Ni-Cd Nickel-Cadmium

Ni-H_2 Nickel Hydrogen

NMC Nickel Manganese Cobalt

RTG Radioisotope thermoelectric generator

TVAC Thermal Vacuum

V Volt

Wh Watt Hour

ANALYSIS OF A MODIFIED EQUIVALENT CIRCUIT MODEL FOR LITHIUM-ION BATTERY MODULES IN CUBESATS

1. Introduction

CubeSats are miniaturized satellites that are typically powered by commercial-off-the-shelf (COTS) electrical components which make up the electrical power subsystem (EPS). A typical CubeSat EPS requires solar arrays to generate power, an EPS board to distribute and regulate power, and batteries to store generated power. Figure 1(a) is an example of a CubeSat EPS stack consisting of the EPS board and battery pack. Figure 1(b) is an example of a body mounted solar panel.

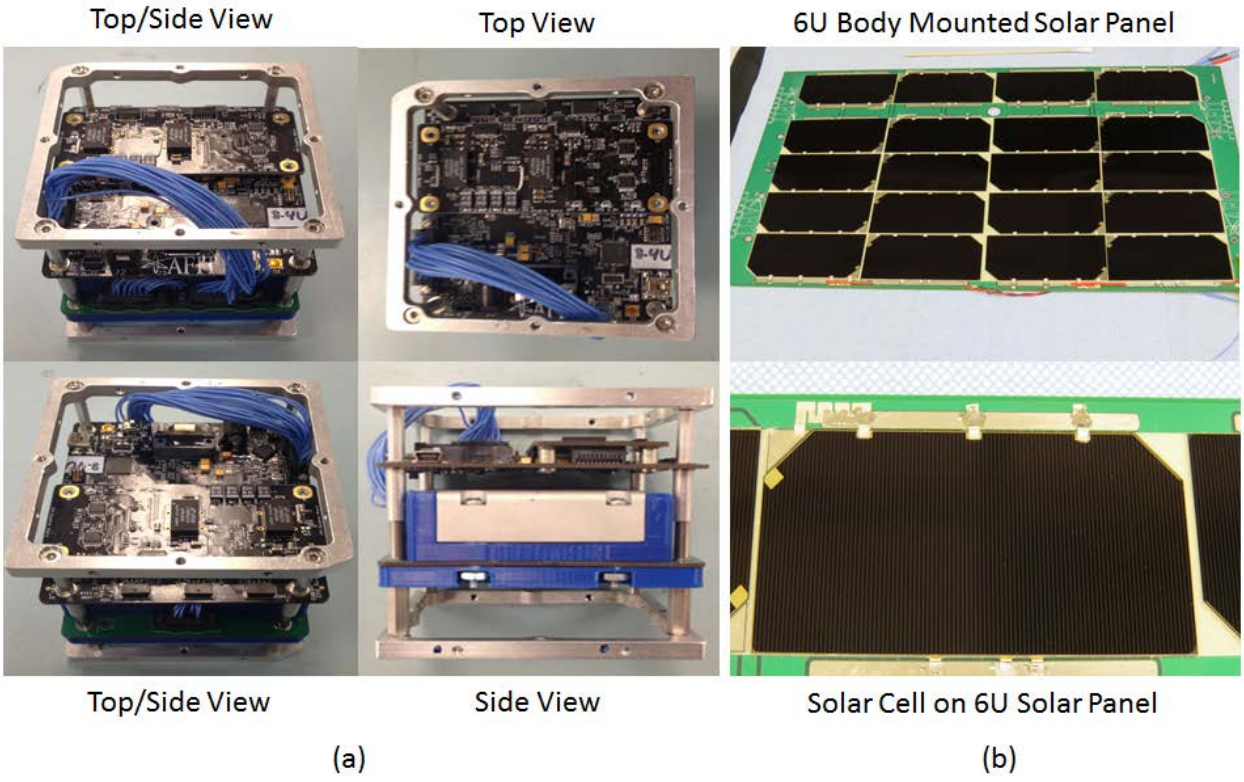

Figure 1: EPS Stack (a) and 6U Body Mounted Solar Panel (b)

Due to risks involved in using COTS components, a CubeSat's EPS must undergo space qualification testing to verify its ability to operate in the space environment. Space qualification is a verification process in satellite design which ensures that components will meet their designed specification. The life of a satellite can be directly related to how long the EPS can provide power in fulfilling a satellite's mission requirements. Once the EPS fails to meet mission power requirements, the satellite's life could be over. Complete or partial failure of the CubeSat's power system almost always means the end for a CubeSat mission; failure of such electrical components motivates space qualifying and testing so there is confidence that the components will survive and operate in space. To characterize the behavior of the components in the space environment, rigorous environmental testing must be conducted. Testing is a crucial step in qualifying components for space applications; however, the ability to accurately model and predict the behavior of such components would provide an effective tool in evaluating an EPS's performance. A model that accurately predicts the behavior of an EPS before a CubeSat is sent into space could provide confidence and reduce uncertainty in meeting power requirements.

The motivation for this research stems from the desire to prevent EPS failure through the development of a model that can accurately predict the performance of an EPS before a CubeSat is designed, built, and operated in space. The challenge behind developing an accurate EPS model is the extensive knowledge required of all components in an EPS. The goal of this research is to establish a foundation in EPS modeling by conducting analysis of modeling for the energy storage component of the EPS using real test data. This research focuses on battery modeling and testing. This chapter provides a background on CubeSats, power systems and batteries, the problem statement, and a preview of the methodology used in this research.

1.1 CubeSats

In 1999, professors Puig-Suari from California Polytechnic State University, San Luis Obispo (Cal Poly SLO) and Twiggs from Stanford University invented the CubeSat as a project for students to design, build, and test a small satellite in a classroom setting [1]. Although CubeSats were originally created to be classroom projects, they are now fully capable of fulfilling a wide range of mission requirements, making them valuable assets in the space industry. Suari and Twiggs defined the standard known as a "1U." A 1U CubeSat is typically defined as a 10 cm x 10 cm x 10 cm (length, width, height) cube whose maximum mass typically does not exceed 1.3 kg [2]. Figure 2 shows an example of a 1U CubeSat. The number in front of the "U" is the nominal designator for the number of 1U sized CubeSats that make up the satellite. For example, a 6U CubeSat is nominally the size and weight of six 1U CubeSats. Today, CubeSats are designed in sizes from 1U all the way up to 27U and are expected to grow larger as a result of improvement to containerized CubeSat dispensers [1].

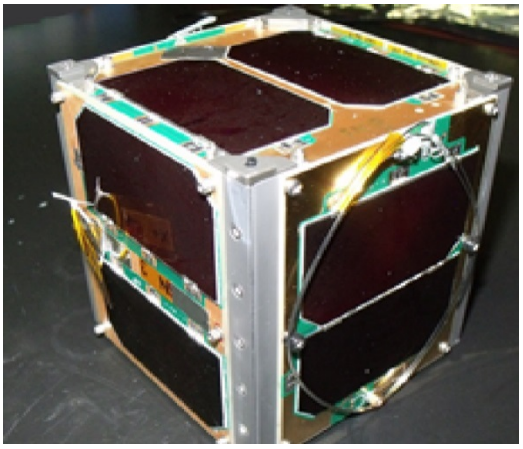

Figure 2: Fox-1 CubeSat from AMSAT [3]

1.1.1 CubeSat Power Systems

Due to size and weight limitations, CubeSat power systems typically do not exceed 100 Watt-Hour (Wh) of stored or 50 W of generated power; however, there are exceptions, especially with newer EPS subsystems. Compared to large satellites that can fit fuel cells, nuclear, or radioisotope thermoelectric generators (RTG), CubeSats are almost always limited to generating electrical power using solar panels and storing this electrical energy using batteries or like devices. Average power generated by the solar panel is limited because a CubeSat's orbits are typically less than 500 kilometers (km) in altitude. During the eclipse phase of the orbit, the CubeSat would not be able to generate any power from the solar panels and must rely on batteries to power the spacecraft. Batteries can be categorized into primary and secondary. Primary batteries are non-rechargeable and disposable after their use. Secondary batteries are rechargeable so they can be used to store and provide power for the CubeSat. Secondary batteries are recharged by solar panels when the panels are illuminated by the Sun. Secondary batteries allow the CubeSat to store electrical energy for the entire duration of the mission. Typically, CubeSats rely on secondary batteries such as Lithium-Ion (Li-Ion), Nickel-Cadmium (Ni-Cd), or Nickel-Hydrogen (Ni-H_2). This research only evaluates secondary batteries, specifically Li-Ion.

1.2 Basic Battery Terminology and Definition

The term battery is often used to describe a source of stored electrical energy. This definition of battery can cause confusion as the term battery could refer to either a single cell or multiple cells in a pack. A battery cell is a single individual electrochemical storage unit. A battery pack is a combination of two or more battery cells connected together in series or parallel to form an electrochemical storage unit to provide more capacity. In this research, the term battery will be used to describe a combination of multiple battery cells [4].

Battery cells are identified through their nominal voltage and rated current capacity. The term nominal refers to a manufacturer specified reference rating. The nominal voltage can also be thought of as the operating voltage of the battery. For Li-Ion battery cells, the nominal voltage is typically rated at 3.6 V. The rated current capacity is the charge a battery cell can hold and is expressed in units of ampere hours (Ah). The rated current capacity of a battery is specific for a given temperature and discharge rate which will be described shortly. In terms of energy storage, the product of nominal voltage and the rated current capacity results in a total nominal energy capacity in units of watt hours (Wh).

Discharge rate, or discharge current is typically expressed as C rate, relative to a cell's rated current capacity. For example, consider a 3.2 Ah capacity battery cell. A 1C discharge rate would have a current draw of 3.2 A and would take approximately one hour to be completely discharged. A C/2 discharge rate would have a current draw of 1.6A and take approximately 2 hours to be completely discharged. A 2C discharge rate would have a current draw of 6.4 A and take approximately 30 minutes to be completely discharged. The total available current capacity in a battery cell decreases more quickly for higher C rates resulting in a shorter discharge time. Alternatively, the total available current capacity decreases more slowly for lower C rates resulting in a longer discharge time.

The cut-off voltage for a battery cell is the minimum voltage that the battery cell can operate at. The cut-off-voltage is used to define the empty state of a battery cell. This will become more important when describing the relationship between state of charge and voltage.

A battery pack's total voltage and current capacity are determined through a series and parallel relationship based on the cell configuration in the battery pack. The voltage of battery cells connected in series is the sum of each individual cell voltages. The current capacity of

battery cells connected in parallel is the sum of an individual cell's current capacity in each parallel string.

1.3 Problem Statement

According to Swartwout [5], half of all first-time CubeSats Projects end up in failure [6]. Common CubeSat failures are caused by the EPS not providing power [7]. Power plays a vital role in determining a CubeSat's success or failure. In the past, AFIT has experienced a failure in their ALICE CubeSat through loss of contact, typically a result of failure of the power or communication system; however, the cause of failure was never determined. As launching CubeSats into space become more widely accessible to the public and universities, the high rate of failure becomes a much greater concern; thus, modeling an entire CubeSat before launch will become more prominent in the CubeSat design process to mitigate risks. Currently, there is minimal to no content publicly available in EPS modeling for CubeSat applications.

1.5 Research Focus

The ultimate goal of this research effort is the eventual development of an accurate EPS model for a CubeSat; however, the focus of this research is the analysis of currently available battery models and evaluating their capability of simulating Li-Ion battery in the space environment. The technique used to evaluate the battery model is the comparison of simulated results from the models to measured results collected from experimental test data. This research will focus on answering the following question: "Can a Thevenin Equivalent Circuit Model be used to accurately predict the performance of a Li-Ion battery module for a CubeSat in a simulated space environment?"

1.6 Research Methodology

The methodology used to answer the research question is to modify an existing Thevenin Equivalent Circuit Model to simulate a battery pack and compare the modified model's output to experimental test data in a simulated space environment. The proposed Thevenin Equivalent Circuit Model is modified through replacement of 80 cells in a series configuration inside the battery model to 4 cells in a two-series, two-parallel configuration (2S2P). This research will compare the modified battery model's output to experimental data of AFIT's 2014 battery pack, shown in Figure 3, obtained through Thermal Vacuum (TVAC) testing.

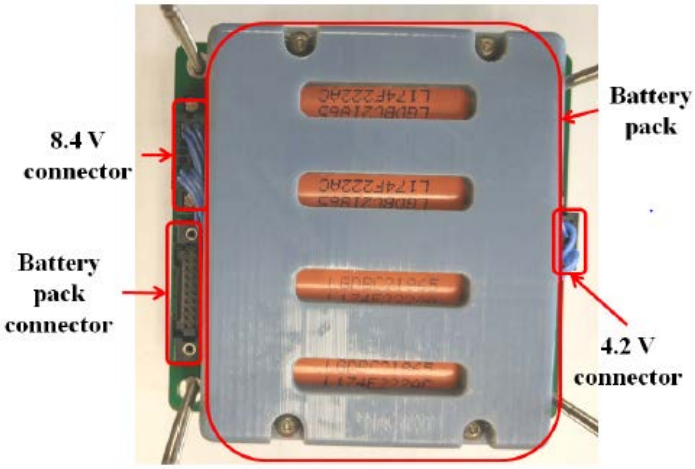

Figure 3: AFIT 2014 Battery Pack [8]

TVAC testing is conducted to simulate the effects the space environmental has on a battery pack. Conducting battery performance tests in TVAC will provide experimental data in space-simulated environment for comparison with the model. The model will provide an analytical basis to be used in prediction and simulation of battery packs in space. Modeling and testing are both used to verify that the battery pack will be qualified for use in space. Further

studies in battery pack modeling are presented in the literature review to provide a background in developing an accurate EPS model.

1.7 Preview

Chapter 2 will focus on an extensive literature review of Li-Ion battery cells and battery cell modeling. A variety of existing battery models will be presented with a proposed model presented at the end of Chapter 2. Chapter 3 will provide a more detailed methodology used to modify a battery model capable of predicting the behavior of AFIT's battery pack in the space environment. Chapter 3 will also incorporate more information on TVAC testing. Chapter 4 will show the results and analysis between model and environmental test data. Finally, Chapter 5 will summarize the research and provide additional future work and recommendations.

II. Literature Review

This chapter will present a thorough description of Li-Ion batteries, battery modeling approaches, and battery testing procedures. First, a background on Li-Ion batteries and factors that affect their performance will be addressed. Then, an extensive review of existing battery modeling techniques will be presented to provide background on techniques used to simulate battery behavior. From the techniques presented, a model will be proposed as the basis of analysis for this research. Finally, a description of battery testing procedures will be presented to describe what performance parameters are needed to evaluate batteries for space applications.

2.1 Lithium-Ion Battery

Li-Ion batteries are electrochemical storage units that convert chemical energy into electrical energy. Prior to the 1980's Ni-Cd was widely used in spacecraft [9]. Between the 1980s and 1990s Ni-H_2 became the more popular type for space applications [9]. Li-Ion batteries were not introduced into the market until they were commercialized by Sony in 1991 [10]. Today, Li-Ion batteries are more widely used in not only spacecraft but also portable electronics such as mobile handheld devices, laptops, and digital cameras. The advantages Li-Ion batteries have over Ni-Cd and Ni-H_2 in space applications, especially in CubeSats, is their specific mass (W/kg) and potential for higher electrical storage capacity due to higher energy density (J/Liter) when compared with Ni-Cd and Ni-H_2 [9]. The specific mass and energy density is important for CubeSats where volumetric size, mass, and power are limited. The disadvantages Li-Ion batteries have compared to Ni-Cd and Ni-H_2 are in safety [11]. Protection circuits are placed in Li-Ion battery cells to limit voltage and discharge current to prevent overcharging, overheating or short-circuiting that would otherwise result in thermal runaway causing a fire or explosion [12]. Li-Ion batteries come in a variety of chemistries which will be described next.

2.1.1 Li-Ion Components

Internally, Li-Ion batteries are composed of the following components: positive electrode, negative electrode, electrolyte and a separator. Figure 4 shows a graphic representation of the internal structure of a Li-Ion Battery cell.

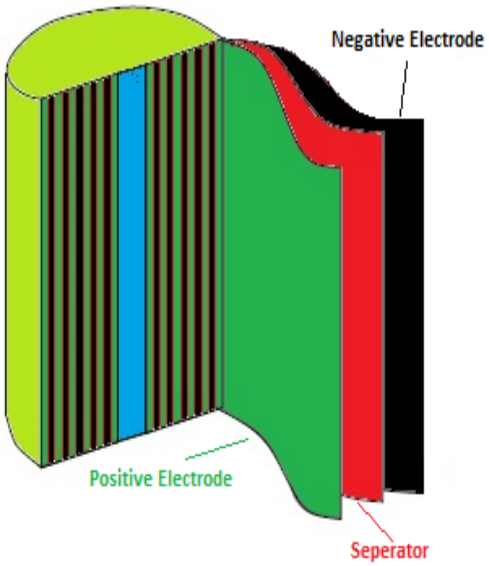

Figure 4: Li-Ion Battery Cell [4]

An electrode is an electrical conductor that allows current to flow through the medium (electrolyte) inside a battery cell. In Li-Ion battery cells, the negative electrode is typically composed of graphite, C_6. For the positive electrode, the material used is more variable, such as Cobalt (LCO), Nickel Cobalt Aluminum (NCA) and Nickel Manganese Cobalt (NMC) [13]. Li-Ion batteries are categorized based on the chemistry of the positive electrode. Each of the chemical composition of the positive electrode differs in cost, safety and energy density [11]. The positive electrode for the battery cells used in this research is of the Nickel Manganese Cobalt (NMC) type [14]. NMC was chosen for this research primarily due to safety

considerations in preventing thermal runaway when testing at high temperatures inside the TVAC chamber. NMC has a higher tolerance to thermal runaway, thus proving better safety ratings at higher operating temperatures when compared to LCO or NCA type battery cells [13].

Most researchers tend to refer to the term cathode and anode to describe the positive and negative electrode, respectively. By definition, cathode is where charge current flows out of the battery and anode is where charge current flows into the battery. In rechargeable battery cells such as Li-Ion, the terms cathode and anode are interchangeable because the current flow through the electrodes changes direction depending on state: charge or discharge. Historically, the term cathode and anode originated from the positive and negative electrodes, respectively, in a primary (non-rechargeable) battery cell during discharge. Thus, in all following discussions, regardless of whether the Li-Ion battery cell is undergoing charge or discharge, the positive electrode is often referred to as the cathode and the negative electrode is referred to as the anode.

The electrolyte is the medium that allows ions to flow between the positive and negative electrodes. The ions flowing through the electrolyte are known as cations and anions. Cations are ions with a positive net charge, and anions are ions with negative net charge. During discharge, the cations move through the electrolyte towards the positive electrode, while the anions move towards the negative electrode. For Li-Ion battery cells, the electrolyte is typically a salt dissolved in a non-aqueous solvent. A non-aqueous solvent is used due to an intense chemical reaction between lithium and water that forms highly flammable hydrogen. A commonly used salt is Lithium Hexaflurophosphate, $LiPF_6$. Solvents used in Li-Ion cells include Ethylene Carbonate, $C_3H_4O_3$, and diethyl carbonate, $C_5H_{10}O_3$. The salt-solvent combination is not a part of the chemical processes in a Li-Ion cell but is still important in facilitating transport of lithium

ions. The electrolyte is mainly a medium for electrical conduction and does not take part in the chemical reaction process of the battery [4].

The separator is a membrane that physically isolates the positive and negative electrodes. Separation between the positive and negative electrodes prevents a short circuit inside the battery. Although the separator's function is to physically isolate the electrodes, the separator is permeable. A permeable membrane allows lithium ions to pass through and intercalate with either electrode during charge and discharge. Typically, separators in commercial Li-Ion battery cells are made out of polyolefin, such as polyethylene or polypropylene [15].

2.1.2 Charge & Discharge Process for Li-Ion Battery Cells

For electrochemical cells, the charging and discharging process is conducted through a redox, or oxidation-reduction, reaction which is a chemical reaction that allows electrons to transfer between two species (atoms, molecules, or ions). During discharge, the negative electrode is oxidized (loses electrons) while the positive electrode is reduced (gains electrons) from the circuit. This process of losing electrons and gaining electrons is termed oxidation and reduction, respectively. During charge the opposite occurs, the negative electrode is reduced and the positive electrode is oxidized [16].

For Li-Ion batteries, the charge and discharge processes are not a redox reaction but an intercalation, or insertion, of lithium ions into the positive and negative electrode. Intercalation allows lithium ions to occupy the empty spaces of the crystal lattice in the structure of the electrode without changing its overall structure. For intercalation to work, the electrodes must have the properties of being an open crystal structure and have the ability to accept electrons simultaneously as lithium ions occupy its empty spaces. Lithium atoms are stored inside the crystal lattice structure and the atom becomes a positively charged lithium ion when it loses an

electron. Inside the electrode, the lithium atoms are able to freely move and are not tightly bonded to the electrode [4].

During discharge, lithium atoms stored inside the negative electrode loses an electron and becomes a positively charged lithium ion. The lithium ions move across the separator and are intercalated into the positive electrode. At the same time, the electron that the lithium atom lost travels from the negative electrode, through the circuit and into the positive electrode where it is rejoined with the lithium ion to form lithium atoms without charge. During charge, lithium ions flow from the positive electrode and insert into the negative electrode while simultaneously, the electrons flow through the circuit from the positive electrode into the negative electrode and recombines with the lithium ion in the negative electrode [4]. This process is illustrated in Figure 5.

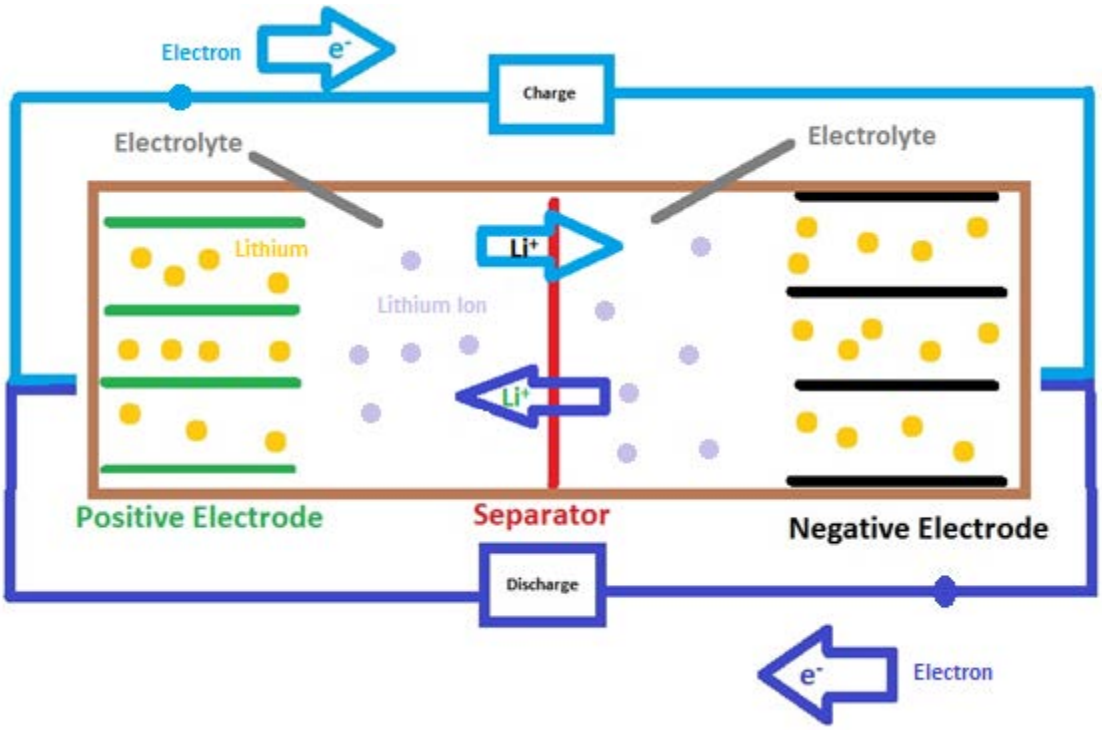

Figure 5: Li-Ion Battery Charge and Discharge

Through the process of intercalation, Li-Ion battery cells are able to supply and store electrochemical energy. During discharge and charge, there is a potential difference between the two electrodes from the electrons lost by the lithium and the electrons gain by the lithium ion at the opposite electrode. This potential difference between the two electrodes is known as the electromotive force (EMF) or cell voltage. EMF or cell voltage is one of the many performance battery cell parameters that will be observed in this research [4].

2.1.3 Li-Ion Performance Characteristics

Li-Ion battery performance characteristics for space applications are categorized into the following: Capacity (charge (Ah) or energy (Wh)), Voltage (V), Depth of Discharge (DOD), and Number of Cycles. Charge capacity is the total amount of charge the battery is capable of storing; whereas, energy capacity is the total amount of electrical energy the battery is capable of storing. In this research, capacity will be referred to as the charge capacity. Voltage is the electrical potential of the battery. DOD is a percentage of the total capacity used up by the spacecraft at any given time. Number of cycles is the number of times a battery can charge and discharge before permanent loss of capability to store power which is also known as capacity fading. Ning et al. [17] presented studies on capacity fading as a result of cycling. Experimental results showed a set of Sony 18650 Li-Ion battery cells that underwent 300 cycles at 1, 2, and 3C discharge rates resulted in a 9.5%, 13.2% and 16.9% permanent loss of their capability to store power. The number of cycles is an important characteristic used to predict the lifetime duration a CubeSat will be able to operational in space because a typical satellite in low Earth orbit (LEO) will pass through an eclipse 15 times per day. McKissock, Loyselle, and Vogel [18] at NASA Glenn Research Center in Cleveland, Ohio established guidelines on the use of Li-Ion for space applications. These guidelines provide a broad overview of factors, such as temperature, charge

and discharge rate, vibration and shock, and radiation, which affect Li-Ion battery performance in the space environment. For this research, the factors being evaluated will be temperature, and discharge/charge rate on a battery cell's voltage and capacity.

2.2 Battery Modeling

Extensive research has been conducted to model a battery cell's behavior and is shown by the abundance of battery modeling techniques that available in literature. Sun and Shu [19] presents the different types of models in an overview which can be organized into four categories: Electrochemical, Mathematical, Electrical, and Adaptive. This research will adhere to Sun and Shu's categorization of battery models.

Alternatively, Shafiei [20] presents a similar overview to battery modeling; however, he categorizes battery modeling into three categories: Electrochemical, Stochastic and Analytical (mathematical), and Electrical circuit. Like Sun and Shu, Shafiei also discusses advanced modeling techniques using Kalman Filtering (adaptive) but doesn't treat it as a separate category. A brief description of each type of model will now be discussed to provide a background on battery modeling, and the proposed model for this research will be discussed in Section 2.4.

2.2.1 Electrochemical Models

Electrochemical models are based on the electrochemical reactions that occur inside a battery cell. As described earlier in Section 2.1.2, Li-Ion batteries operate based on intercalation that allows ionization of lithium, diffusion of lithium ions from one electrode to another, and reabsorption of electrons by the lithium ion at the electrode to recombine back into lithium. This diffusion and concentration of ions is modeled in electrochemical models. For lithium ion battery cells, an electrochemical battery model is presented by Doyle, Fuller, and Newman (DFN) [21]. Their model employs six coupled non-linear differential equations to describe the behavior of

lithium ion battery cells. Their model specifically describes the diffusion of lithium ions as well as the concentration of lithium ions distributed between the electrolyte, separator, and electrodes. [22] It is advised to refer to[21] for more details on the DFN model.

The DFN model has been shown to accurately model Li-Ion battery behavior, but the complexity of the model prevents it from being used for practical real time applications such as spacecraft simulation. Forman et al. [23] utilized an algorithm on the DFN model to identify 88 parameters needed to model a battery cell. DualFoil is an open source program coded in FORTRAN that utilizes DFN's electrochemical model [24]. Due to its high accuracy, researchers often use the DualFoil program to validate their own battery models [25]. The main disadvantage of utilizing the DualFoil program is that extensive knowledge of battery chemical properties and internal battery parameters are required to accurately model a battery cell.

Although proven to be highly accurate, the complex nature of electrochemical models is the main reason electrochemical models are not used as the modeling approach in this research to predict battery behavior. For more information on electrochemical battery cell modeling, refer to *Modeling and Simulation of Lithium-Ion Batteries from a Systems Engineering Perspective* [26].

2.2.3 Mathematical Models

Mathematical models are battery models that typically use empirical equations to describe the behavior of a battery cell. Mathematical models can be broken down into two different types of model: Analytical and Stochastic.

Analytical Models are battery models that describe the properties of a battery using only a few mathematical equations. Peukert's law is the simplest type of analytical model. Peukert's law uses an empirical equation to describe the lifetime of a battery based on current and capacity. The limitation of Peukert's law is its simplicity. Peukert's law is not accurate in describing the

battery's behavior due to variable loads [27]. Because satellites have varying loads, Peukert's law would not be an ideal model to use to describe battery behavior. Another analytical model that accurately predicts battery behavior due to varying load is presented by Rakhmatov and Vrudhula (RV). The RV model, also known as the diffusion model, combines Fick's law, which describes the one-dimensional diffusion process of lithium ions, and Faraday's law, which describes the relationship between flux of lithium ions and current, to obtain an analytical solution. Refer to *An Analytical High-Level Battery Model for use in Energy Management of Portable Electronic Systems* for more information on the RV model [27]. The RV model is able to accurately describe battery behavior over varying loads much better than Peukert's law. RV compares their model and Peukert's law to the DualFoil program. RV's results show a maximum of 6% error for the RV model and 42.6% error for Peukert's law when comparing battery lifetime on a constant load profile with the DualFoil simulation under heavy loads. When comparing varying loads to the DualFoil simulation, their results showed a maximum of 2% error for the RV model and 14.4% error using Peukert's Law. The limitation of the analytical models presented is the inability to capture important battery performance characteristics such as the dynamic relationship between current and voltage. Both the RV and Peukert's models tend to predict only the lifetime of a battery cell and do not incorporate temperature as part of their mathematical equation.

A Stochastic model is another type of Mathematical model that utilizes stochastics to simulate the electrochemical processes of a battery cell. Stochastic models are able to model the recovery behavior of a battery cell which is observable when a battery is discharged and then allowed to settle to an equilibrium state. The battery will return to a state at a much higher voltage than under load. In Stochastic models, the recovery behavior is described as a random

process, hence the term stochastic. Chiasserini and Rao present a stochastic battery model, referred to as the CR model, using Markov chains to model a Li-Ion battery. Markov chains are a process that describes the probability of going from one state in time to another without any influence from past or future states, specifically the state described is the state of charge of the battery cell and its relationship to the voltage and capacity of the battery cell.

Chiasserini and Rao compared their model to the DualFoil program for a Li-Ion cell. Their comparison resulted in a maximum error of 4% in a comparison of overall lifetime capacity of the battery cell due to recovery effects. Chiasserini and Rao's results confirm that the CR model is a good model for simulating the recovery effect of a battery cell. For more information on the CR model, refer to *Energy Efficient Battery Management* [28]. Stochastic models are accurate in modeling the recovery effects in battery cells, but they do not by themselves incorporate other factors that affect battery performance such as variable charge or discharge rates.

Overall, Mathematical models are accurate in predicting the lifetime of a battery. However, the use of empirical equations and probability makes them less ideal for use in real time spacecraft simulation or battery performance prediction that incorporates variable temperature and loads. Analytical models do not incorporate temperature into their empirical equations, while Stochastic models do not accurately predict responses to variable loads. For these reasons, this research will not use Mathematical models to simulate battery pack behavior.

2.2.4 Electrical Models

Electrical models incorporate electrical circuit theory to predict the behavior of a battery cell. Electrical models are intuitive for electrical engineers to relate battery performance

parameters such as voltage and current to the electrical components of a spacecraft. Electrical models are categorized into the following: Thevenin, Impedance, and Runtime.

2.2.4.1 Thevenin Equivalent Circuit Model

Thevenin equivalent circuit models use a circuit network consisting of a voltage source ,V_{oc}, a series resistor, R_i, and a parallel resistor-capacitor (RC) network ,R_t *and* C_t, to predict battery behavior. Figure 6 shows a basic Thevenin Equivalent Circuit Model with a voltage source, resistor, and a single RC network.

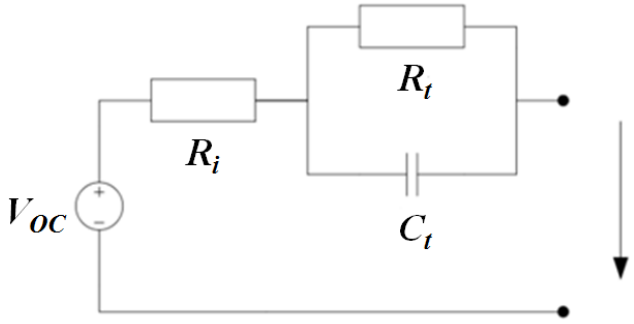

Figure 6: Thevenin Equivalent Circuit Model

V_{oc} is the open circuit voltage of the battery. The open circuit voltage of a battery is the potential difference between a battery cell's cathode (positive) and anode (negative) when the battery is not connected to a closed circuit. V_{oc} describes the voltage of the battery when not in use.

R_i is the ohmic resistance of the battery cell. The ohmic resistance creates the drop in voltage due to current flowing from one electrode to another. R_t is the resistance that models the polarization of the battery. Polarization is the deviation observed between the open circuit voltage and terminal voltage as a result of applied discharge or charge current. C_t is used to directly influence or control the transient response of the simulated battery. R_t and C_t are used to change the behavior of the charging, discharging, and recovery responses of a battery cell.

Thevenin electrical models use battery cell experimental data to create lookup tables for each parameter in the circuit. The limitation of Thevenin electrical models is the requirement of experimental data to establish the necessary RC parameters used in the model. Thevenin electrical models typically have one or two RC networks to keep the number of parameters small that have to be extracted from the experimental data; however, more networks can be added to model other effects. For more information on how to extract parameters from experimental data, refer to *Time-Domain Parameter Extraction Methods for Thevenin-Equivalent Circuit Battery Models* by Hentunen, Lehmuspelto and Suomela [29].

Due to the simplicity and insight on a battery cell's voltage due to current draw, a Thevenin Equivalent Circuit model will be used in this research. Research has been conducted in adding thermal effects to the model making it ideal in providing a battery cell model capable of simulating the space environment. A one RC network Thevenin Equivalent Circuit model will be analyzed in this research to determine the level of accuracy in the model's voltage output.

2.2.4.2 Impedance Battery Model

Impedance models typically utilize a Randle's circuit to model the behavior of a battery cell. Figure 7 shows the Randle's circuit.

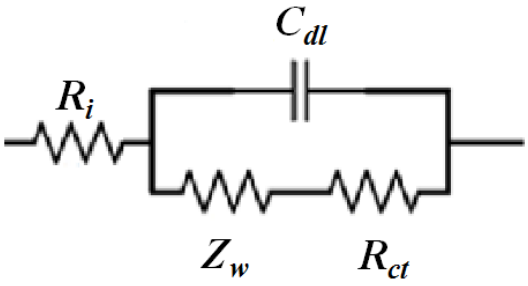

Figure 7: Randle's Circuit [30]

The Randle's circuit contains an ohmic Resistance, R_i, an activation polarization resistance, R_{ct}, a concentration polarization, Z_w, and a double layer capacitance, C_{dl}. The ohmic resistance, R_i, defines the overall resistance inside the battery. The activation polarization resistance, R_{ct}, directly influences the charge transfer process of a battery which is the ionization process at the electrodes which separates lithium into lithium ions and electron. The concentration polarization, Z_w, is also known as the Warburg impedance and influences the diffusion process of lithium ion inside the battery cell. The double layer capacitance, C_{dl}, models the storage of electrical energy inside the battery cell [31].

Impedance models typically utilize a method known as electrochemical impedance spectroscopy (EIS) to collect experimental data. In the EIS method, the battery cell's impedance is measured using a frequency response from a sinusoidal input. The resulting output response is dependent upon the battery cell's impedance. EIS data is represented in either a Nyquist or a Bode plot. From which the parameters of the Randle circuit can be extracted. For more information on EIS and parameter extraction of the Randle's circuit, refer to *Basics of Electrochemical Impedance Spectroscopy* by Gamry [32].

Impedance models are based on alternating current (AC) theory. Typically, a spacecraft operates under components that generate (solar panels) and store (batteries) power through direct current (DC). Batteries produce direct current; thus, it would be more intuitive to use DC circuit theory to model batteries. This research will not utilize impedance models for the reason that impedance based modeling would not be practical in system based modeling applications such as a spacecraft that is primarily DC powered.

2.2.4.3 Runtime-based models

Runtime-based models are similar to Thevenin Equivalent Circuit Models in terms of utilizing DC theory; however, Runtime-based models use a combination of multiple resistor-capacitor circuits to model a battery cell's response. Runtime-based models are more complex than Thevenin and are typically used in modeling applications in Simulation Program with Integrated Circuit Emphasis (SPICE). Alternatively, Runtime-based models can be combined with Thevenin Equivalent Circuit Models to create Hybrid Battery models which are described next. For more information on Runtime-based models, refer to *A PSPICE macromodel for lithium-ion batteries* by S. Gold [33].

2.2.4.4 Hybrid Electrical Battery Models

Dougal et al. [34] present a dynamic model of a single lithium-ion battery that that is capable of modeling the important effects of temperature. The model presented is a hybrid between electrical and electrochemical models. The hybrid model closely matches the manufacturer's data sheet and experimental results. Unfortunately, the authors do not quantitatively specify how closely their models match the experimental results. The experimental results presented in the literature showed that the model agreed with the experimental data and the manufacturer's data sheet. However, the model was only based on discharge characteristics and did not include charging characteristics. At lower temperatures (-20° C) or at high discharge rates (~1.8C), their model did not match experimental data. Although the model presented by Dougal et al. incorporates the effects of temperature, this specific model will not be used in this research because the model is used for analysis of a single battery cell and does not present a capability to be modified for simulation of multiple battery cells in a battery pack configuration.

Chen [35] presents an electrical battery model that models the dynamic characteristics of the battery. Chen's model proposes a combination of a Thevenin Equivalent Circuit Model,

Impedance model and Runtime-based models. Chen utilized 10 Li-ion battery cells, each tested individually, and extracted curves for the parameters in his model. The parameters extracted are single variable functions based on a battery's state of charge (SOC). The single variable empirical functions along with Chen's proposed model are presented in Figure 8.

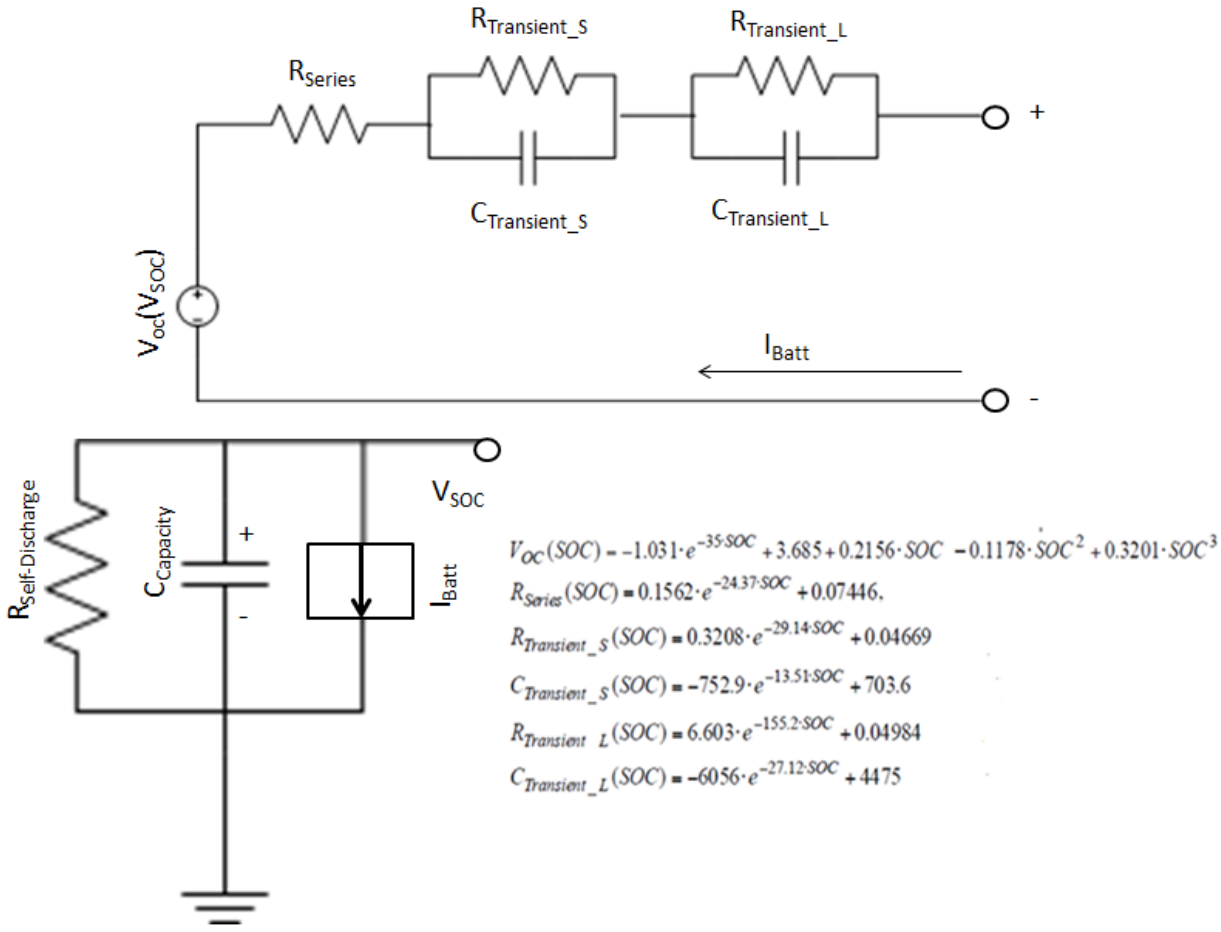

Figure 8: Chen's Battery Model [35]

The functions were used by Chen to simulate and compare to experimental data resulting in a battery runtime error of 0.1% and a maximum voltage deviation of 21 mV out of 3.6V. Although comparison between experimental data and simulation showed high accuracy, Chen's model did not take into account number of cycles, and temperature. Chen's model is not a viable

option for spacecraft battery simulation because the model ignores two main performance factors: temperature and number of cycles.

Erdinc, Vural, and Uzunoglu [36] present a battery model that modified Chen's work and introduced capacity fading and temperature effects through a correction factor term showing that battery dynamics are highly affected by not only the temperature and capacity fading, but also the charge and discharge rates. The results presented by the authors justify that temperature, capacity fading, and charge and discharge rates must be incorporated into the model to accurately simulate a battery cell's dynamics. The authors did not compare experimental data with simulated predictions. Instead, data was presented to show changes to battery run time as a result of temperature and number of cycles. Their model captures the right trend of the battery, but does not show the exact behavior. This model is an ideal model that can be used to simulate battery cell dynamics in spacecraft. The modified Chen's model takes into account capacity fading (decrease in capacity due to number of cycles over time), temperature, and charge/discharge rates that are prominent in spacecraft battery performance measurements. However, this model is not used in this research.

2.2.5 Adaptive Models

Finally, Adaptive battery models are a subcategory of electrical models that use Kalman filtering techniques to estimate a battery's state of charge and simulate behavior in real time. Measured input and output data from the current state of the battery is used to update the model and predict the future state of the battery. Adaptive models are empirical and cannot be used to predict behavior of another different battery pack without additional experimentation on the new battery pack. For more information on adaptive models using Kalman filtering, refer to *On-line adaptive battery impedance parameter and state estimation considering physical*

principles in reduced order equivalent circuit battery models: Part 1. Requirements, critical review of methods and modeling by Fleischer, Waag, Heyne, and Sauer [37]. Adaptive models are suited for battery monitoring and control rather than battery prediction and simulation. Adaptive models will not be used in this research for battery modeling and will be a discussion for further research.

Overall, electrical models are capable of simulating and predicting battery cell dynamics with expected accuracy in predicting responses somewhere between electrochemical and mathematical models. Their main disadvantage is the requirement for experimental data to estimate RC parameters. Electrical modeling accuracy is highly dependent on the conditions under which experimentation have taken place. Electrical models become less accurate for temperature, discharge, or charge behavior not present in the experimental data used to estimate the RC parameters.

2.3 Summary of Battery Models

Table 1 summarizes the advantages and disadvantages of each type of battery model. Overall, the electrical battery models are the most intuitive for electrical engineers and will be the focus for this research. An electrical battery model that incorporates thermal effects is ideal for simulating spacecraft battery behavior. A proposed electrical model that incorporates thermal effects will be used in this research to simulate and model a battery pack.

Table 1: Summary of Battery Models

Battery Model	Advantages	Disadvantages	Expected Accuracy
Electrochemical Model	Models battery cell based on physics and electrochemical process	Complex	~1% error from experimental data
		Too time consuming to be used for simulation	
	Highest accuracy of all battery cell models	Requires extensive knowledge of internal battery chemistry parameters	
Mathematical	Simplistic	Empirical equations used to model battery are non-intuitive	~4-6% error from experimental data for battery lifetime
	Models a battery cell using a few equations	Equations do not provide information of dynamic relationship between current and voltage	
Electrical	Provides battery performance characteristics	Requires experimental data to estimate parameters	~5- 10% error from experimental data
	Intuitive for electrical engineers	Not as accurate as other methods	
	Simplistic		

2.4 Proposed Model

Although the Modified Chen's Model is ideal in simulating battery cell dynamics, simulation of battery pack dynamics would require further investigation. Thus, an alternative approach is proposed to model the behavior of a battery pack. The proposed model in this research is presented by Huria, Jackey, Gazzarri, and Ceraolo (HJGC) [38]. The author's electrical model utilizes Simulink and SIMSCAPE in MATLAB to create a Thevenin Equivalent Circuit based battery cell model that incorporates temperature effects. Additionally, HJGC's battery cell model is capable of integrating into a system of multiple battery cells models to form and simulate a battery pack. Each battery cell model also introduces RC parameters that are variable based on temperature. These RC parameters can be acquired through experimental data

and a tool in Simulink known as Simulink Design Optimization. Refer to *High Fidelity Electrical Model with Thermal Dependence for Characterization and Simulation of High Power Lithium Battery Cells* for more information on the HJGC model [38]. This research will modify the HJGC model along with generating RC parameters based on experimental data to validate a 2S2P battery pack. This research will also utilize the modified HJGC model to predict the behavior of a 4S2P battery pack.

2.5 Battery Testing Method

NASA's Johnson Space Center (JSC) created a guide on battery test planning [39]. Battery testing methods can be categorized into performance and abuse testing. Performance testing determines the capabilities of the battery cell under a variety of operating conditions. Abuse testing determines the limits of physical and operational abuse that a battery cell can endure.

This research will primarily focus on performance testing of battery cells. Performance tests of battery cells used for space applications are conducted in a thermal environment chamber to simulate the conditions that a battery is likely to encounter in space. Load tests, charge and discharge of a battery cell under a load, are conducted in conjunction with thermal environmental cycling to simulate the charge and discharge process a battery experiences on a spacecraft.

For this research, a load test under vacuum and thermal conditions is required to gather experimental data. The experimental data is used to estimate RC parameters in the proposed HJGC model. Extracted experimental data under various thermal conditions is expected to show changes in RC parameters for each temperature test scenario.

2.6 Summary

Research in terms of Li-Ion batteries, battery models, and battery testing was presented in this review. The chosen model to simulate spacecraft battery behavior is the Thevenin Equivalent Circuit based model presented by Huria, Jackey, Gazzari, and Ceraolo [38]. The proposed HJGC model provides a simplistic yet intuitive approach to simulating battery pack performances. The model takes into account the effects of environmental temperature through variable RC parameters based on temperature. The HJGC model is a Thevenin Equivalent Circuit Model, thus experimental data is required to present an accurate model capable of predicting the performance of a CubeSat battery pack. Chapter 3 will address the methodology used to modify the equivalent circuit model in MATLAB. Chapter 3 will also address the testing approach used to acquire experimental data for parameter extraction.

III. Methodology

This chapter will first describe the chosen procedure for modeling, testing, and extracting battery parameters. First, the proposed battery pack model will be modified. Next, AFIT's battery pack will undergo environmental testing in the TVAC chamber to simulate operation in the space environment. Environmental test data from a Li-Ion cell will be used to extract the RC parameters for the battery model. Incorporating the extracted parameters into the modified battery model, the modified model will simulate AFIT's battery pack under a range of temperatures. Finally, the model simulation results will be compared to the environmental test data. The analysis between model results and experimental data will show the level of accuracy in predicting battery pack behavior. Thus, the modified model with extracted RC parameters will attempt to answer the research question of can we predict battery pack behavior in a space environment.

3.1 Battery Model Modification

This research will begin with modifying the battery pack model presented by HJGC [38]. The HJGC battery model utilizes an add-on toolbox for MATLAB known as SIMSCAPE that allows the user to model systems using blocks that represent physical components such as a resistor or capacitor. For more information about SIMSCAPE, refer to the Mathworks website for tutorials [40]. The HJGC Model built in Simulink/SIMSCAPE is shown in Figure 9.

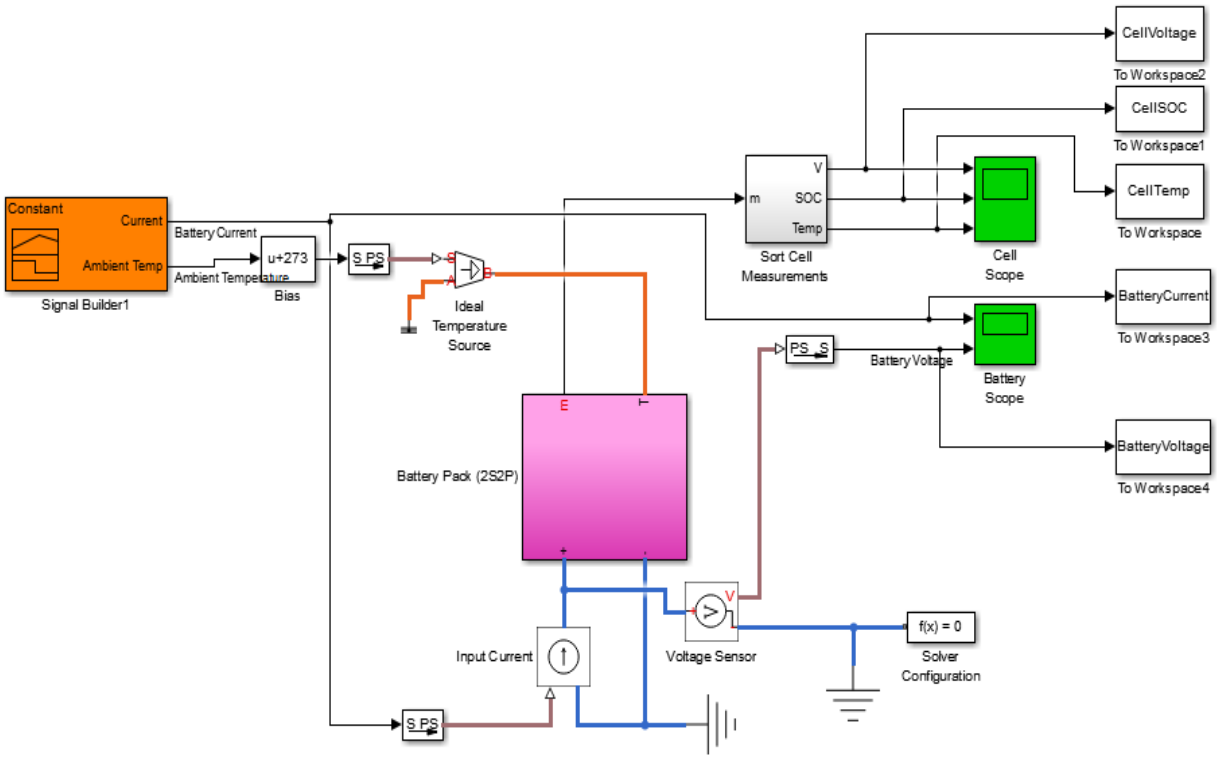

Figure 9: HJGC Battery Model presented in MATLAB using Simulink and SIMSCAPE. A *Signal Builder* block provides the current and temperature input into the *Battery Pack (2S2P)* mask which displays and stores the outputs through the two scopes.

The HJGC model's battery pack architecture is layered using masks which are customizable user interface blocks that hide the contents inside the mask. Names of the blocks and masks used in the HJGC model will be italicized. The hierarchy of the battery pack architecture of the HJGC battery model broken down from top to bottom is shown in Figure 10. From left to right the masks on the left contain the masks on the right.

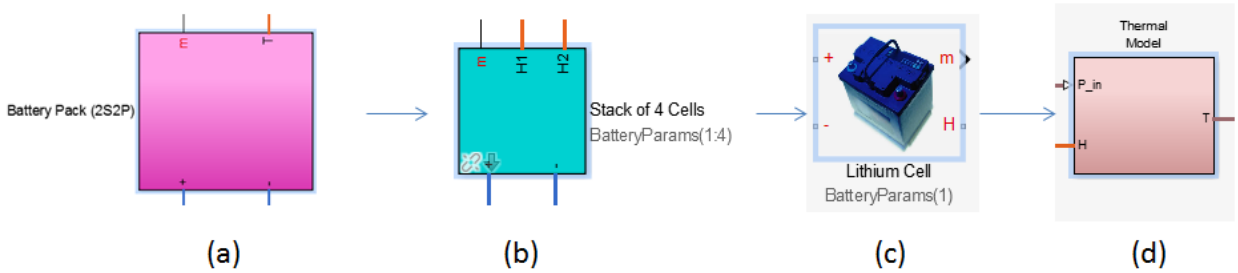

Figure 10: HJGC Battery Pack Architecture. The masks used in the HJGC Battery model are presented from left to right. The mask on the left contains the mask on the right. The *Battery Pack (2S2P)* mask (a) contains the *Stack of 4 Cells* mask (b). The *Stack of 4 Cells* mask contains four *Lithium Cell* masks (c). Each *Lithium Cell* Mask contains a *Thermal Model* mask (d).

The *Battery Pack (2S2P)* mask, Figure 10(a), represents the overall battery pack. The *Stack of 4 Cells* mask, Figure 10(b), represents the stack of cells that make up the battery pack of which there is only one in the modified HJGC model. The *Lithium Cell* mask, Figure 10(c), represents an individual Li-Ion battery cell of which there are four in the modified HJGC model. Lastly, *Thermal Model* mask, Figure 10(d), represents the temperature behavior a Li-Ion cell experiences due to environmental temperature and internal heating from the resistors.

The content inside the *Battery Pack (2S2P)* mask from the original HJGC model is shown in Figure 11. The original HJGC model was designed to model the behavior of 80 cells in a series configuration. There were a total of 10 *Stack of 4 Cells* masks, referred to as *Stack of 8 Cells* in the original model, each containing 8 *Lithium Cell* masks. The contents inside the *Stack of 8 Cells* mask are shown in Figure 12.

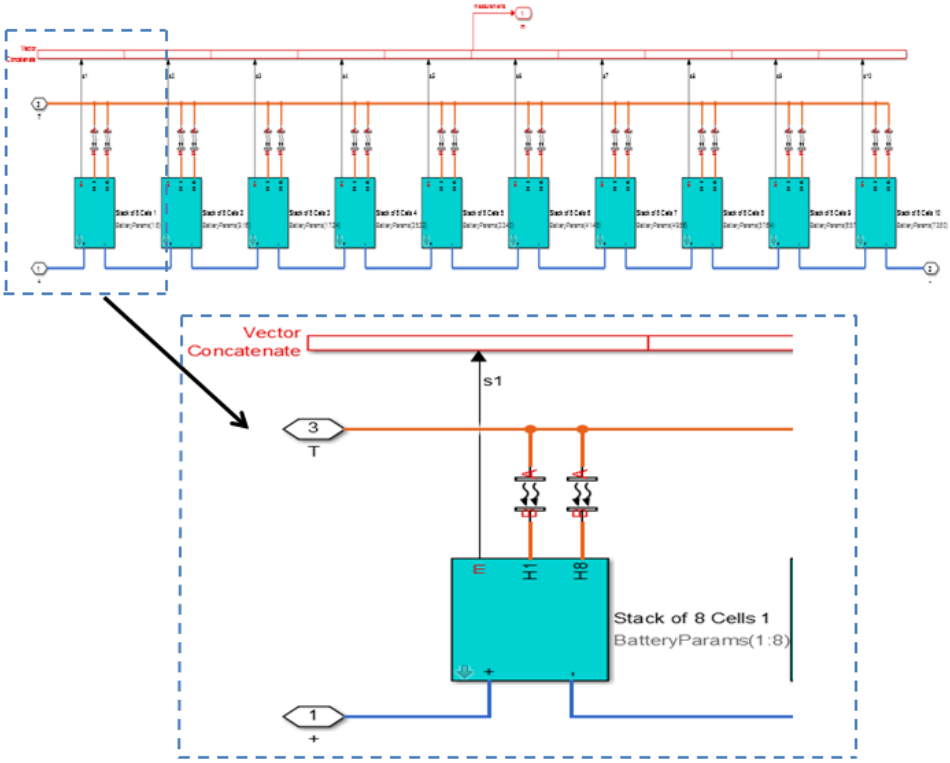

Figure 11: Battery Pack (2S2P) mask contents before modification. The original HJGC model contained 10 *Stack of 8 Cells* masks each containing 8 *Lithium Cell* masks.

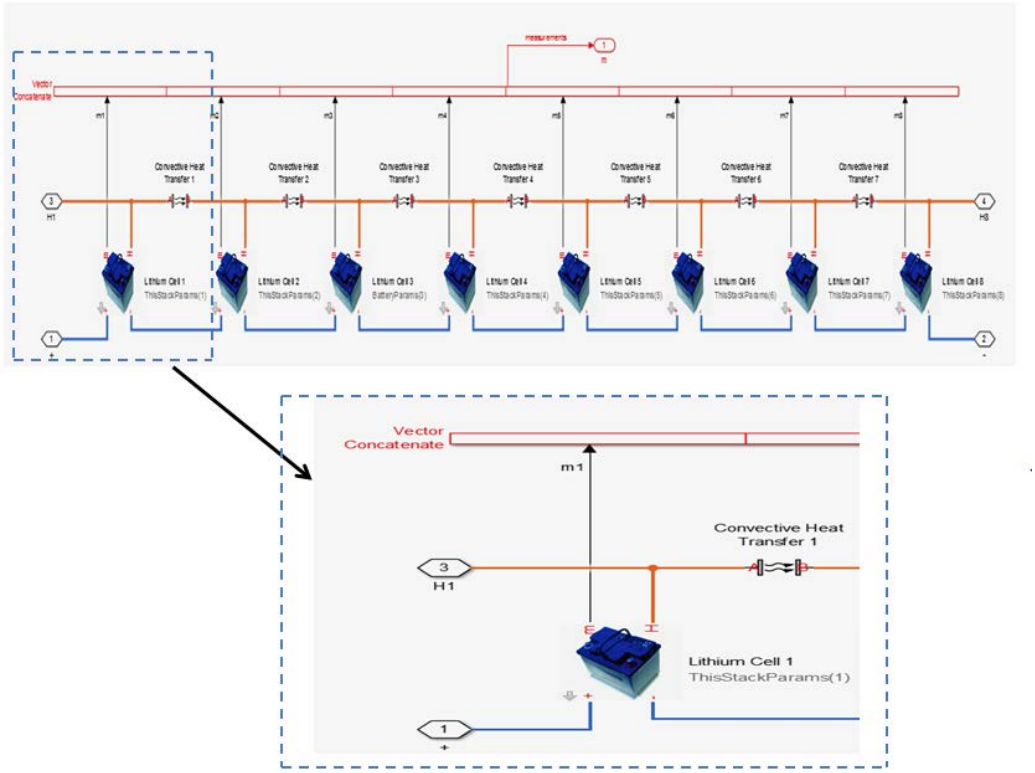

Figure 12: *Stack of 8 Cell* contents before modification. The original HJGC model contained 8 *Lithium Cell* masks in a series configuration inside each *Stack of 8 Cell* mask.

The modification from the original HJGC model was to use only one *Stack of 4 Cells* mask to represent one battery pack and is shown in Figure 13. Block 1 labeled “m” is the measured outputs from all four *Lithium Cell* mask. Blocks 1 and 2 labeled “+” and “-” is the input of current from the *Signal Builder* shown in Figure 9. Block 3 labeled “T” is the input of temperature from the *Signal Builder*. The two blocks linked to H1 and H2 on the *Stack of 4 Cells* mask, and block 3 is used to represent the energy transfer of heat through convection between the surrounding temperature and the battery cells.

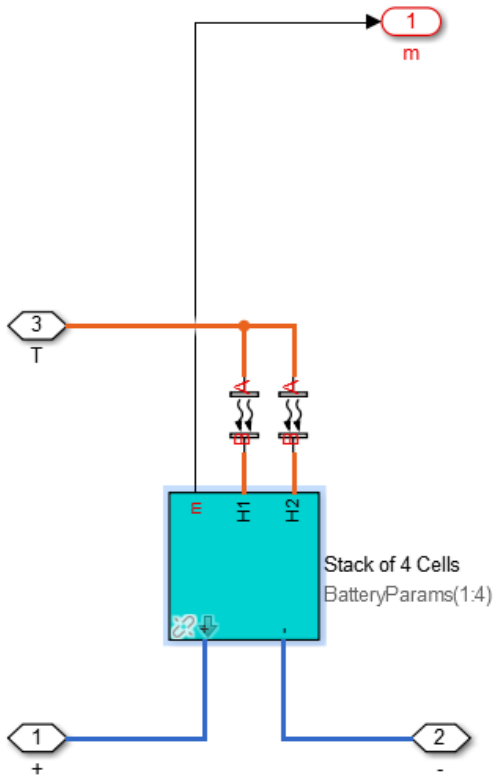

Figure 13: *Battery Pack (2S2P)* Mask Contents after modification. Modifications made to the original HJGC model was to delete the other 9 *Stack of 8 Cell* masks and change the contents inside the last *Stack of 8 Cells* mask to contain 4 *Lithium Cell* mask.

In the modified HJGC model, the *Stack of 8 Cells* from the original HJGC model is renamed as the *Stack of 4 Cells* mask which represents a battery pack that has two cells connected in series and two cells connected in parallel (2S2P). The four *Lithium Cell* masks inside this the *Stack of 4 Cells* mask were configured to simulate AFIT's 2S2P battery pack. It is expected that multiple battery pack configurations are feasible inside this mask. The modified content inside *Stack of 4 Cells* mask for a battery pack in a 2S2P configuration is shown in Figure 14.

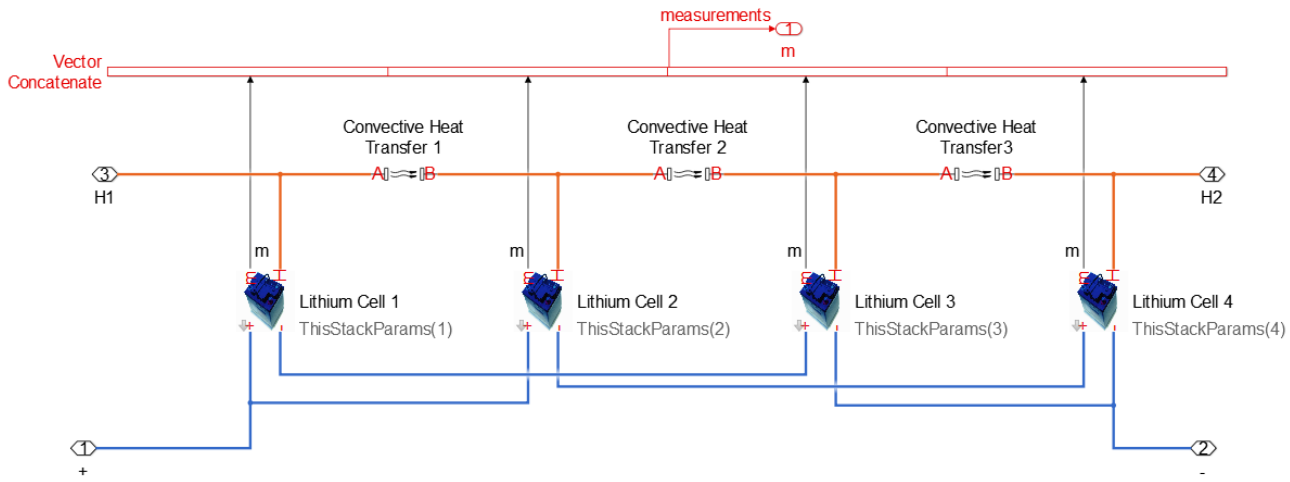

Figure 14: *Stack of 4 Cell* contents after modification. Four *Lithium Cell* masks are arranged in a 2S2P configuration.

Inside the *Stack of 4 Cells* mask are four more masks called *Lithium Cell*. Each of the four *Lithium Cell* mask represents an individual Li-Ion battery cell in a 2S2P battery pack configuration. Similarly to the *Stack of 4 Cells* mask, blocks 1 and 2 are the inputs of current from the *Signal Builder*; while blocks 3 and 4 are the temperature inputs from the *Signal Builder*. The *Convective Heat Transfer* block between each *Lithium Cell* mask simulates the heat transfer between each Li-Ion battery cell.

The contents inside the *Lithium Cell* mask contain a Thevenin Equivalent Circuit Model using a single RC network and the *Thermal Model* mask. Figure 15 shows the contents of the *Lithium Cell* mask. The blocks inside this mask labeled *Em_table*, *R0*, *R1*, and *C1* represent the voltage source, ohmic resistance and the RC network from a Thevenin Equivalent Circuit respectively. Each of these blocks inside the *Lithium Cell* mask utilizes a lookup table to model the individual battery cells. The lookup table is based on extracted parameters from experimental data. Data for the lookup table is stored in an initiation file, along with other information of the

battery cell such as battery dimensions and weight that is used by the *Thermal Model* mask. The modified HJGC Model as well as the original, utilizes an initiation file that provides the input used primarily by the blocks inside the *Lithium Cell* mask.

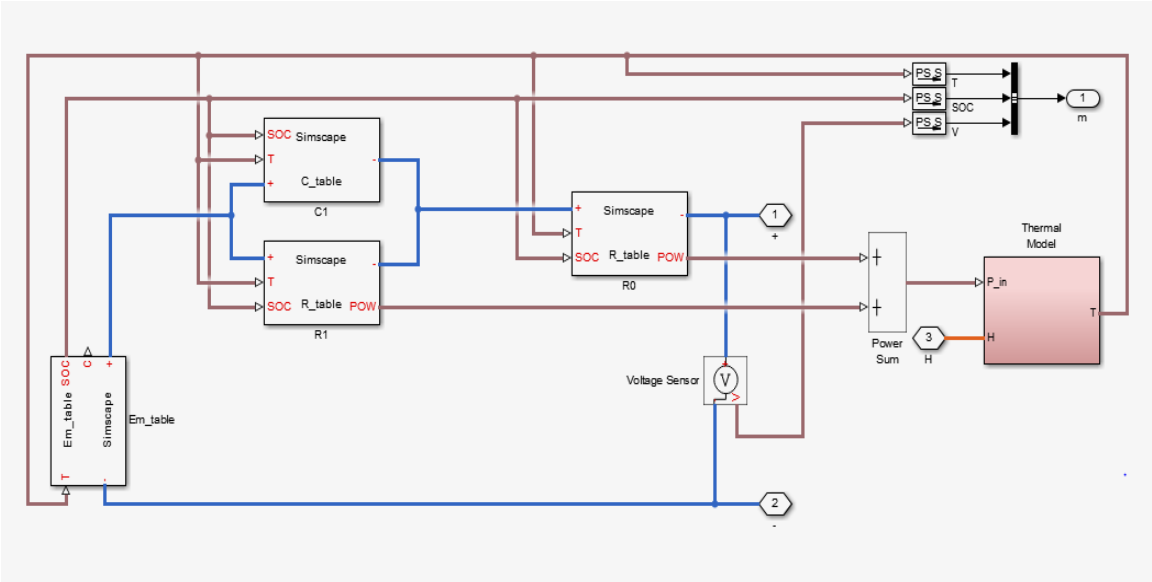

Figure 15: HJGC *Lithium Cell* Mask Contents. The HJGC *Lithium Cell* mask contains the *Thermal Model* mask and the Thevenin Equivalent Circuit Model. The voltage is represented by the block *Em_table*, the RC network is represented by blocks *R1* and *C2*, and the ohmic resistance is represented by the block *R0*.

The *Thermal Model* mask in the *Lithium Cell* mask can be used to predict the change in behavior of the battery cell due to temperature and change in temperature from the resistors. The change in temperature from the resistors is inputted to the *Thermal Model* mask as the power generated by the current flowing through the resistors, *P_in*, and the temperature of the environment input is from the *Signal Builder* and is represented by the variable *H*. Figure 16 represents the thermal model inside the *Lithium Cell* Mask.

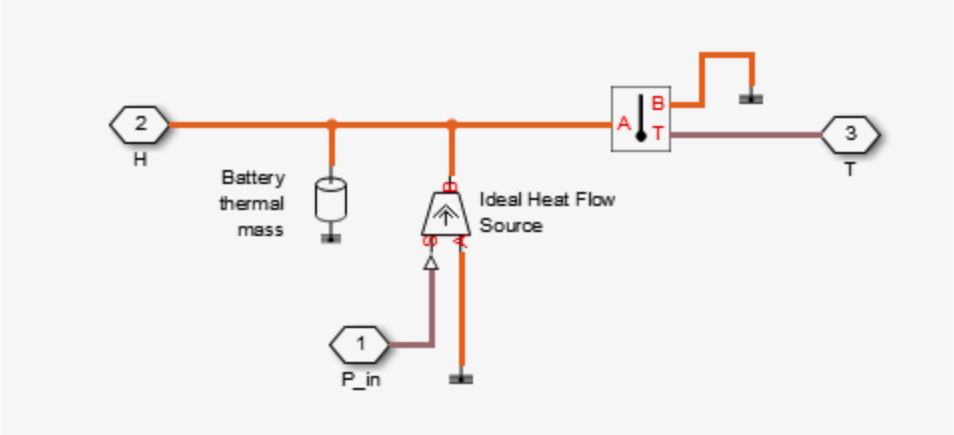

Figure 16: *Thermal Model* Mask Contents.

The block labeled *Battery thermal mass* represents a battery's ability to store internal energy. Block 1 labeled *P_in* is the power input from the resistors. Block 3 labeled *T* contains the temperature output from the battery. Lastly, the block directly connected to Block 3 is the temperature sensor in the thermal model used to generate the temperature output.

3.2 Battery Model Flowchart

Once the model has been modified, it can be used to simulate the performance of a 2S2P battery. A flowchart, shown in Figure 17, depicts the input files needed to build the model, the actual model file that is used to generate the simulation, and the outputs from the model. Modeling a battery pack starts with an initiation file, loading the HJGC prebuilt *Lithium Cell* mask, and modifying the *Signal Builder* with a desired load and temperature profile. The *Signal Builder* uses the same the temperature and the current draw found in the experimental data as the desired load and temperature profile.

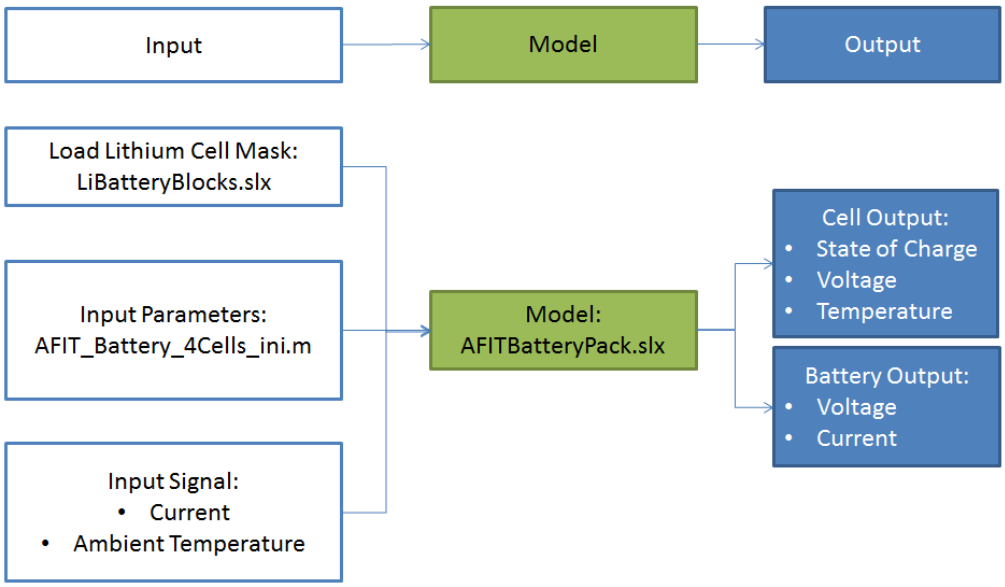

Figure 17: Battery Model Flowchart

The initiation file contains information specific to the battery cell modeled such as the lookup tables for each RC parameter, the battery cell's dimension, and the battery cell's weight. The initiation file, when compiled, stores the information of the lookup tables inside MATLAB's workspace which is accessed the *Lithium Cell* mask. The other information such as the battery cell's dimension and weight is also stored in MATLAB's workspace and is accessed by the *Thermal Model* mask.

Battery cell dimensions can be measured or based off the manufacturer's specification sheet. For this research, the initiation file's lookup tables, battery dimensions and weight are based on extracted parameters from experimental data of a battery cell, and the manufacturer's specification sheet. Once the input files have been loaded and compiled, running the model will output temperature, voltage, and state of charge information for each battery cell and voltage and current for the battery pack. The output is compared with experimental data collected from AFIT's battery pack in experiments described next in Section 3.3. Before running the model and

using it for comparative analysis, collection of experimental data of the battery cell and AFIT's battery pack is required for parameter estimation.

3.3 Environmental Testing

Environmental testing is conducted to estimate parameters at various operating temperatures. Environmental test data of the battery pack is also compared with the model's simulation output. This section will describe the equipment, setup, and test cases used to gather the test data for parameter estimation and comparative analysis.

3.3.1 List of Equipment

In order to gather experimental data, the each of the following equipment will be used and explained in detail next.

- ABBESS Thermal Vacuum (TVAC) Solar Simulation System
    - Type-K Thermocouples
    - TVAC Interfacing Connectors
- CADEX C8000 Battery Testing System
    - CADEX Power Port Cables
- LG ICR18650C2 Battery Cell
- AFIT 2S2P Battery Pack (Cells only)

Along with the computer, the following programs are required to gather data:

- TVAC Chamber and Thermocouple Software (ABBESS and LabVIEW)
- CADEX C8000 Software (BatteryLab)

3.3.1.1 ABBESS Thermal Vacuum Solar Simulation System

Figure 18 shows the ABBESS TVAC used to simulate the space environment. The ABBESS TVAC chamber contains the following major components: vacuum chamber, thermal platen/shroud, and solar simulator. This research will only utilize the vacuum chamber and thermal platen/shroud to test the battery. Type K Thermocouples and Interfacing Connectors will be described next. The Type K thermocouples are used to monitor the external temperature of the battery cell and battery pack to provide thermal data of the batteries. The LabVIEW software is used to record temperature data from the thermocouples. The interfacing connector is what allows the battery pack and battery cell inside the chamber to be connected with the CADEX C8000 Battery Testing System outside the chamber.

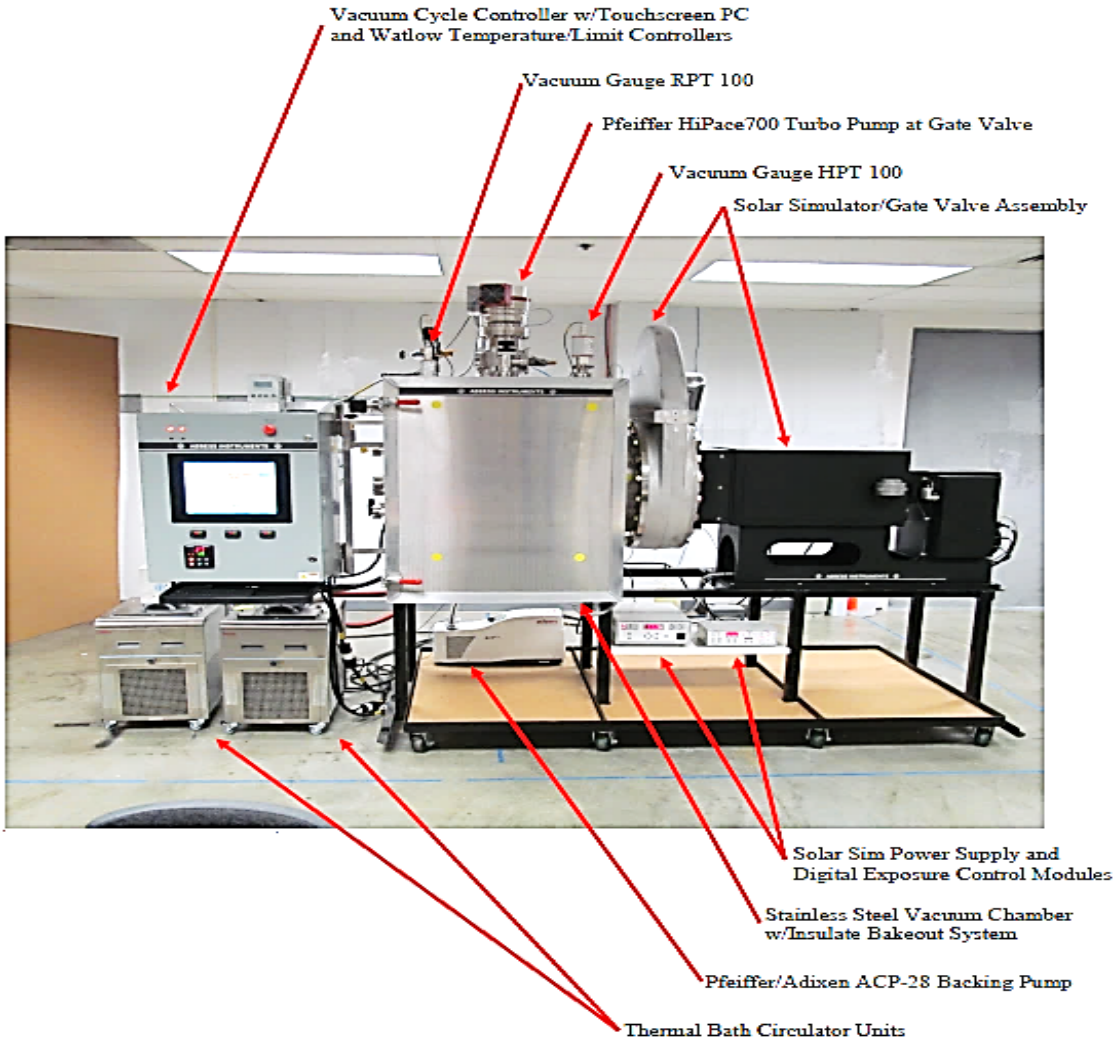

Figure 18: ABBESS Thermal Vacuum Solar Simulation System [41]

3.3.1.2 CADEX C8000 Battery Testing System

Figure 19 shows the CADEX C8000 Battery Testing system used to gather battery cell and battery pack data. The CADEX C8000 is capable of charging and discharging the battery pack and battery cell through programs in its BatteryLab software. The test cases for this research are processed through user created programs inside the BatteryLab software. An example of the program used in BatteryLab can be found in the CADEX user manual[42].The CADEX C8000 comes equipped with Power Port Cables that are used to connect with the

batteries. With four channels, the CADEX C8000 can run four battery pack and individual cell tests simultaneously. Refer to the CADEX C8000 product page or the user manual for more information on the CADEX C8000 Battery Testing System [42].

Figure 19: CADEX C8000 Battery Testing System [43]

3.3.1.3 LG ICR18650C2 Battery Cell

Since this research focuses on modeling the behavior of the LG ICR18650C2 cells in a 2-series, 2-parallel (2S2P) battery pack configuration, testing a single LG ICR18650C2 battery cell, shown in Figure 20, is necessary for parameter extraction. The model using extracted parameters will be validated using test data from a 2S2P battery pack configuration. Figure 21 is a table from the manufacturer that shows the battery specifications for a single LG ICR18650C2 cell.

Figure 20: LG ICR18650C2 battery cell

Item	Condition / Note	Specification
2.1 Capacity	Std. charge / discharge	Nominal 2800mAh (C_{nom}) Minimum 2700mAh (C_{min})
2.2 Nominal Voltage	Average	3.72V
2.3 Standard Charge (Refer to 4.1.1)	Constant current Constant voltage End current(Cut off)	0.5C (1350mA) 4.30V 50mA
2.4 Max. Charge Voltage		4.30V
2.5 Max. Charge Current		1.0C (2700mA)
2.6 Standard Discharge (Refer to 4.1.2)	Constant current End voltage(Cut off)	0.2C (540mA) 3.0V
2.7 Max. Discharge Current	-20 ~ 5℃	0.5C (1350mA)
	5 ~ 45℃	2.0C (5400mA)
	45 ~ 60℃	1.5C (4050mA)
2.8 Weight	Approx.	Max. 50.0 +/- 3.0 g
2.9 Operating Temperature	Charge Discharge	0 ~ 45℃ -20 ~ 60℃
2.10 Storage Temperature (for shipping state)	1 month 3 month 1 year	-20 ~ 60℃ -20 ~ 45℃ -20 ~ 20℃
2.11 Cell Voltage (for shipping state)	Voltage range	3.7 ~ 3.9V

Figure 21: LG ICR18650C2 Battery Cell Specifications [44]

3.3.1.4 AFIT Battery Pack

The 2014 AFIT battery pack, shown previously in Figure 3, includes four LG ICR18650C2 cells; when combined in a 2S2P configuration, the battery pack has a total energy capacity of 41.66 Wh at a nominal voltage of 7.44 V. To achieve a 2S2P configuration, the individual battery cells are welded together using tabs. Figure 22 shows the “tabbed” LG battery cells.

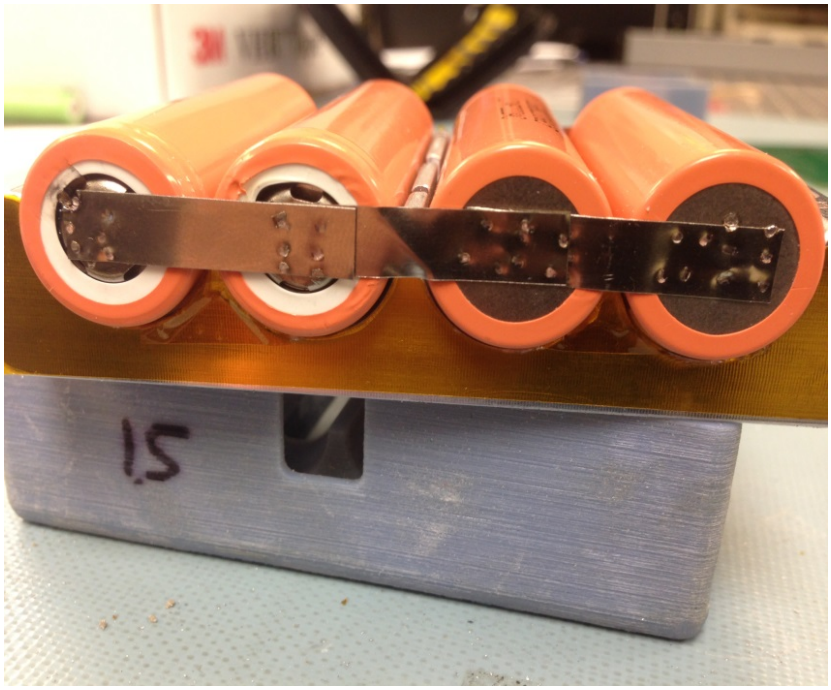

Figure 22: Tabbed LG ICR18650C2 Battery Cells

The battery pack is capable of reaching a peak voltage of 8.6 V at a maximum state of charge. Battery pack voltage and capacity can be determined using fundamental circuitry laws for series and parallel circuits. For batteries in a series configuration, voltages are added together; however, current remains the same. For batteries in a parallel configuration, current is added together; however, voltage remains the same. Thus, for four battery cells rated at 4.3 V and 2.8 Ah each in a 2S2P configuration, the voltage is added together for two cells, to equate 8.6 V, and

the current is added together for two cells to equal 5.6 Ah. To get the energy capacity in Watt hours (Wh), the total capacity in Ah is multiplied by the nominal voltage, not the peak voltage. For the LG batteries, the nominal voltage is 3.72 V— resulting in a total nominal voltage of 7.44 V for the battery pack. Thus, the total energy capacity of AFIT's battery pack is 41.66 Wh [44].

For this research, AFIT's battery pack will be tested using only the cells from inside the battery pack with no accompanying battery control electronics. The reason is to provide a better characterization of the cells inside the battery pack by eliminating any deviations in test data caused by wiring and circuitry inside the battery board. The HJGC model does not model the losses due to wiring and circuitry for a battery pack.

3.3.2 TVAC Test Setup

This section will describe the experimental test setup of the TVAC chamber. Figure 23 shows the block diagram layout of the CADEX C8000 Battery Testing System, battery cells, and ABBESS TVAC Chamber.

3.3.2.1 Battery Setup

The individual cell and the "tabbed" cells inside the battery pack stack were setup in a TVAC-ready configuration, shown in Figs. 24 and 25, prior to beginning TVAC test.

In a TVAC ready configuration, the batteries rest on a metallic casing which is used as a battery cell container and is placed on the chamber platen to provide thermal contact between the platen and cells. Figure 26 shows the metallic casing used to hold the batteries inside the TVAC chamber.

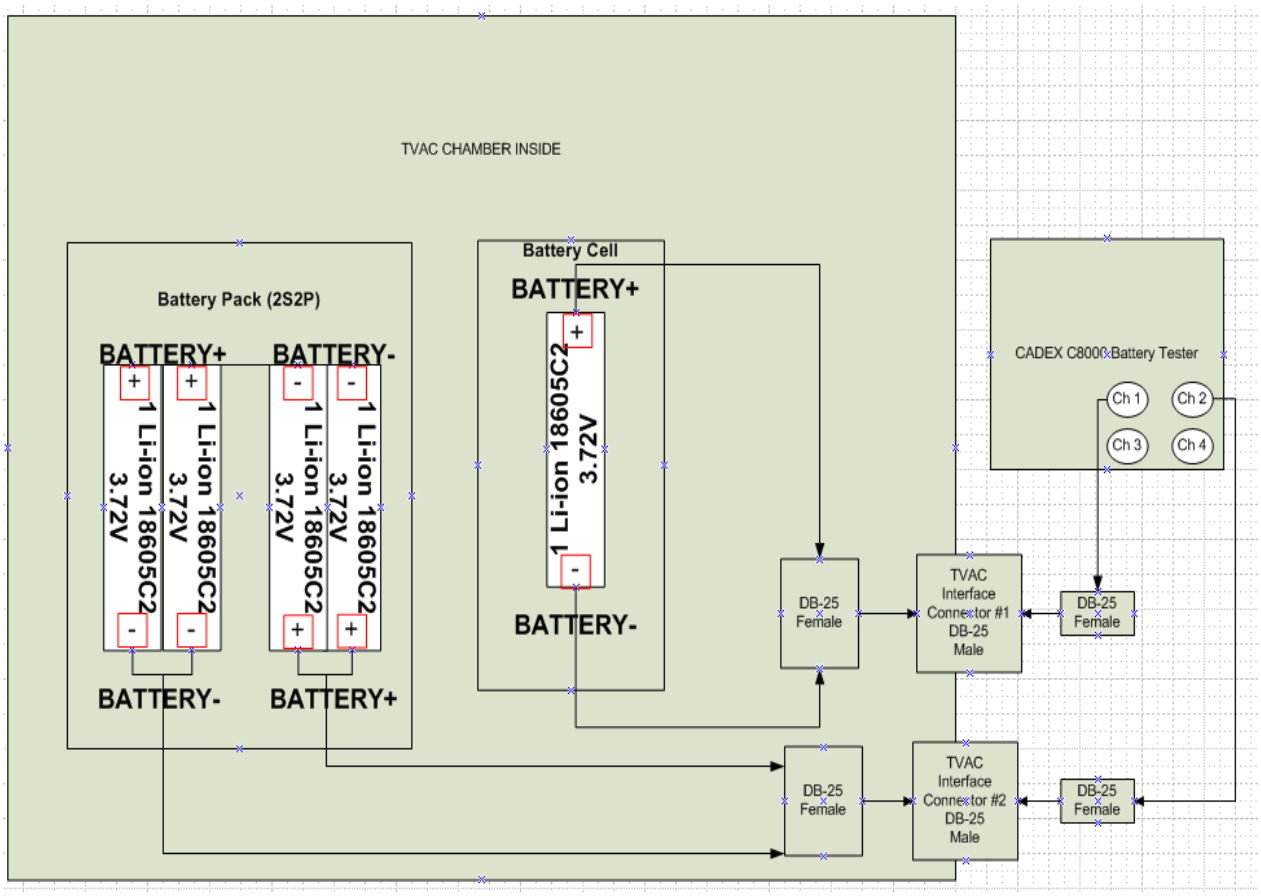

Figure 23: TVAC Test Setup. The setup shows the battery pack and battery cell connection to the CADEX Battery Testing System. From inside the chamber to outside the chamber, the battery cell is connected to channel 1, while the battery pack is connected to channel 2 on the CADEX.

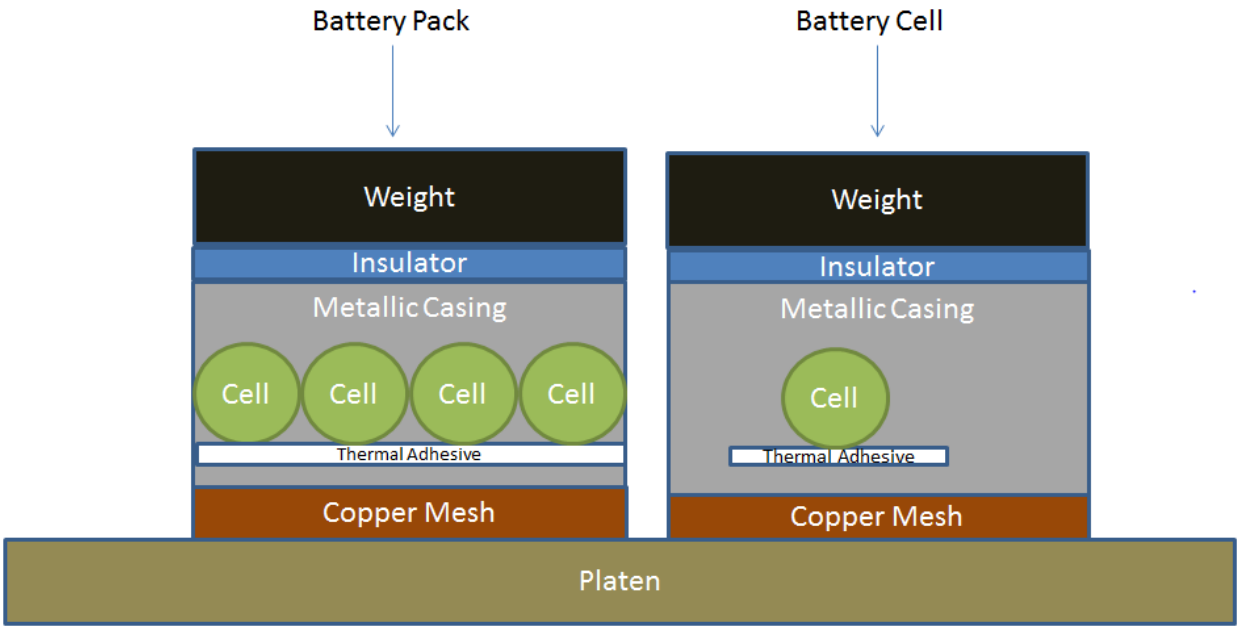

Figure 24: Battery Setup inside TVAC Chamber

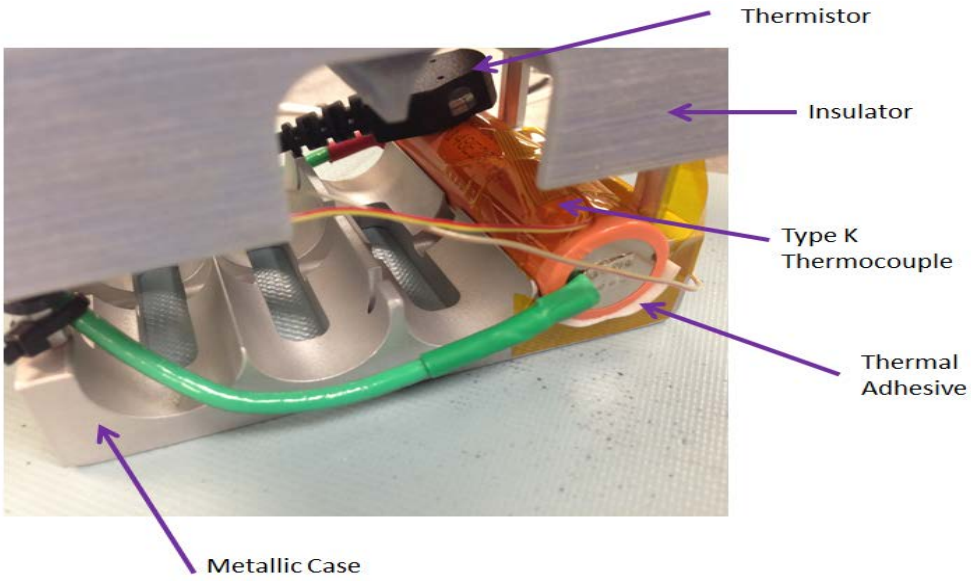

Figure 25: Battery Cell in TVAC-Ready Configuration

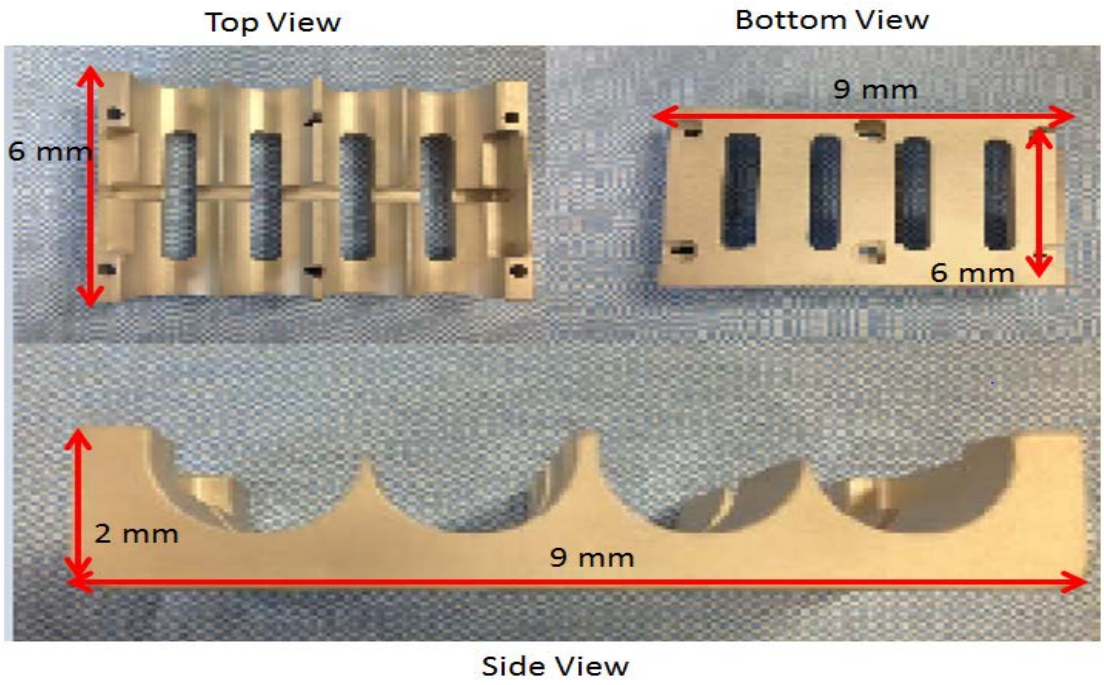

Figure 26: Battery Pack Metallic Casing

Between the metallic casing and the battery cells is a thermal adhesive that is used to keep the battery from sliding out of the metallic case during setup inside the TVAC chamber and provide a thermal path between the battery cell and case. The thermal adhesive used is 3M VHB 4930 double-sided sticky tape. The properties for the tape can be found in the manufacturer's specifications sheet [45]. Figure 27 shows the adhesive applied to the battery cells prior to placement on the metallic case. During setup inside the chamber, a copper mesh, shown in Figure 28, is placed between the metallic case and platen to reduce the thermal resistance between the metallic case and platen.

Figure 27: Thermal Adhesive on Battery Cells

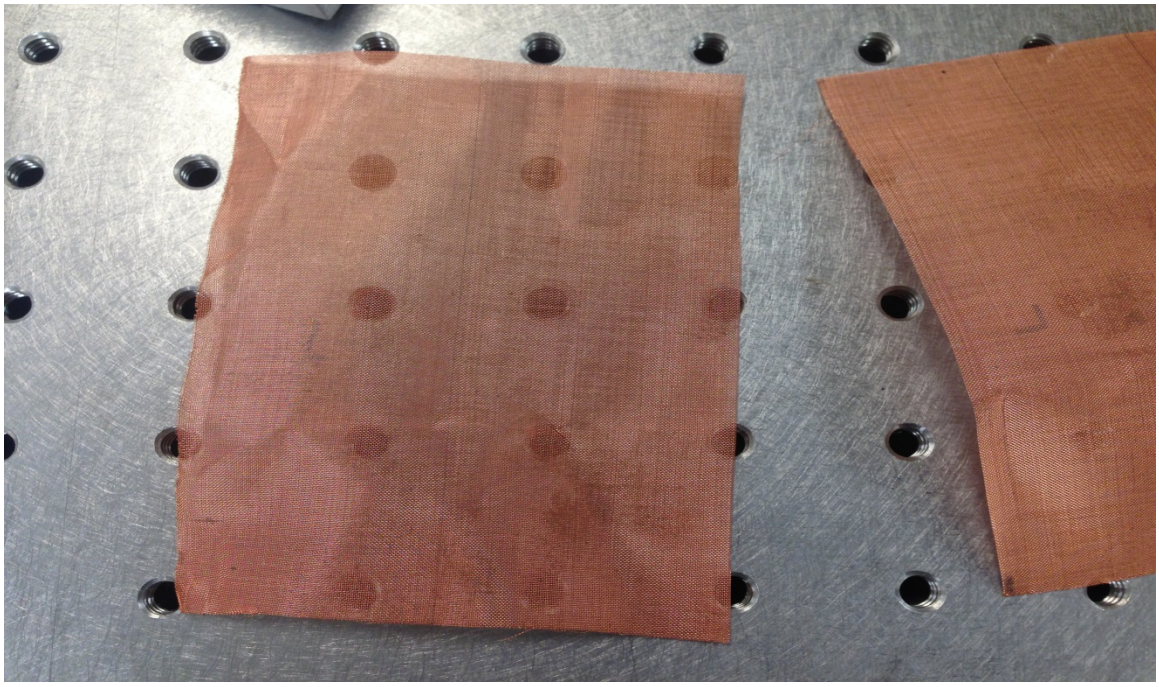

Figure 28: Copper Mesh

Prior to integrating the batteries into the TVAC chamber, thermocouples and thermistors were installed on the batteries to monitor the temperature of the cells. Figure 29 shows a depiction of the general location of the Type K thermocouples on the pack and individual cell.

Figure 30 shows a photograph of the placement locations of each Type K thermocouples on the test hardware. The placement of the Type K thermocouple on the chamber platen will be shown in a later figure. The thermocouples are secured to the test articles using Kapton tape.

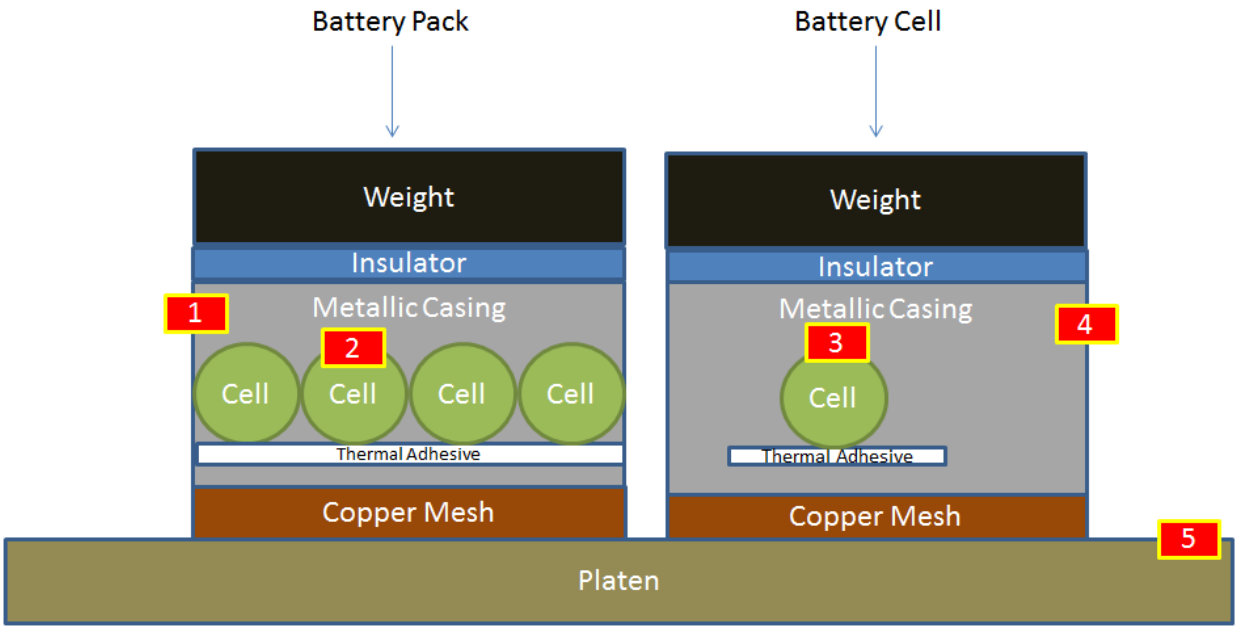

Figure 29: TVAC Chamber Thermocouple Locations Numbers 1 through 5

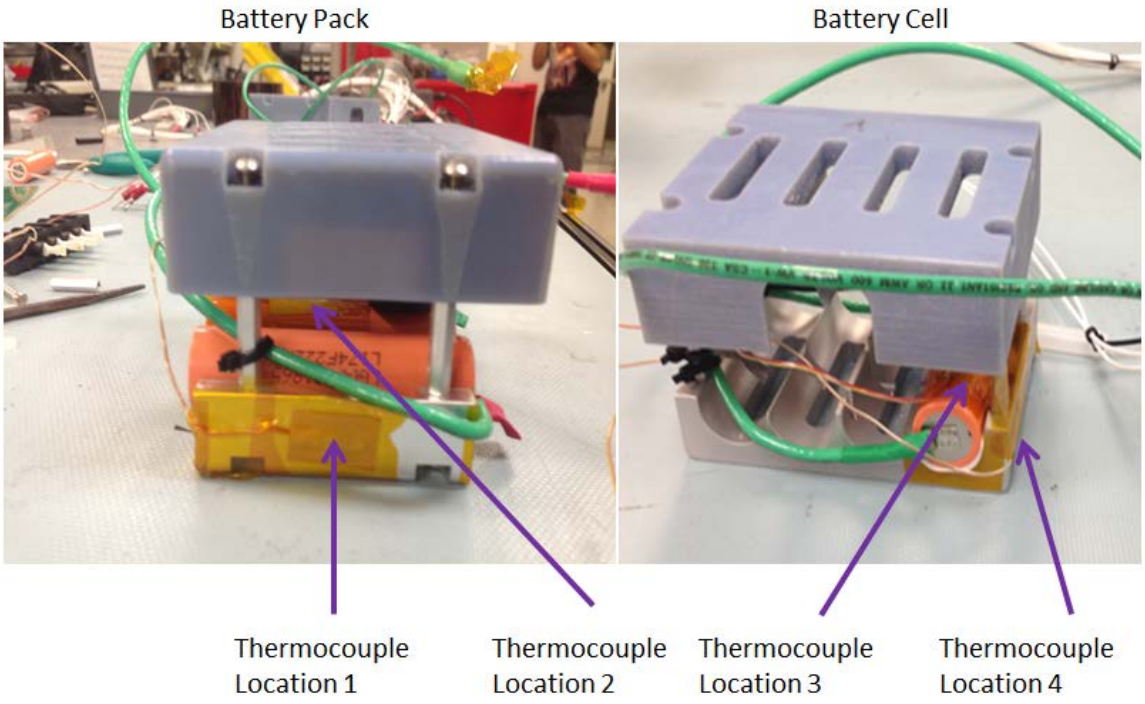

Figure 30: Thermocouple Locations

Thermistors, attached to the batteries near the same location as the thermocouples, act as the monitor sensors for the CADEX C8000 Battery Testing System. This separate temperature sensing system allows testing to be cut off or temporarily suspended if the battery cells exceed preset operating temperatures and will resume testing once the measured temperature from the thermistor has dropped 5°C below that limit. Figure 31 shows a depiction of the placement location of the thermistor setup inside the TVAC chamber. Figure 32 shows the placement location of the thermistors on the test article. The thermistors are secured to the battery cell through magnets located in the thermistor sensor head package. Figure 25 shows the placement location of both the Type K thermocouple and thermistor on the battery cell.

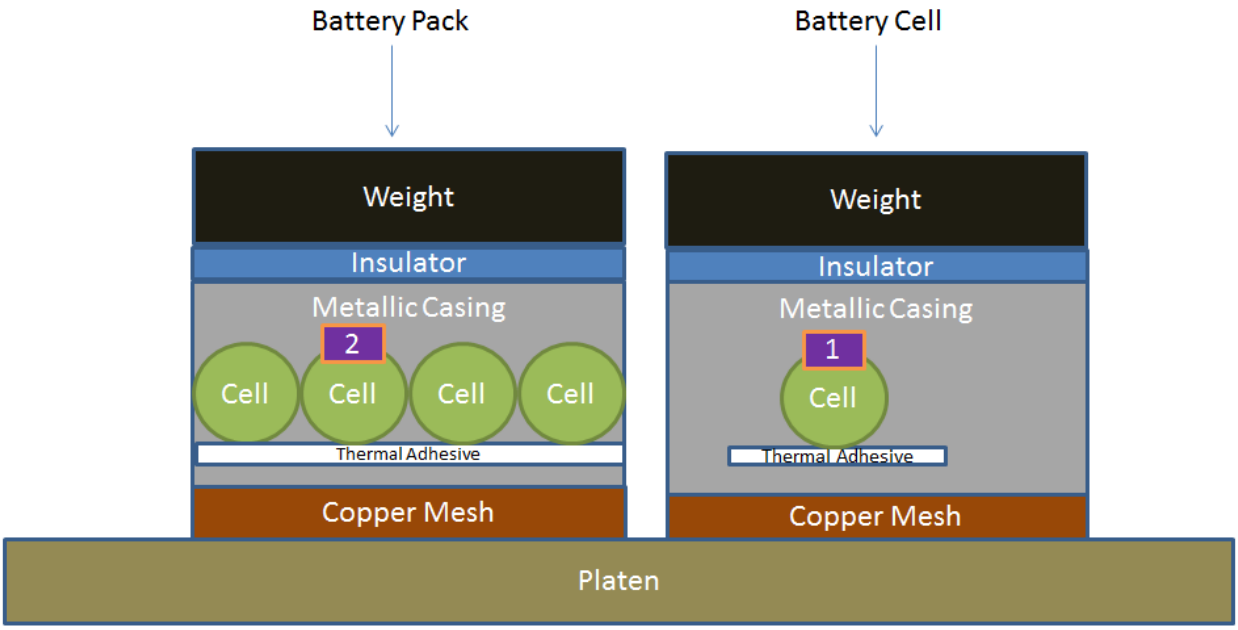

Figure 31: TVAC Chamber Thermistor Locations Numbers One and Two

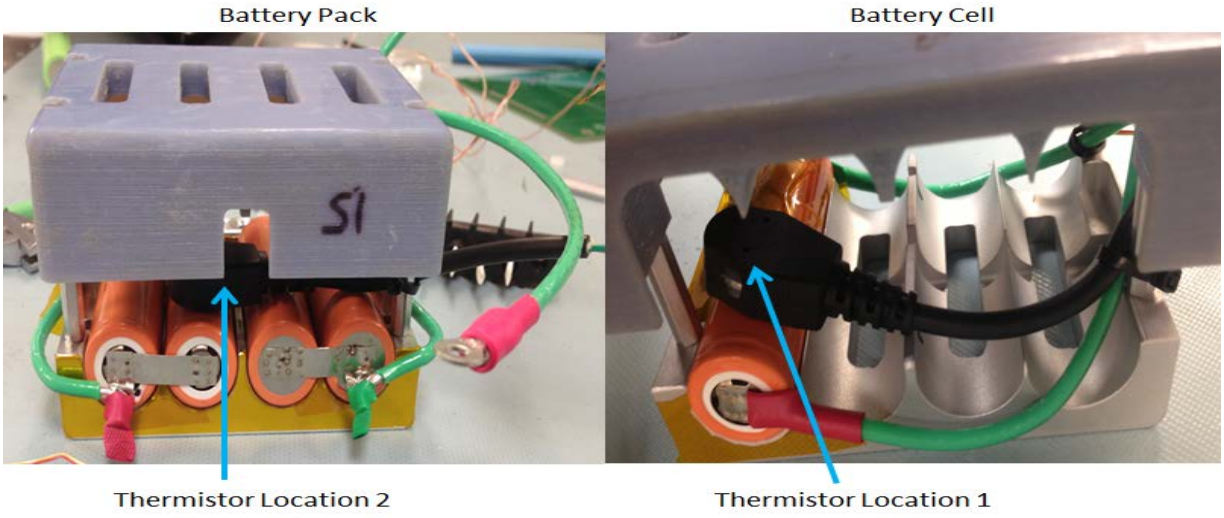

Figure 32: Thermistor Locations

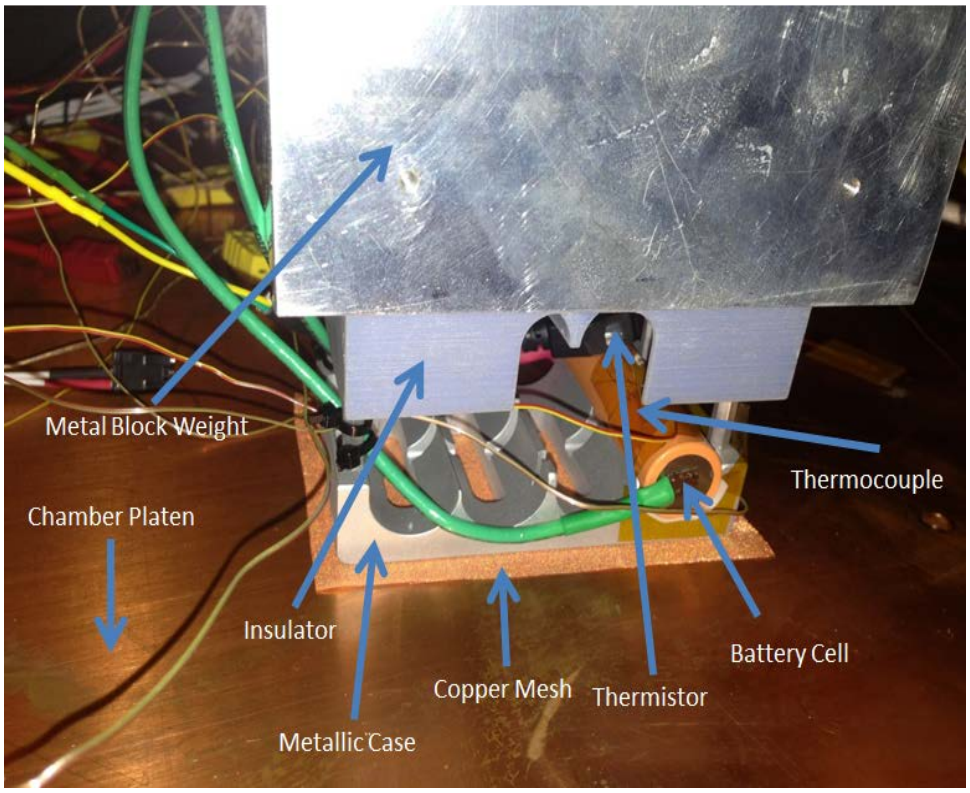

Figure 33: Battery Test Setup with Weight and Insulator

Figure 33 shows the insulator and a metallic block weight on top of the battery cell inside the TVAC chamber. The purpose of the weight insures full contact between the metallic case, copper mesh and the chamber platen. Figure 34 shows the full test setup inside the TVAC chamber without the weight on the battery pack and cell. The placement of the Type K thermocouple on the chamber platen is also shown in Figure 34. Lastly, Figure 35 shows the same image but with the metallic block weight on the battery pack and cell. Figure 35 is the final version of the test setup.

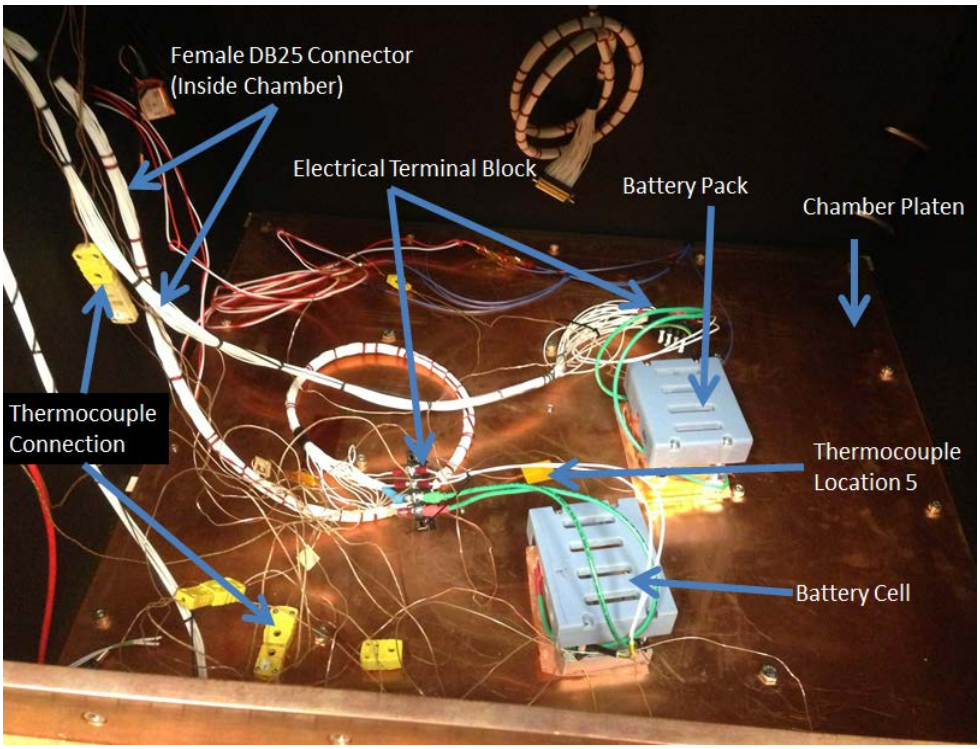

Figure 34: Test Setup inside Chamber without Metal Block Weight

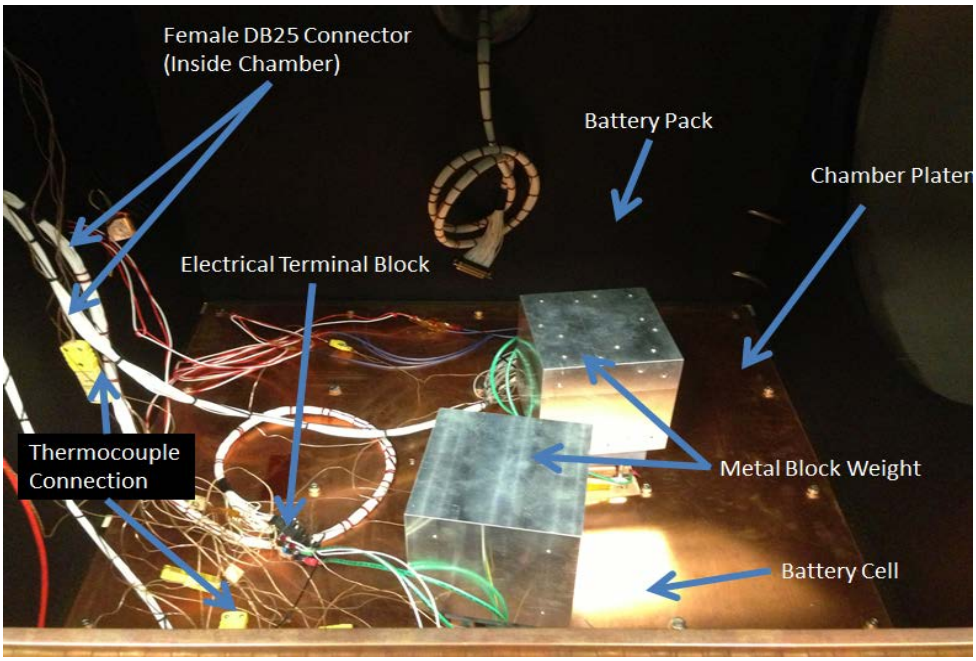

Figure 35: Test Setup inside Chamber with Metal Block Weight

3.3.2.2 TVAC Interfacing Connectors

The TVAC interfacing connectors are used to connect the battery cells to the CADEX C8000 Battery Testing System. Four female DB25 connectors are required to connect the battery cell stacks through the TVAC Chamber to the CADEX C8000 Battery Testing System. Each pin and wire on the female DB25 connectors is capable of handling a maximum current draw of 2 A. Multiple pins and wires are used to discharge the batteries at a current greater than the 2 A limit. The custom-made female DB25 is capable of drawing out a maximum 22 A; however, the limitation in current draw is 10 A per channel on the CADEX. Figure 36 shows one of two female DB25 connectors used outside the TVAC chamber that connects the CADEX C8000 to the TVAC chamber's male DB25 interfacing port shown in Figure 37.

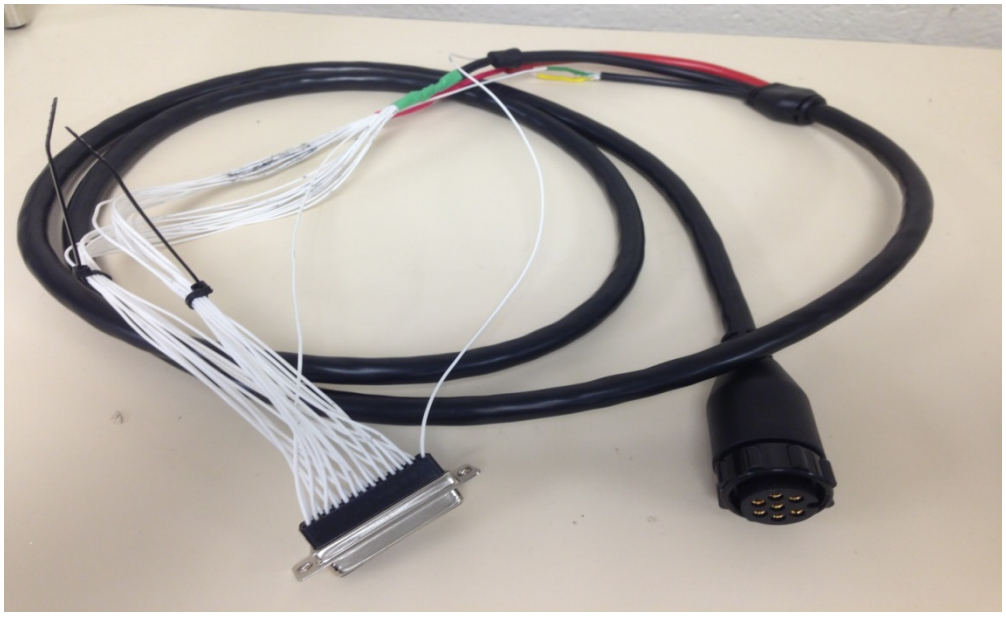

Figure 36: Custom Female DB25 Connector (Outside Chamber)

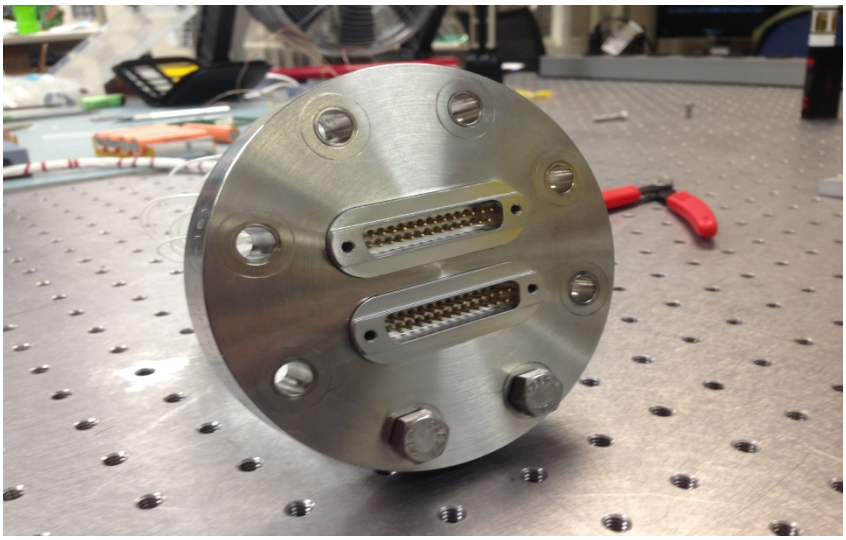

Figure 37: Male DB25 TVAC Interface Port

Figure 38 shows the connection between the female DB25 interface connector (outside the chamber) from the CADEX C8000 Battery Testing System to the male DB25 TVAC interface port.

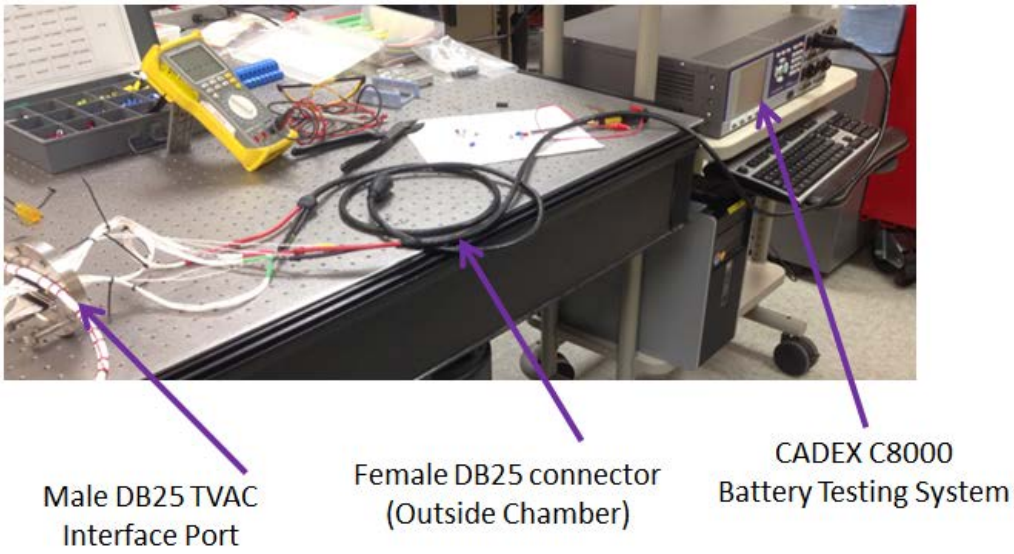

Figure 38: Outside TVAC Chamber Connection

Figure 39 shows the connection for inside the chamber from the battery cell to the male DB25 interface port using one of two female DB25 connectors (inside the chamber) and an electrical terminal block.

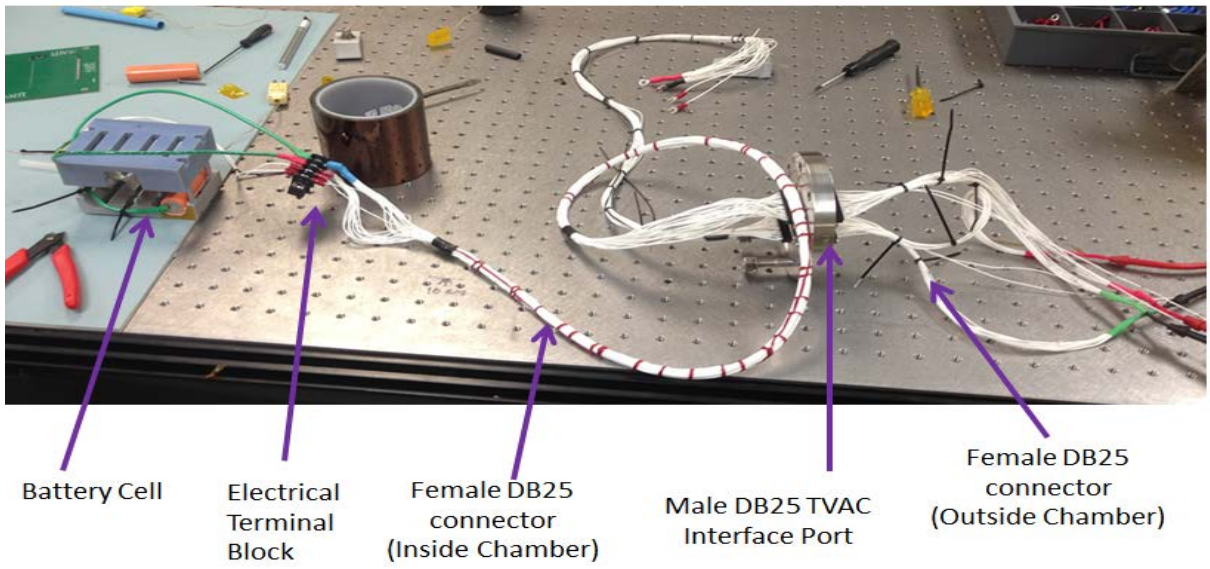

Figure 39: Inside TVAC Chamber Connection

The female DB25 connector used inside the chamber is connected to an electrical terminal block shown in Figure 40. One electrical terminal blocks is used for each test article. The electrical terminal block allows the user to connect the battery pack or cell to the male DB25 TVAC interface port without directly connecting wires from the battery to the female DB25 (inside chamber) connector.

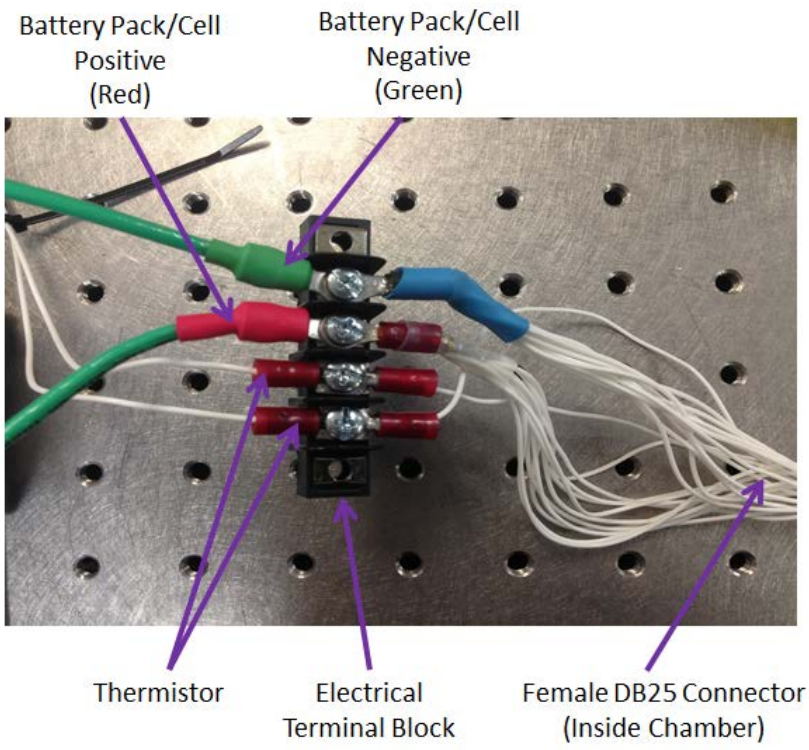

Figure 40: Electrical Terminal Block Connection

3.3.2.3 CADEX C8000 Battery Testing System Setup

The female DB25 coming out of the TVAC chamber are not directly connected to the CADEX C8000. The DB25 is connected to the CADEX C8000 through the CADEX C8000 Battery Port using a modified Power Port Cable shown previously in Figure 36. The unmodified Power Port Cable, shown in Figure 41, utilizes banana plugs and a temperature sensor to test battery cells. Modifications were made to the Power Port Cable by cutting off the V sense, V Drive and Temperature sensor.

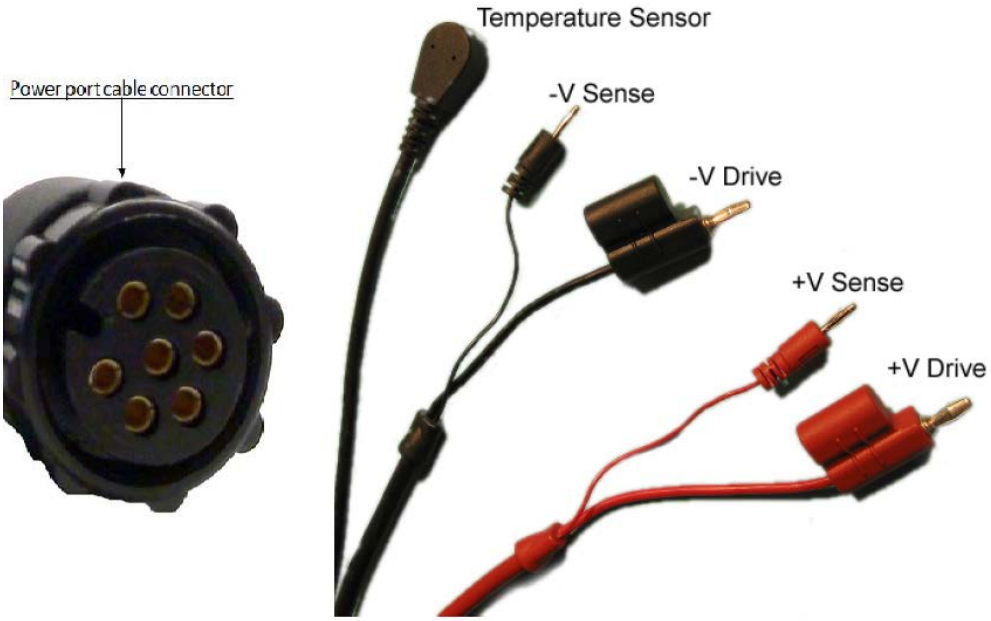

Figure 41: CADEX C8000 Power Port Cable [42]

The cut off temperature sensor is used inside the TVAC chamber and routed through the electrical terminal block and female DB25 (inside chamber) connector. The temperature sensor is the thermistor attached to the battery. It will be used to gather battery temperature data alongside the thermocouple and act as the temperature failsafe mechanism to stop testing if the battery surpasses its nominal operating limit.

3.4 TVAC Test Cases

Data collection from the individual battery cell test article, for model parameter extraction, and the battery pack, for comparative analysis, was conducted using the test cases presented in Table 2. Each test case will be tested at the following chamber temperatures: 0°, 25°, and 40° C. These test cases are presented in more rigorous detail in a test plan to ensure all data is gathered and recorded (see Appendix 1.0).

Table 2: Battery Test Cases

Test Name	Article Tested	Type of Test	Purpose
High Current (1.5C)	Battery Pack	Constant Current Charge and Discharge	Analyze Model Behavior for High Current Scenario
Normal Current (1C)	Battery Pack	Constant Current Charge and Discharge	Analyze Model Behavior for Normal Current Scenario
Low Current (0.5C)	Battery Pack	Constant Current Charge and Discharge	Analyze Model Behavior for Low Current Scenario
Dynamic (1C)	Battery Cell	Pulse Discharge	Parameter Estimation for Model

3.5 Parameter Estimation

Single Cell parameter estimation is conducted using the parameter estimation toolbox in Simulink to create lookup tables. HJGC created a model separate from the battery model presented earlier in Section 3.1 that uses the parameter estimation toolbox to generate lookup tables for the *Lithium Cell* mask [46]. This model, referred to as the *Parameter Estimation Model*, is a Simulink model presented in Figure 42. The *Parameter Estimation Model* is used to extract parameters from experimental data to be used in the modified HJGC model.

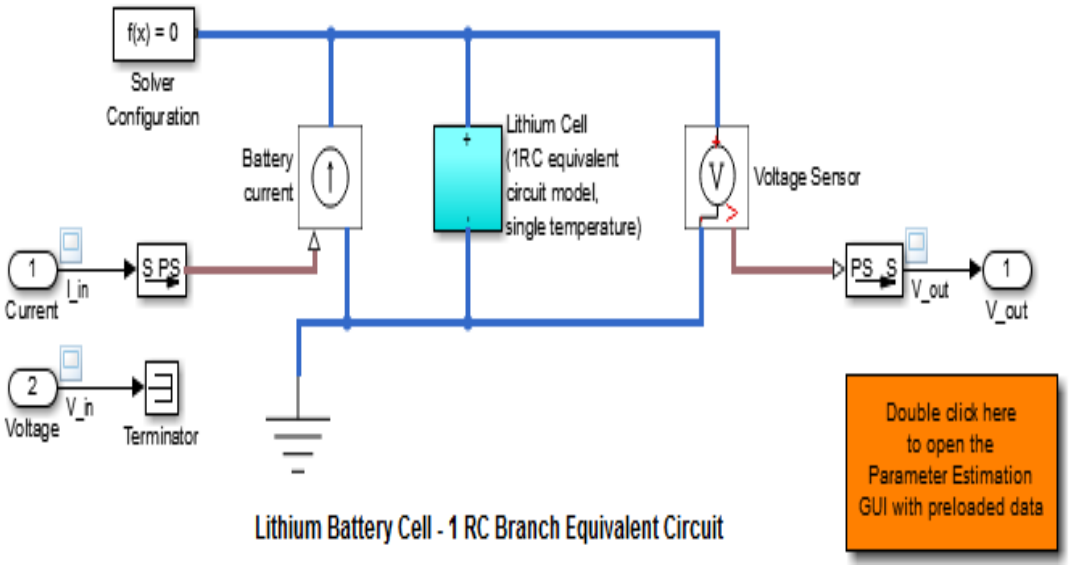

Figure 42: HJGC *Parameter Estimation Model* for *Lithium Cell* Mask [46]

The CADEX C8000 Battery Testing System stores experimental data in a text file. The text file is converted to a XLS file through Microsoft Excel and is imported into MATLAB. Test data from the Dynamic test case is used to estimate parameters and develop a lookup table. The lookup table will have parameters based on temperatures at 0°, 25°, and 40°C. The modified HJGC model interpolates between these the three lookup tables in generating an output. For more information on how to use the parameter estimation toolbox in MATLAB, refer to the Mathworks website [47].

The lookup tables generated from the *Parameter Estimation Model* are transferred into the initiation file to begin modeling the 2S2P battery pack. Comparison analysis between the modified HJGC Model and Low, Normal and High Current test cases is conducted in the next chapter to validate the model.

3.6 Summary

This chapter presents the methods used to modify the HJGC model, collect data for parameter estimation, and insert parameters estimated into the modified HJGC model. The following chapter will comparatively analyze the modified HJGC model and experimental data for the 2S2P battery pack.

IV. Analysis and Results

This chapter will first present the results of the experiment, the estimated parameters in the form of a lookup table, and the model output using the estimated parameters. Then, comparisons between model and experimental results will be analyzed, in an attempt to determine the level of accuracy of the HJGC model for battery pack performance prediction.

4.1 Experimental Results of Battery Cell

The experimental results for the dynamic test cases conducted at 0°, 25° and 40° C are shown in Figs. 43, 44, and 45, respectively. The experimental testing procedure for the dynamic test case was derived from HJGC where a battery cell was tested under partial discharge and rest cycles [38] . For the dynamic test case presented in this research, the battery cell was charged to full capacity then discharged at increments of 6 minutes at a rate of 1C in vacuum ($< 10^{-3}$ Torr). Each 6 minute discharge increment equates to a nominal 10% depth of discharge reduction. The discharge time for each 10% depth of discharge was calculated using coulomb counting, which is integrating current over time to determine the amount of charge leaving the battery. After each 6 minute discharge, the battery cell was allowed to rest for 30 minutes. Using 6 minutes as the time constant, the rest period of 30 minutes was calculated using the relationship between the time constant of a RC circuit, and resistance and capacitance. It takes 4 (24 minutes) to 5 (30 minutes) time constants for the battery cells to reach a steady state [30]. The purpose of the 30 minute rest period, also referred to as the relaxation period, is to capture the recovery effects of the battery cell. The experimental results are used with the HJGC *Parameter Estimation Model* to extract the RC parameters for the HJGC Battery Model.

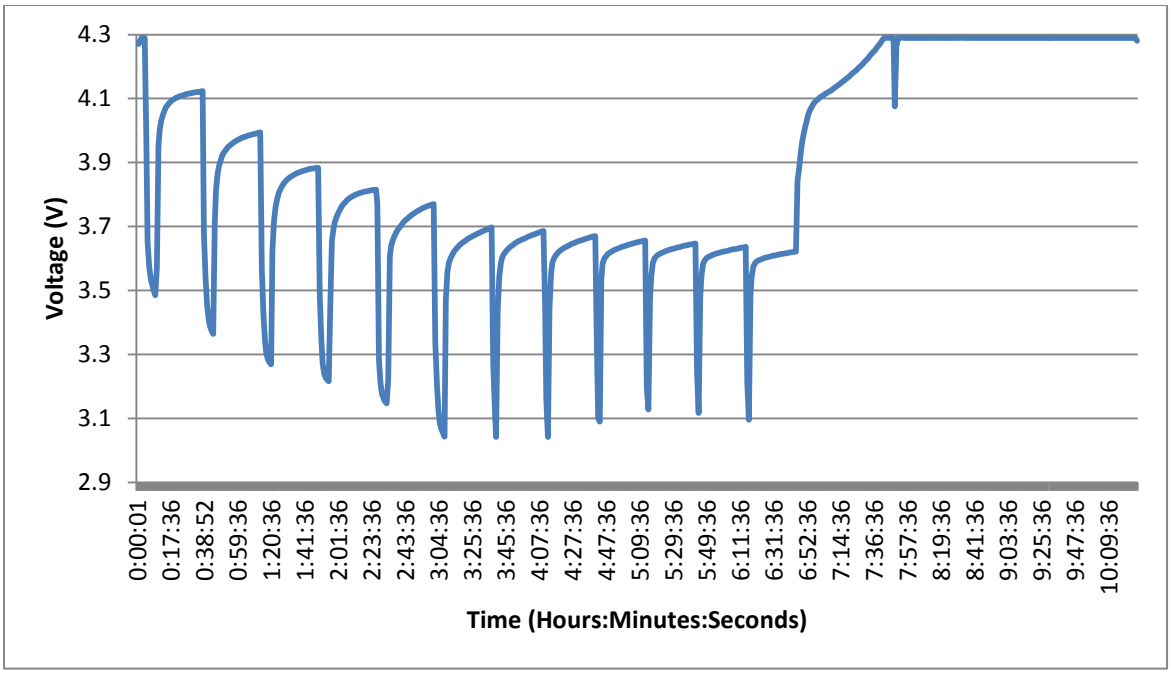

Figure 43: Dynamic Test Case Result: 0° C

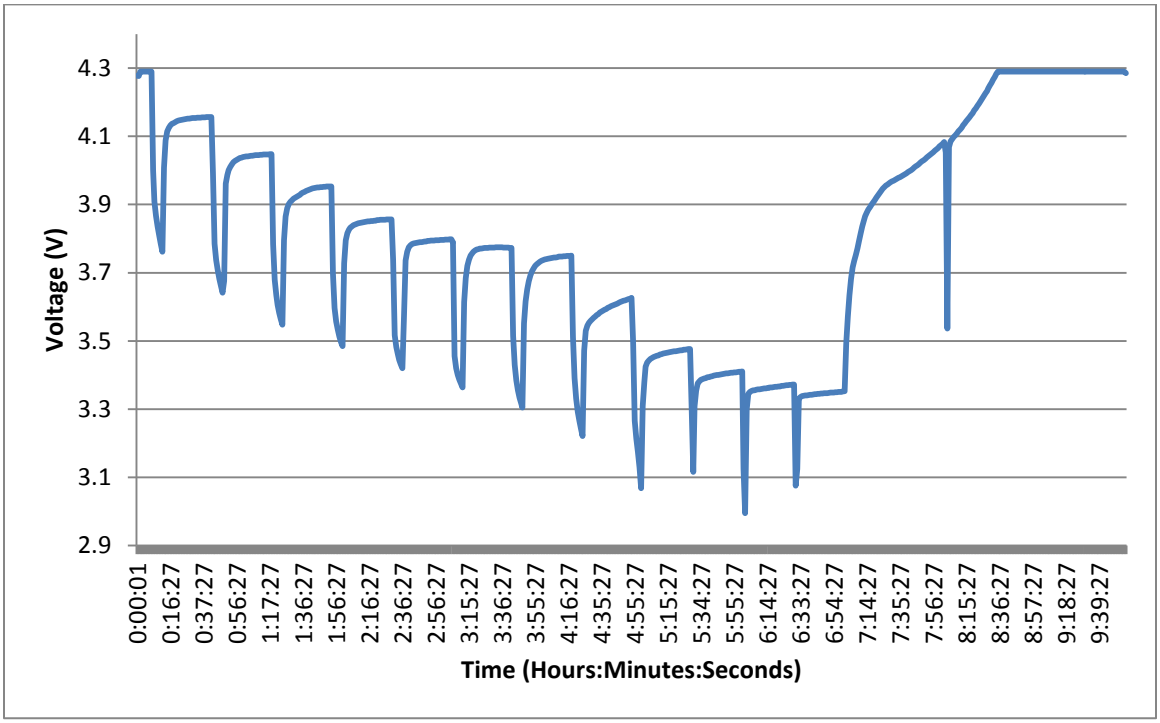

Figure 44: Dynamic Test Case Results: 25° C

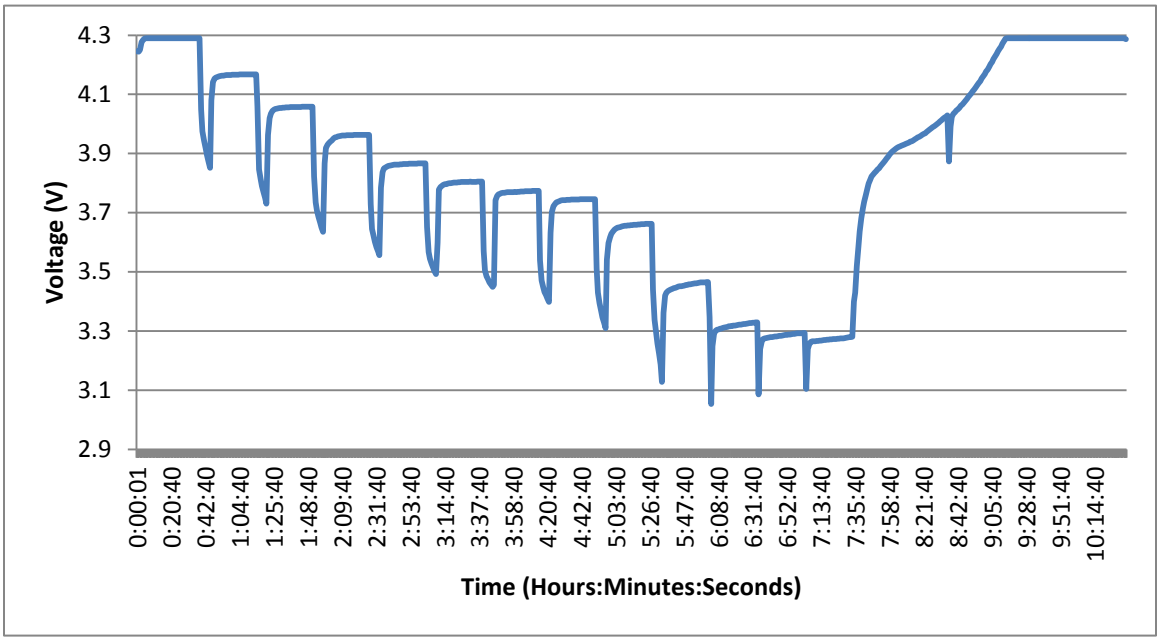

Figure 45: Dynamic Test Case Results: 40° C

4.2 Parameter Extraction

4.2.1 Calculation of Initial RC parameters

An initial guess is required to utilize the HJGC *Parameter Estimation Model*. The initial guess was calculated using the equations shown in Figure 46. ΔV_0 is the drop in voltage from the initial application of current. ΔV_0 is calculated as the difference between the initial battery cell voltage and the relaxed battery cell voltage. ΔV_∞ is the difference in voltage from the battery at the end of a discharge pulse to the voltage of the battery at the end of a relaxation period. T is the rest period for the battery cell to reach the relaxed voltage. For this experiment, the rest period is set to 30 minutes or 5 time constants. Calculating initial parameters of voltage, R0, R1, and C1 from these equations are only valid for an equivalent circuit model using one RC network [30].

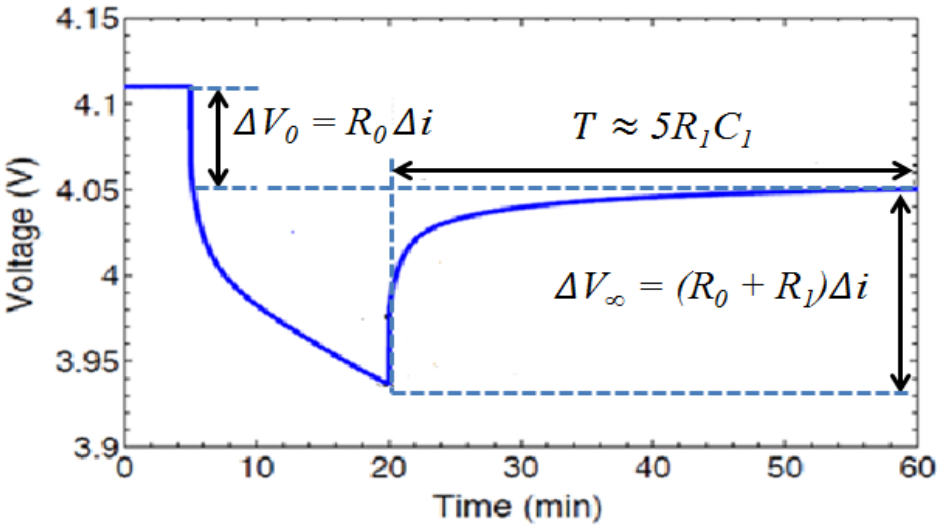

Figure 46:Parameter Estimation Initial Guess Formula [30]

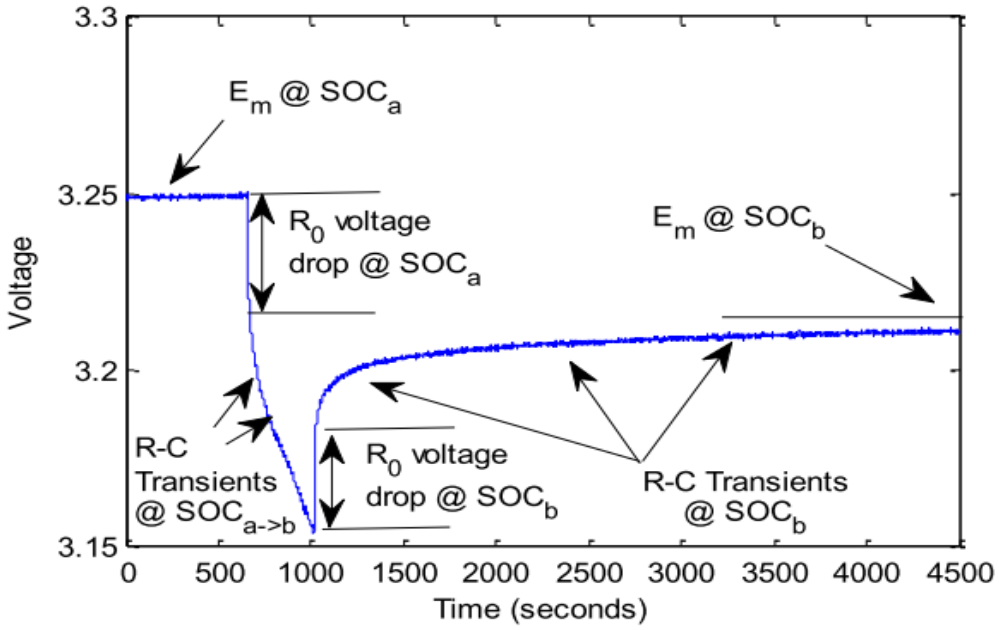

Figure 47: Extraction of Parameters from a Single Pulse[48]

Figure 47 supplements the formulas shown in Figure 46 by providing a visual of the relationship between the pulse discharge curve and each RC parameter. E_m represents the electromotive force or voltage at each state of charge (*SOC*). R_0 is the ohmic resistance and *R-C*

Transients represent the parameters of the RC network based off the number of RC circuits in the Thevenin Equivalent Circuit Model. The initial guess of the parameters are presented in Tables 3, 4, and 5.

Table 3: Initial Guess 0° C Lookup Table

SOC (%)	E_m (V)	R0 (Ω)	R1 (Ω)	C1 (F)
100	4.29	0.059643	0.168214	2140.127
90	4.123	0.046071	0.178929	2011.976
80	3.994	0.039643	0.179643	2003.976
70	3.883	0.024286	0.189643	1898.305
60	3.815	0.016071	0.206429	1743.945
50	3.77	0.026071	0.2075	1734.94
40	3.697	0.003929	0.226071	1592.417
30	3.686	0.005714	0.218571	1647.059
20	3.67	0.005	0.192857	1866.667
10	3.656	0.003214	0.182143	1976.471
0	3.647	0.003929	0.181429	1984.252

Table 4: Initial Guess 25° C Lookup Table

SOC (%)	E_m (V)	R0 (Ω)	R1 (Ω)	C1 (F)
100	4.29	0.05	0.085714	4200
90	4.15	0.035714	0.103571	3475.862
80	4.05	0.035714	0.103571	3475.862
70	3.95	0.035714	0.096429	3733.333
60	3.85	0.017857	0.117857	3054.545
50	3.8	0.007143	0.139286	2584.615
40	3.78	0.010714	0.146429	2458.537
30	3.75	0.046429	0.092857	3876.923
20	3.62	0.05	0.089286	4032
10	3.48	0.046429	0.061071	5894.737
0	3.411	0.021786	0.088214	4080.972

Table 5: Initial Guess 40° C Lookup Table

SOC (%)	E_m (V)	R0 (Ω)	R1 (Ω)	C1 (F)
100	4.29	0.042857	0.071429	5040
90	4.17	0.039286	0.078571	4581.818
80	4.06	0.035714	0.082143	4382.609
70	3.96	0.032143	0.078571	4581.818
60	3.87	0.021429	0.092857	3876.923
50	3.81	0.014286	0.1	3600
40	3.77	0.007143	0.117857	3054.545
30	3.75	0.032143	0.092857	3876.923
20	3.66	0.067857	0.053571	6720
10	3.47	0.05	0.05	7200
0	3.33	0.014286	0.057143	6300

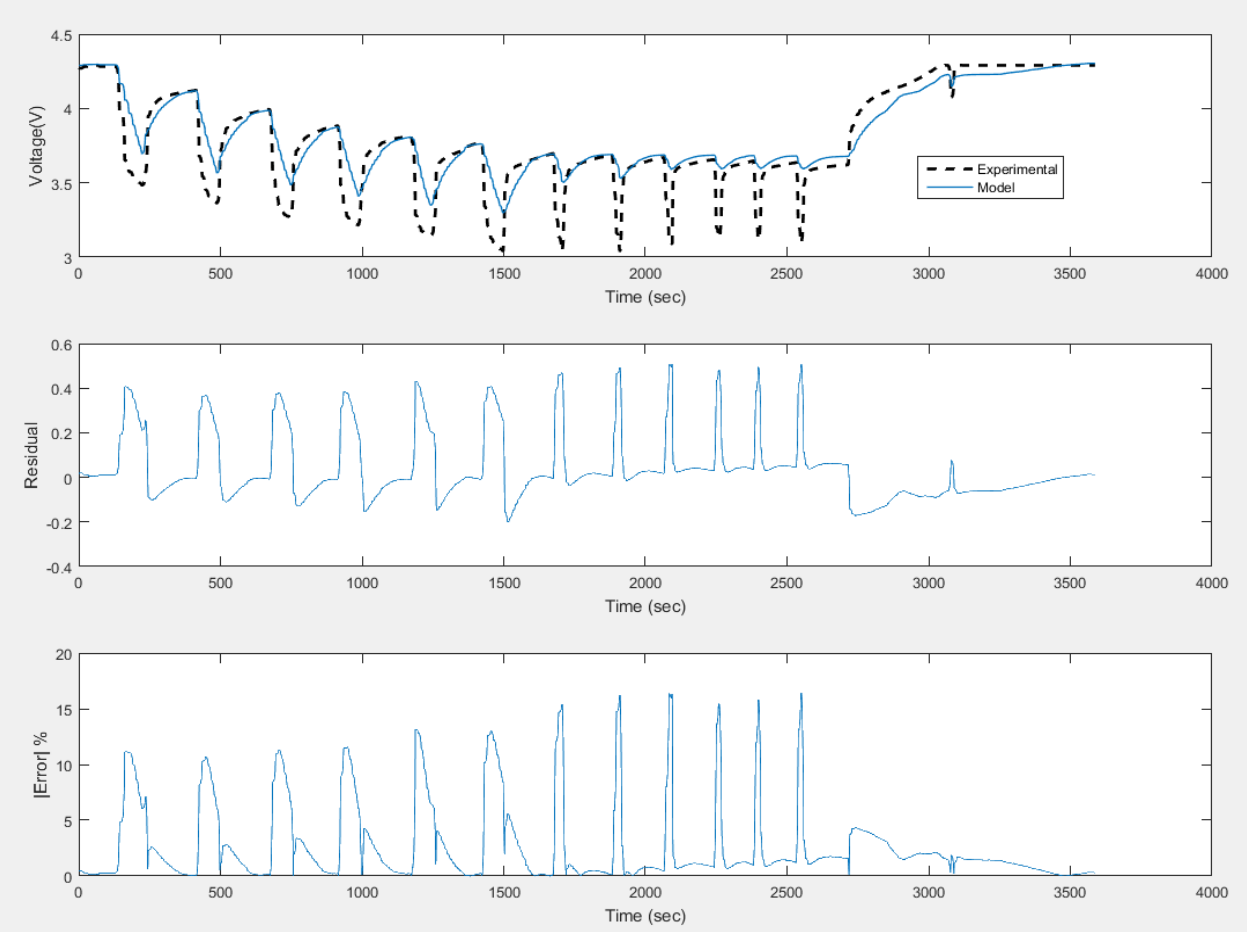

Figure 48: Parameter Estimation Analysis using Initial Guess at 0° C

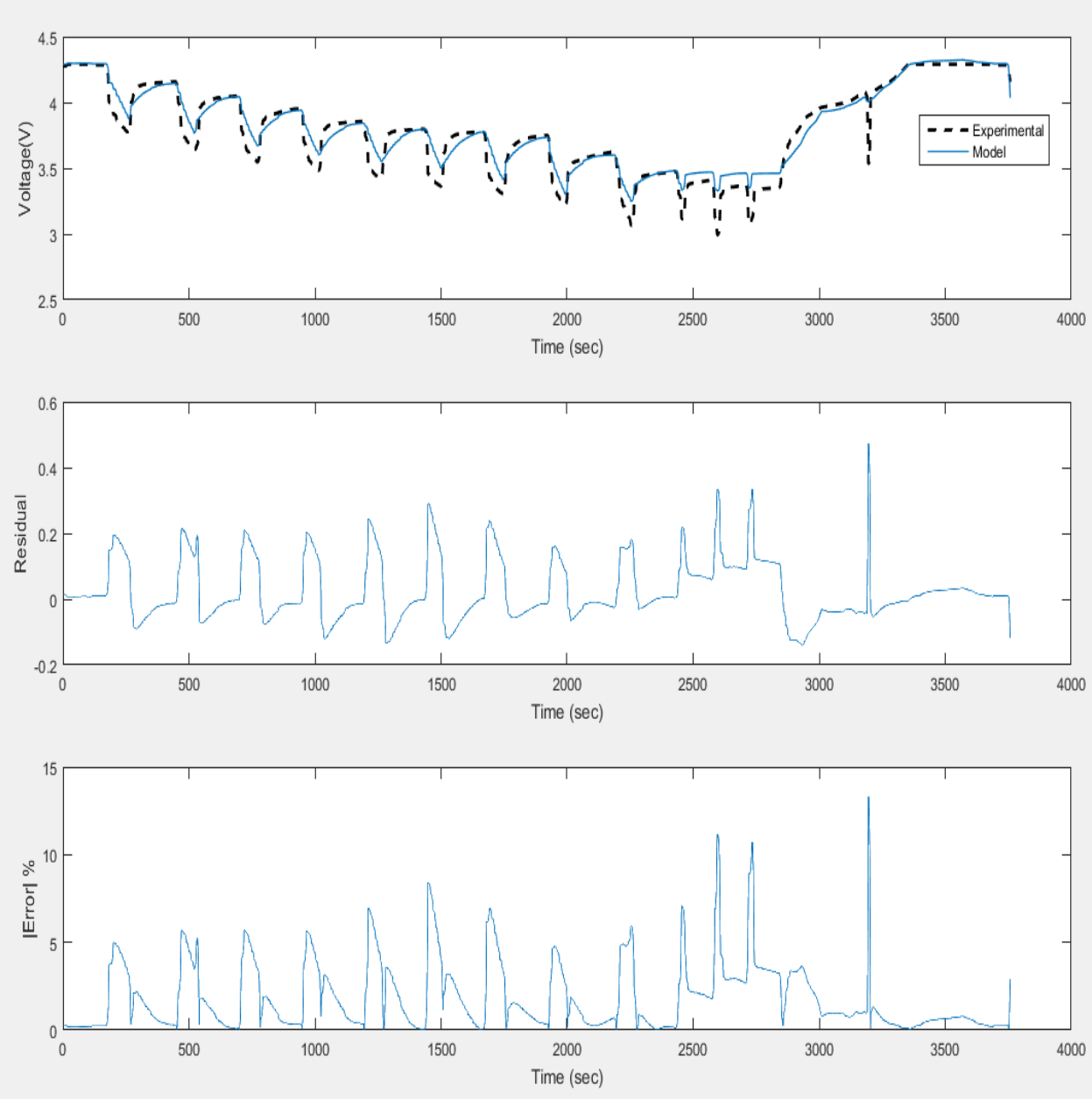

Figure 49: Parameter Estimation Analysis using Initial Guess at 25° C

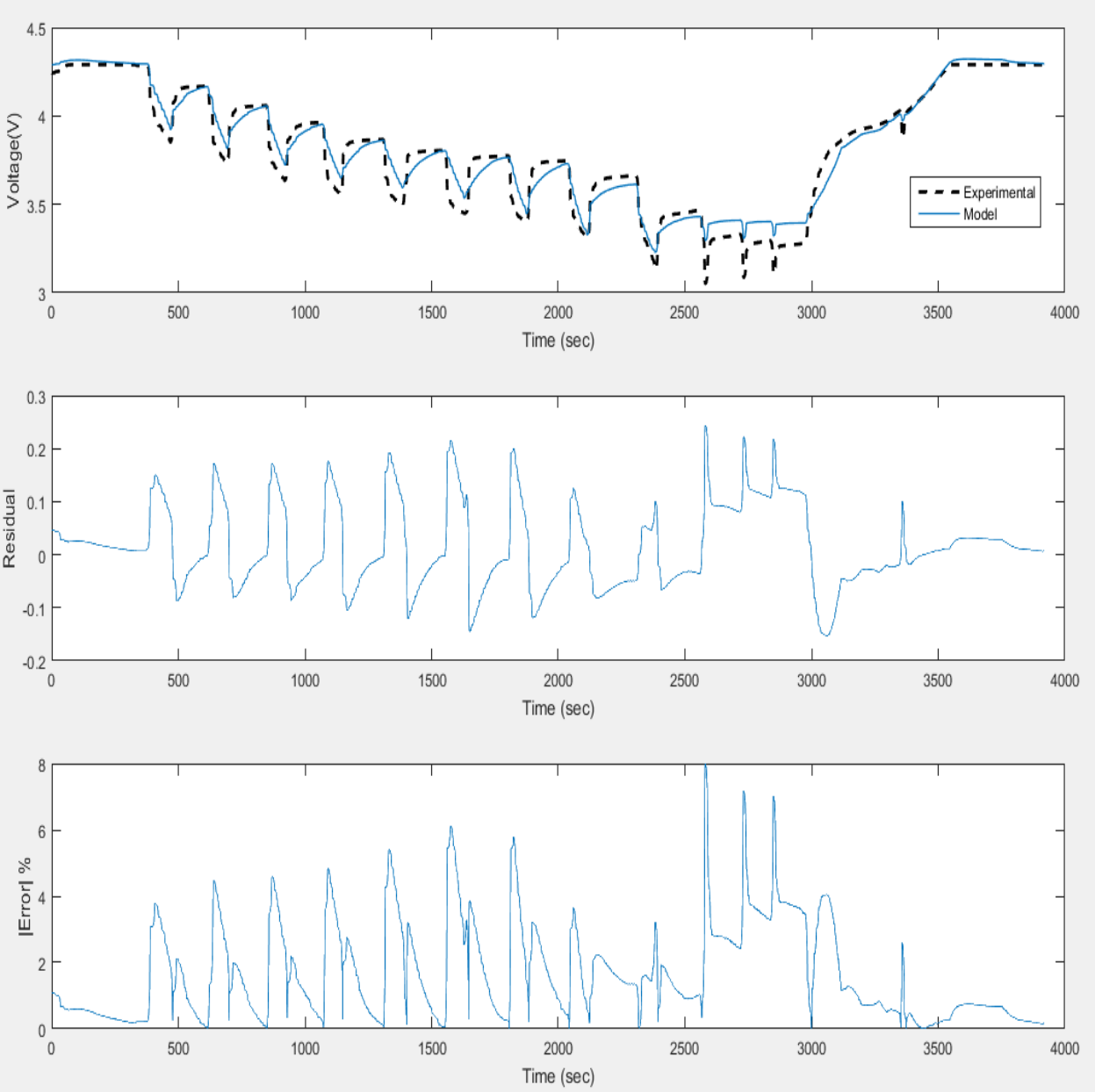

Figure 50: Parameter Estimation Analysis using Initial Guess at 40° C

Using just the initial guess, the HJGC *Parameter Estimation Model* had difficulty matching the experimental results. The maximum absolute percent error, shown in Figs. 48, 49, and 50, between the experimental results and the *Parameter Estimation Model* using the initial guess was 16.39%, 13.32% and 7.98% for the 0°, 25° and 40° C case respectively. The average

absolute percent error across the entire dataset was 2.75%, 1.87%, 1.67% for the 0°, 25° and 40° C case respectively. As a comparison to expected results between model and experimental data, HJGC was able to achieve a maximum absolute error under a 2%, shown in Figure 51 , using a 1RC network Thevenin Equivalent Circuit Model, so one could expect a similar level of agreement with the results presented here. HJGC does not present an average absolute percent error for comparison.

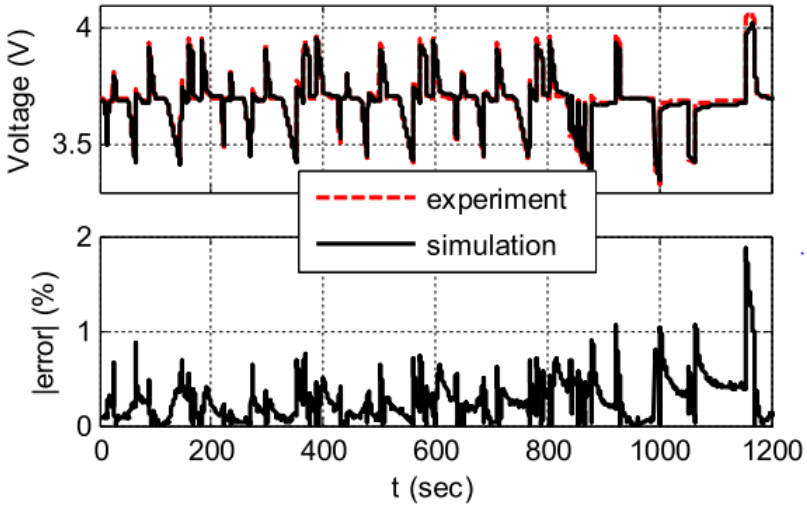

Figure 51: HJGC presents an Absolute Error Percent Under 2% [38]

The initial guess using the equations presented in Figure 46 is shown to not be a valid method estimate of the RC parameters. Observation of Figs. 48, 49, and 50 shows that the parameters, R0, R1, and C1, calculated for the *R-C Transients* section of the model is the likely cause for error.

To estimate parameters where the simulated model matches the experimental data, a trial and error method of adjusting each set of parameters was used. To minimize the error between simulated and measured data, the voltage, ohmic resistance and RC parameter were adjusted by

manually inputting guesses for each parameter until the simulated plot closely matched the measured curve. The trial and error method showed that the resistances R0 and R1 affects the drop in voltage, the Em or voltage affects the relaxation voltage, and C1 affects the curvature of the *RC Transient* section of the plots.

As stated previously, a maximum absolute error under 2% between experimental data and the single cell model is presented by HJGC [38]. Using the trial and error method, the simulated HJGC *Parameter Estimation Model* was able to achieve a maximum absolute error percentage, shown in Figs. 52, 53, and 54, of 12.97 %, 10.68% and 5.90% for the 0°, 25° and 40° C case respectively. The average absolute percent error across the entire dataset using the trial and error method was 0.79%, 0.81%, 0.54% for the 0°, 25° and 40° C case respectively.

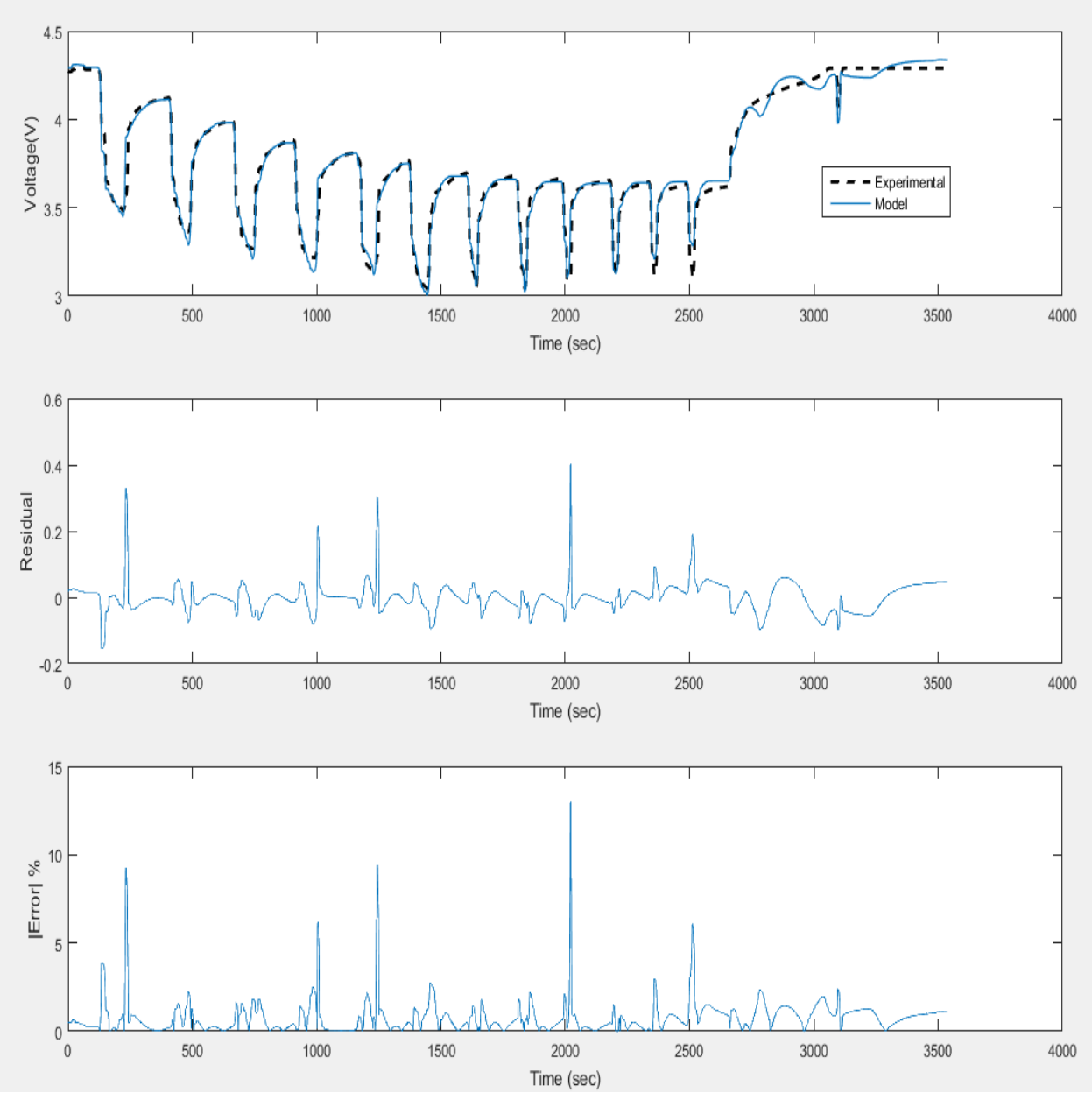

Figure 52: Parameter Estimation using Final Values at 0° C

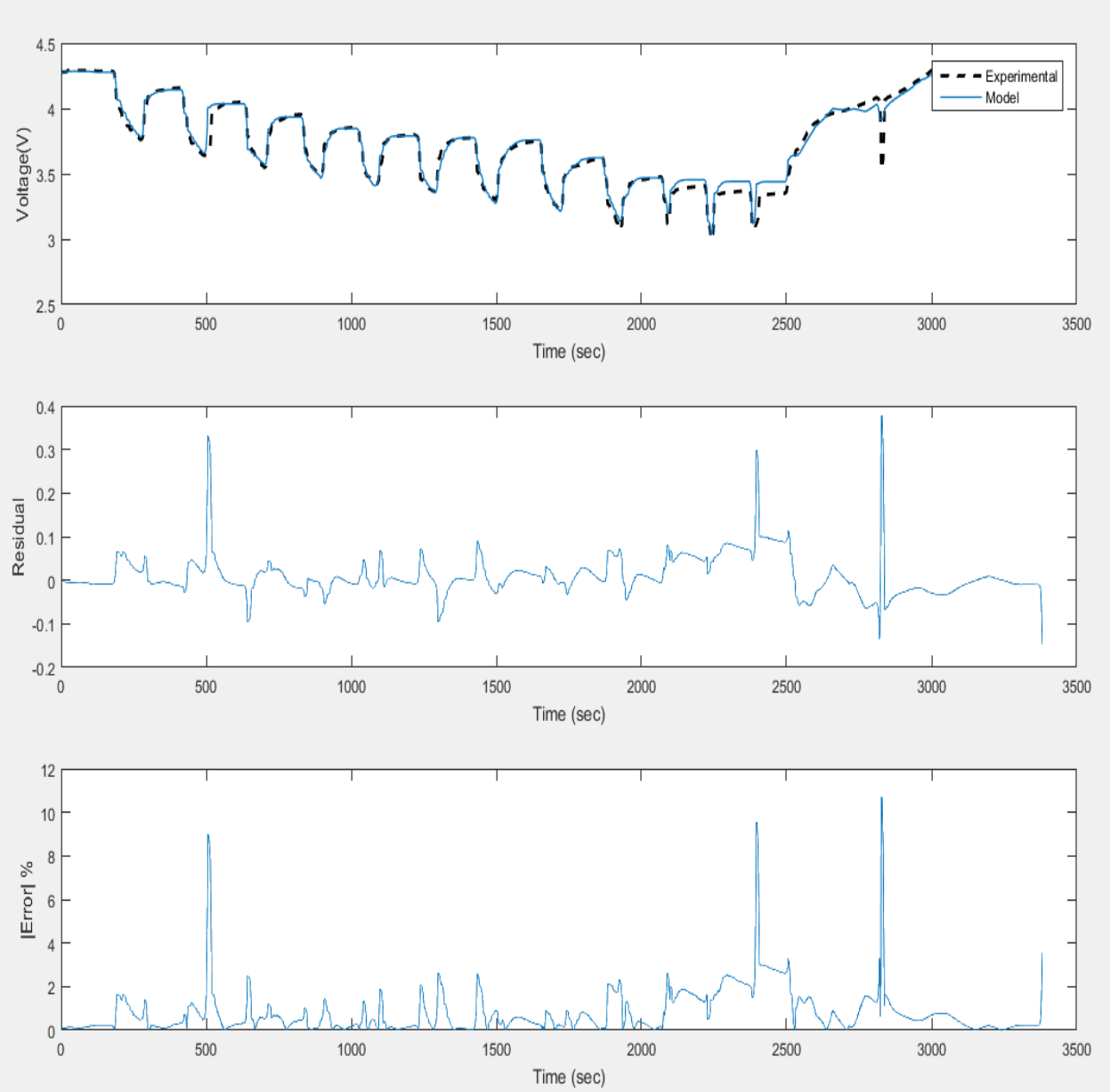

Figure 53: Parameter Estimation using Final Values at 25° C

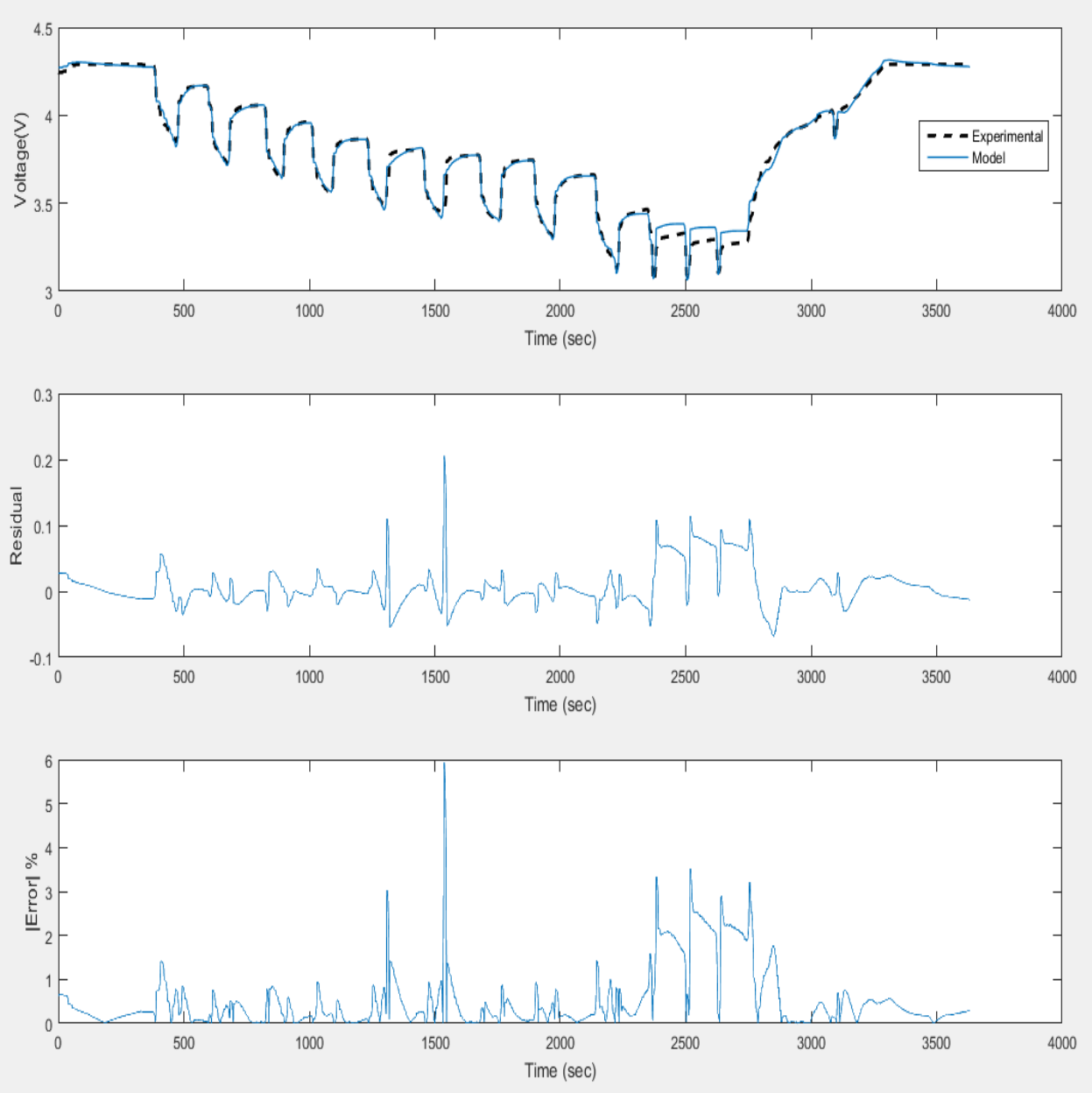

Figure 54: Parameter Estimation using Final Values at 40° C

The simulation and measured voltage plots, shown in Figs. 52, 53, and 54, are shown to be not identical, especially around the *R-C Transients* section of the curve. Suggestions for improvement in the level of accuracy in estimated parameters would be to research alternative methods used to estimate parameters or through adding more RC networks into the Thevenin Equivalent Circuit Model. To more closely match the measured data, HJGC used three RC

networks to achieve an even higher accuracy of 0.002% maximum error relative to the nominal voltage, 3.6 V, of their battery cell [48]. Using more RC networks is an area of future research that should be explored for a more accurate battery model overall. Overall, the trial and error method implemented to estimate the parameters was able to bring the average absolute error, for all 3 temperature cases, below 1%.

The final lookup table for each test case generated by the HJGC *Parameter Estimation Model* using the trial and error method is presented in Tables 6, 7, and 8. These values are later used in the HJGC Battery model and are the same parameters that produced the simulated curve shown in Figs. 52, 53, and 54.

Table 6: Final Lookup Table Values at 0° C

SOC (%)	E_m (V)	R0 (Ω)	R1 (Ω)	C1 (F)
100	4.2925	0.23826	0.43293	4770.6
90	4.1156	0.15978	0.12066	2333.8
80	3.9877	0.16857	0.10116	2299.2
70	3.8719	0.12662	0.1266	965.28
60	3.8194	0.19193	0.045512	6805.1
50	3.7569	0.1474	0.19697	1505.7
40	3.684	0.12183	0.11493	965.57
30	3.6371	0.15365	0.18211	783.12
20	3.67	0.001	0.015	750
10	3.656	0.001	0.001	750
0	3	0.001	0.001	200

Table 7: Final Lookup Table Values at 25° C

SOC (%)	E_m (V)	R0 (Ω)	R1 (Ω)	C1 (F)
100	4.273	0.069784	0.058319	1001.8
90	4.1477	0.10013	0.018314	8831.6
80	4.039	0.12346	0.010624	3518.2
70	3.9414	0.097481	0.040095	1703.4
60	3.8536	0.067991	0.070611	1000.1
50	3.7913	0.078285	0.056201	1004.6
40	3.776	0.052089	0.10985	1004.2
30	3.7717	0.092989	0.079407	1877.4
20	3.6456	0.094768	0.063552	3604.2
10	3.4682	0.051122	0.092277	1006.9
0	3.3627	0.29928	0.00021	1000.5

Table 8: Final Lookup Table Values at 40° C

SOC (%)	E_m (V)	R0 (Ω)	R1 (Ω)	C1 (F)
100	4.2716	0.069503	0.046078	7118
90	4.1729	0.088688	0.041087	3068
80	4.0619	0.095503	0.027136	8110.4
70	3.9625	0.079509	0.042271	3448.1
60	3.8679	0.077609	0.026512	3326.5
50	3.8218	0.087043	0.06007	6243.6
40	3.7761	0.086588	0.050126	3571.1
30	3.7571	0.093051	0.029761	6292.3
20	3.6907	0.09868	0.037837	3874.7
10	3.5426	0.094264	0.010629	3336.4
0	3.171	0.1245	0.080597	7008.3

4.3 Comparison between Experimental Test (2S2P) and Model Prediction

Figure 55 shows the comparison between the experimental data and the model's output voltage for the battery pack at 0° C for the Low, Normal and High current test scenarios. Upon close inspection of the voltage, the model tracks the experimental data accurately with an average absolute error of 1.26% for the entire data set. Error peaks right between the end of

discharge and the beginning of charge portions of the graph shown at times 62110 (Low), 309300 (Normal), and 542100 (High) sec. The model starts to deviate and peak in error by a maximum absolute error of 20.56, 21.79 and 21.25% from the experimental data for the Low, Normal and High test case scenarios during these times. This deviation can be attributed to factors such as temperature or the estimated RC parameters.

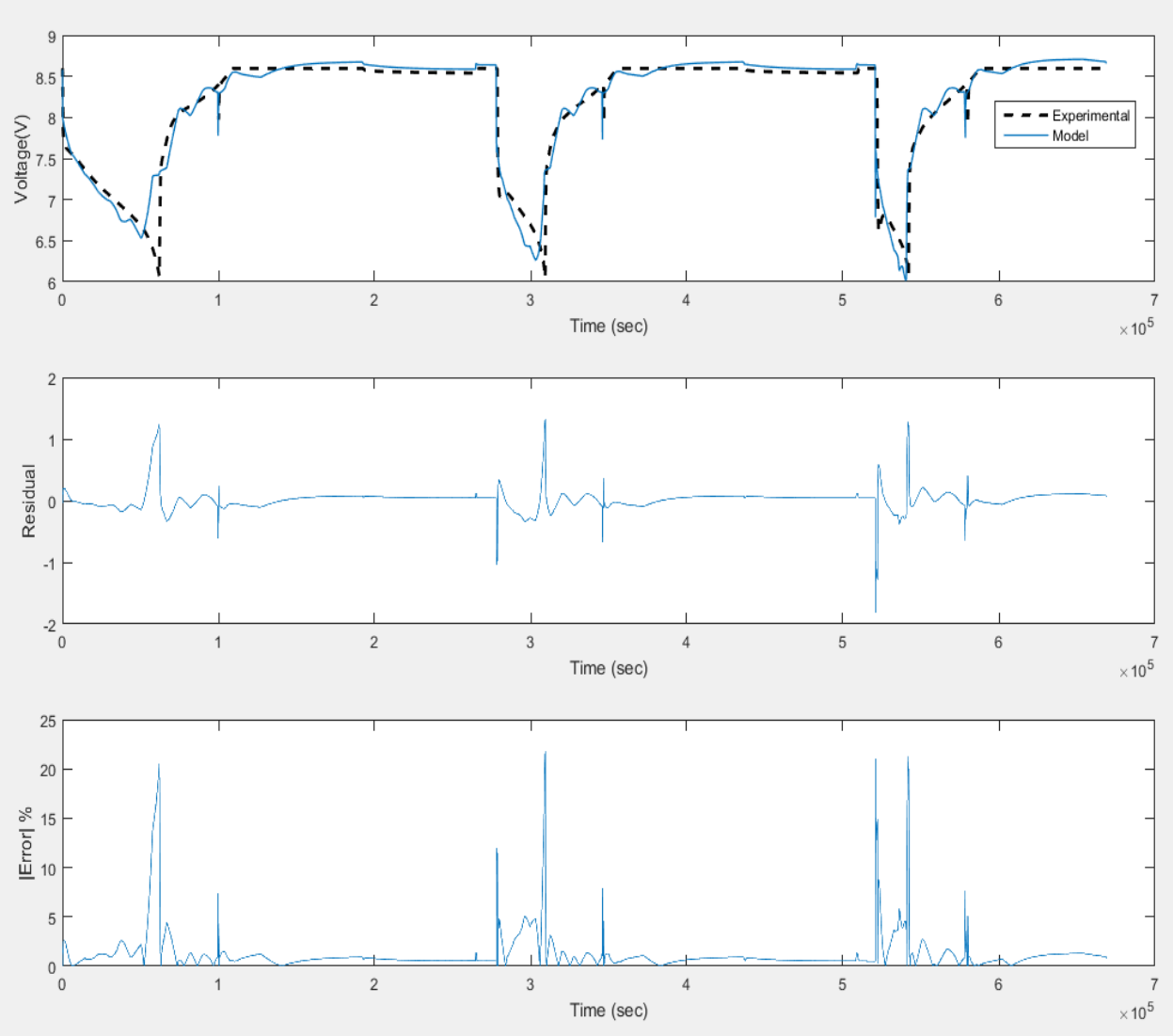

Figure 55: Battery Pack Voltage Analysis at 0° C

One factor is due to the thermal model not accurately predicting the battery pack's temperature at lower states of charge, which will be analyzed in a later section. Alternatively, deviations based on the estimated RC parameters for the single cell causes an overall deviation in the battery pack model. However, there is no observable correlation between the maximum absolute error from the estimated parameter model using the final lookup table values, shown in Figure 52 and the battery pack model, shown in Figure 55. The battery pack model is able to track the fully charged, 8.6 V, steady-state portions of the experimental data with an absolute error between 0.5 to 0.8%. The difference between the charge portion of the model and experimental data is due to using only discharge data to model both charge and discharge. The difference in voltage between charge and discharge in a battery cell is likely caused by the effects of hysteresis. Hysteresis is the lag, or jump in voltage, that occurs between the initial applications of current during a charge or discharge cycle. Hysteresis is a common attribute of battery cells that is not accounted for in this model due to the use of a single RC circuit and using only discharge data. Incorporating hysteresis effects into the model is an area that is suggested for future work. HJGC incorporates the hysteresis effect through the addition of more RC networks which is shown to provide an overall higher accuracy [48].

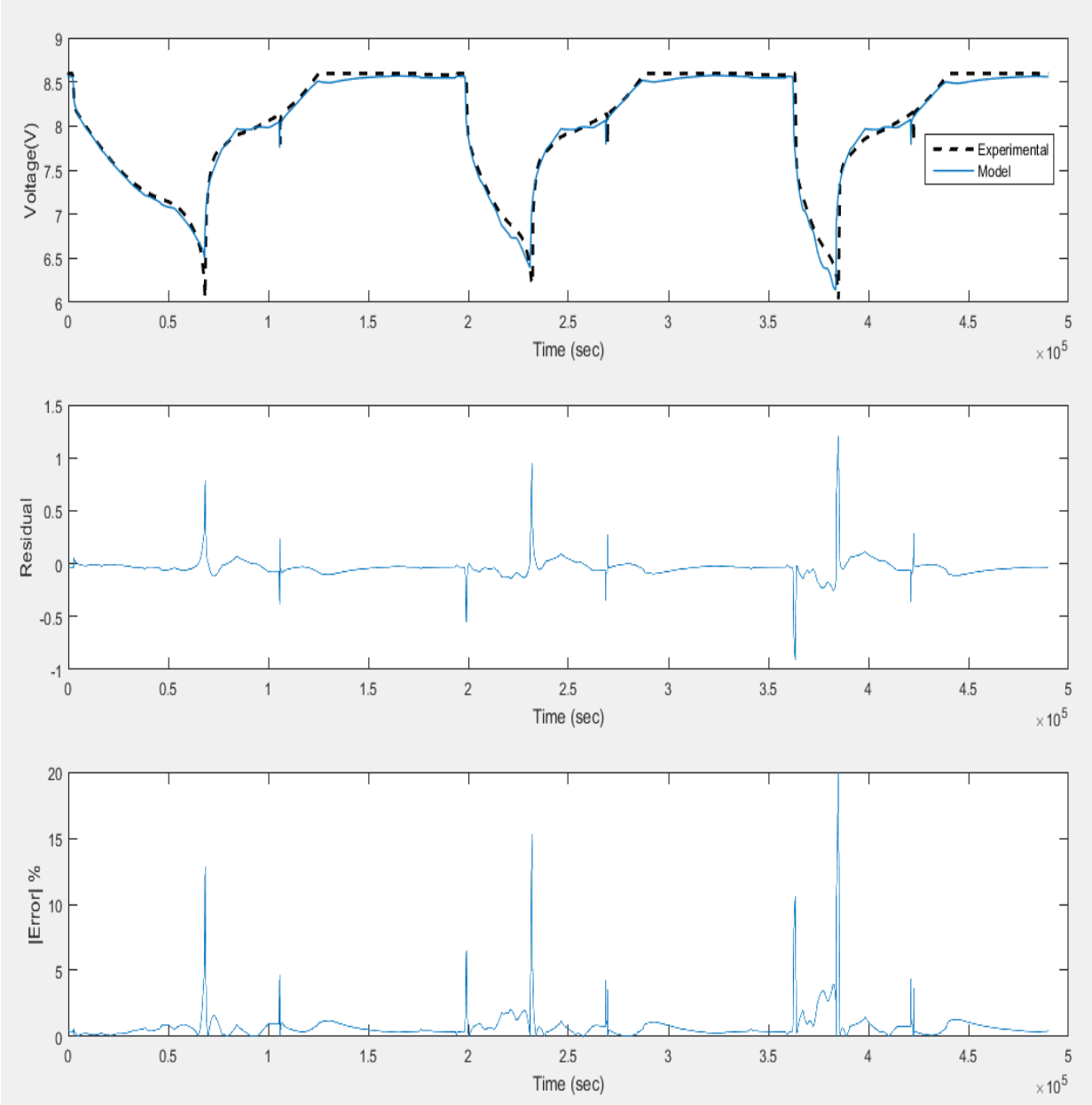

Figure 56: Battery Pack Voltage Analysis at 25° C

Figure 56 shows the comparison between the experimental data and the model's output voltage for the battery pack at 25° C. For the 25° C case, the model tracks the experimental data more accurately than the 0° C case with an average absolute error of 0.76%; however, deviation is still apparent near the end of discharge and the initiation of charge portion of the curves at times 68410 (Low) ,232100 (Normal), and 380000 (High) sec. The maximum absolute errors at

these times are 12.87, 15.31, and 19.93% for the Low, Normal and High current test case scenarios respectively. For the 25° C case at time 68410 sec for the Low current test scenario, the battery pack model outputs a voltage of 6.6 V whereas the experimental data voltage is at 6 V at a 0 % state of charge. The likely cause for deviation is due to the estimated E_m parameter in the final lookup table presented in Table 7 where at a 0% state of charge, the voltage is approximately 3.3 V. This shows that the battery model is highly dependent on the estimated parameters. The role of temperature also plays an effect in the model's output voltage as the Normal and High test case scenario's discharge current were able to reach closer to 6 V. The likely correlation is due to the interpolation of Em values between the 25° C and the 40° C lookup table used for the Normal and High test case sections of the graph at times 232100 and 380000 sec respectively. The Normal and High test case sections of the graph reach temperatures closer to 40° C; thus these sections use parameters based on the lookup table for the 40° C case.

Figure 57 shows the comparison between the experimental data and the model's output voltage for the battery pack at 40° C. As with the 25° C case, the 40° C case is consistent in matching the experimental data for the entire dataset, with an average absolute error of 0.61%. As with the 0° and 25° C case, maximum absolute error peaks at the end of discharge and the beginning of charge sections of the curve at times 89530 (Low), 302700 (Normal), and 908100 (High) sec. The maximum absolute errors associated at these times are 12.47, 13.98, and 14.27% for the Low, Normal, and High test case scenarios respectively. Although not as apparent in the 0° or 25° C case, the 40° C case shows that the model is not able to predict instantaneous drops in voltage due to current spikes caused by the OhmTest function on the CADEX C8000 Battery Testing System that is used to measure the internal resistance of the battery during the charging

portion of the curves. The instantaneous spikes are located at times 127400, 340900, and 957800 sec which resulted in an absolute maximum error of 7.66, 11.4 and 16.19 % respectively.

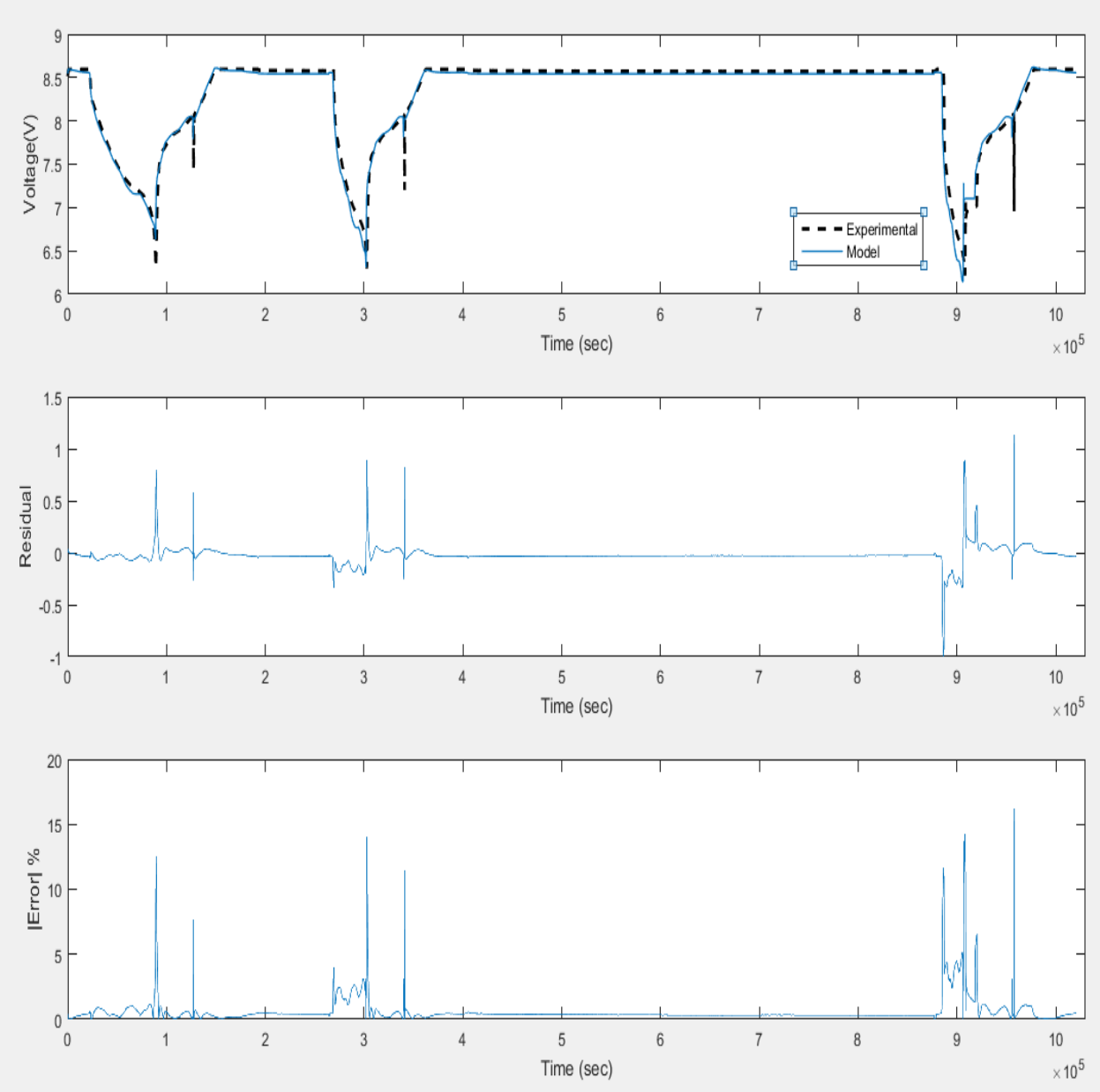

Figure 57: Battery Pack Voltage Analysis at 40° C

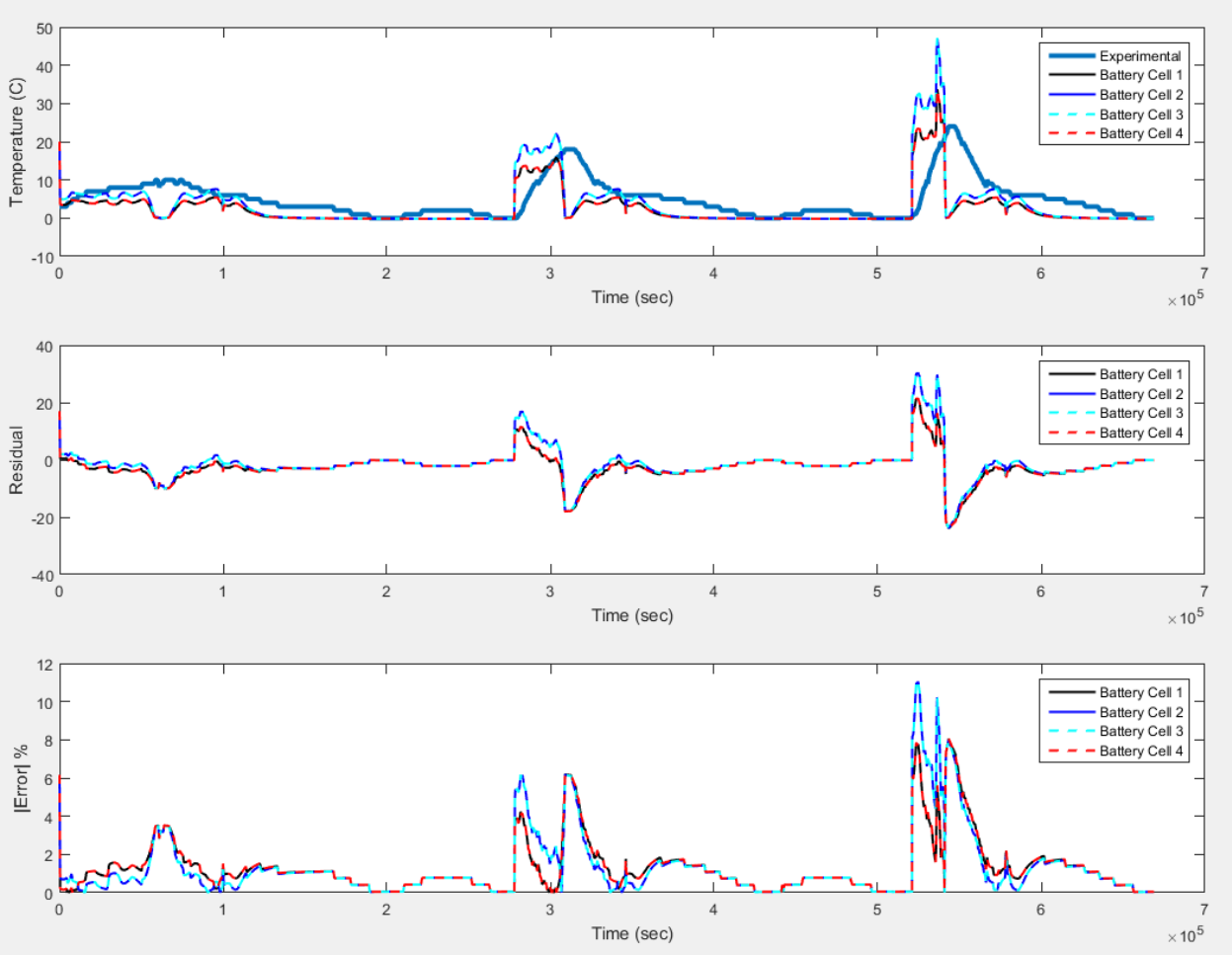

Figure 58: Battery Cell Temperature Analysis at 0° C

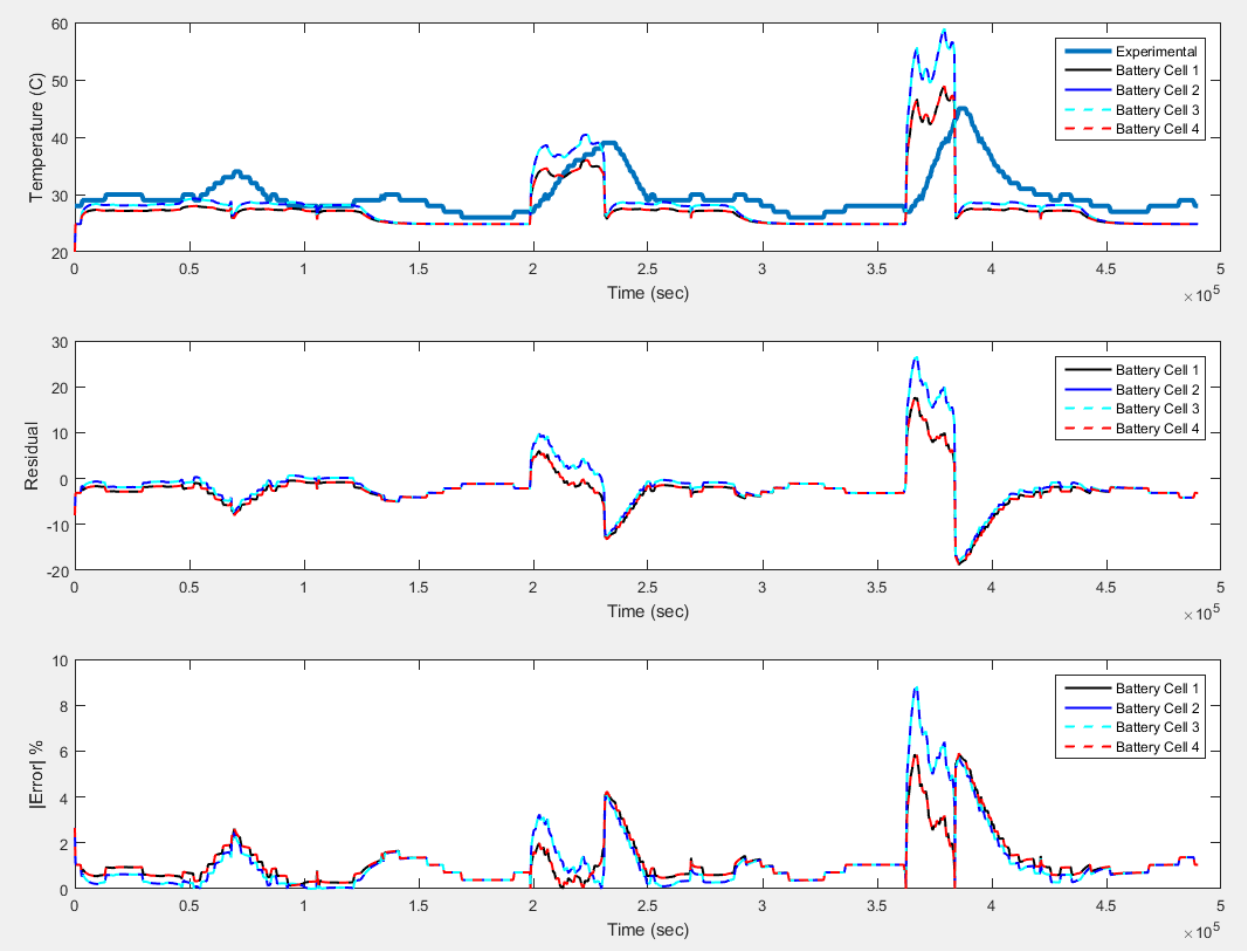

Figure 59: Battery Cell Temperature Analysis at 25° C

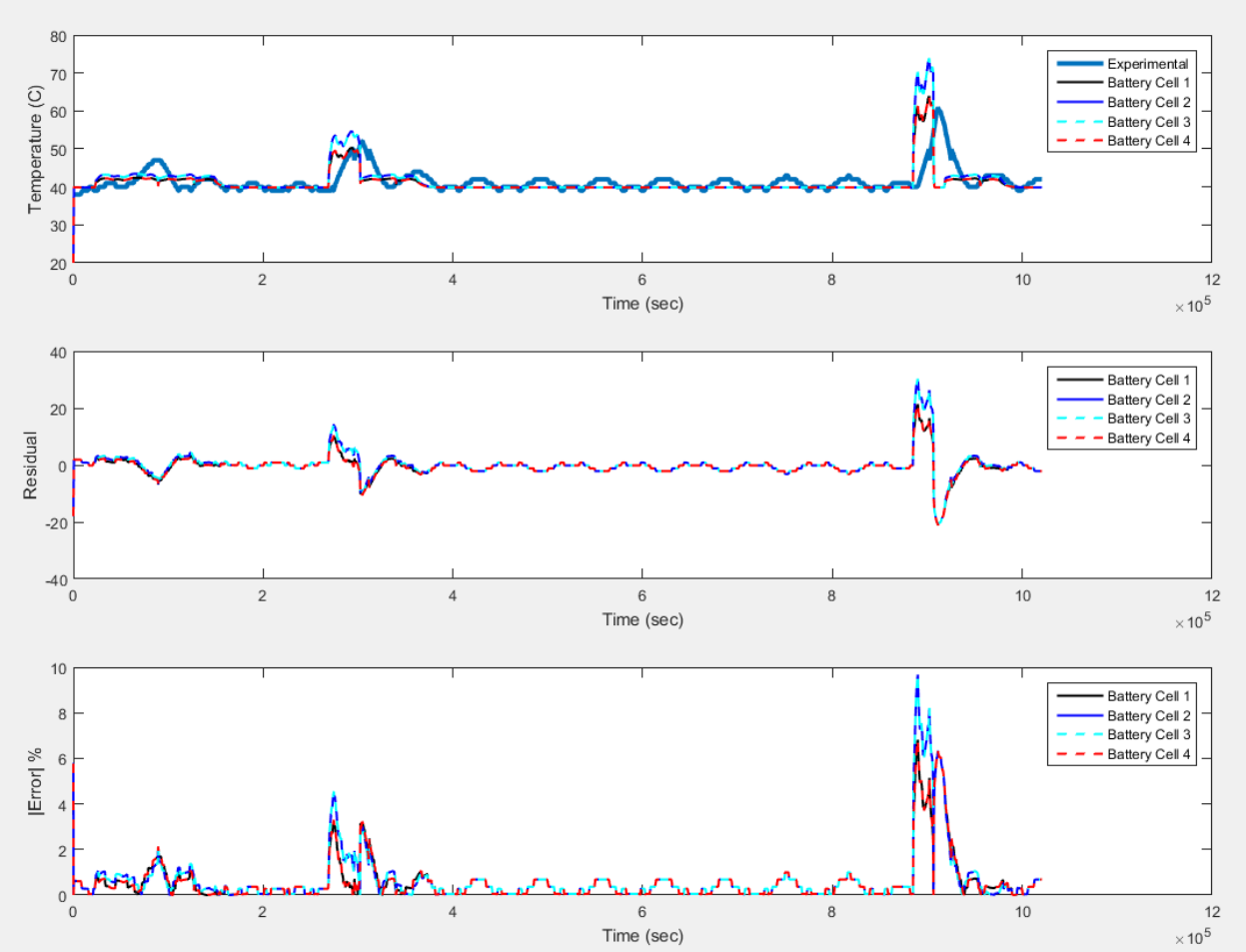

Figure 60: Battery Cell Temperature Analysis at 40° C

Figs. 58, 59, and 60 compares the temperature output from each battery cell in the modified HJGC Battery model with the experimental data collected from the thermistor. The model shows an average absolute error of 1.2901, 1.1682, and 0.5799% for the 0°, 25°, and 40° C test case respectively. This average absolute error directly corresponds to battery cells 1 and 4 which represent the outer most cells in the battery pack. The average absolute error for battery cells 2 and 3 representing the inner most cells are 1.2921, 1.1659, and 0.6750% for the 0°, 25°, and 40° C test case respectively. Similar to the comparison of voltage between the model and experimental data for the battery pack, shown previously in Figs. 55, 56, and 57, the model

struggles to match the experimental temperature during the transition period between end of discharge and beginning of charge. For the 0° C case at Low, Normal and High test scenarios, the peak absolute errors, shown in Figure 58, are 3.53, 6.20, and 11.05 % at times 63910 (Low), 309100 (Normal), and 524700 (High) sec respectively.

The peak absolute errors for the 25° C case, shown in Figure 59, are 2.61, 4.23, and 8.81 % at times 69610, 232100, and 367300 sec respectively. Lastly, the peak absolute errors for the 40° C case, shown in Figure 60, are 2.13, 4.55, and 9.67 % at times 89320,274400, and 889800 sec respectively. These error peaks are a result of the thermal model predicting rapid temperature rise versus the experimental data showing a gradual rise in temperature. The likely cause of such an error is due to the thermal model's assumption of convection heat transfer between the cell and the environment rather than conduction and radiation. Although not visible in the 0° and 25° C case, the 40° C case shows oscillations in the absolute error and the experimental data. This oscillation is due to the PID controller for the temperature monitor of the TVAC chamber. Future work should explore the effects of the thermal model on the prediction of the battery pack. As a result of the thermal model deviating at these specific time points, it is likely a cause for error between the battery pack model output voltage and experimental data, shown previously in Figs. 55, 56, and 57.

In the modified HJGC model, the thermal model was not modified from the original HJGC model and uses the assumptions of battery cell temperature based on convective heat exchanged between the cell and the environment. Further investigation of the thermal effects between the battery cell, the environment and the internal battery temperature through conduction and radiation should be conducted to improve the thermal aspect of the modified

HJGC model. The modified HJGC model does not include any loses due to radiation and conduction and should be an area future work.

4.4 Analysis of Temperature Data

The thermocouple data presented in this section is temperature data collected during the experimental test process from 0° C to 40° C to 25° C and back down to 0° C. Figure 61 shows only the measured temperature data between the cell, the metallic case, and the chamber platen. Oscillation of the chamber platen temperature is observed and is caused by the PID controller of the temperature monitor on the TVAC chamber. For the single cell experiment, the metallic case and chamber platen temperature closely agree which indicates low thermal resistance between the case and the platen due to the presence of copper. The average deviation in temperature between the Chamber Platen and Single Battery Cell is 1.83° C with a maximum deviation of 17.78° C throughout the entire dataset. The average deviation in temperature between the Chamber Platen and Metallic Case is 0.638° C with a maximum deviation of 8.575° C. The average deviation in temperature between the Single Battery Cell and Metallic Case is 1.47° C with a maximum deviation of 10.32° C. When the battery cell is undergoing its Dynamic Test case, the platen and case measured temperature do not match by a maximum deviation of 8.575° C. The thermal energy released by the battery causes an increase in the case temperature which becomes more apparent in the battery pack test article.

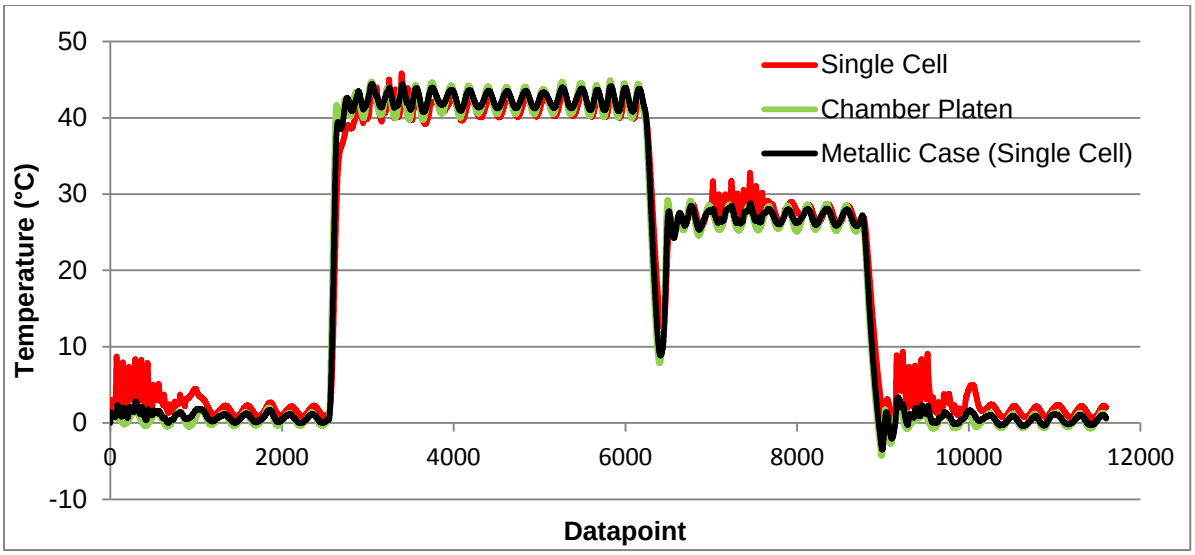

Figure 61: Measured Temperature Data from Thermocouples on a Single Battery Cell

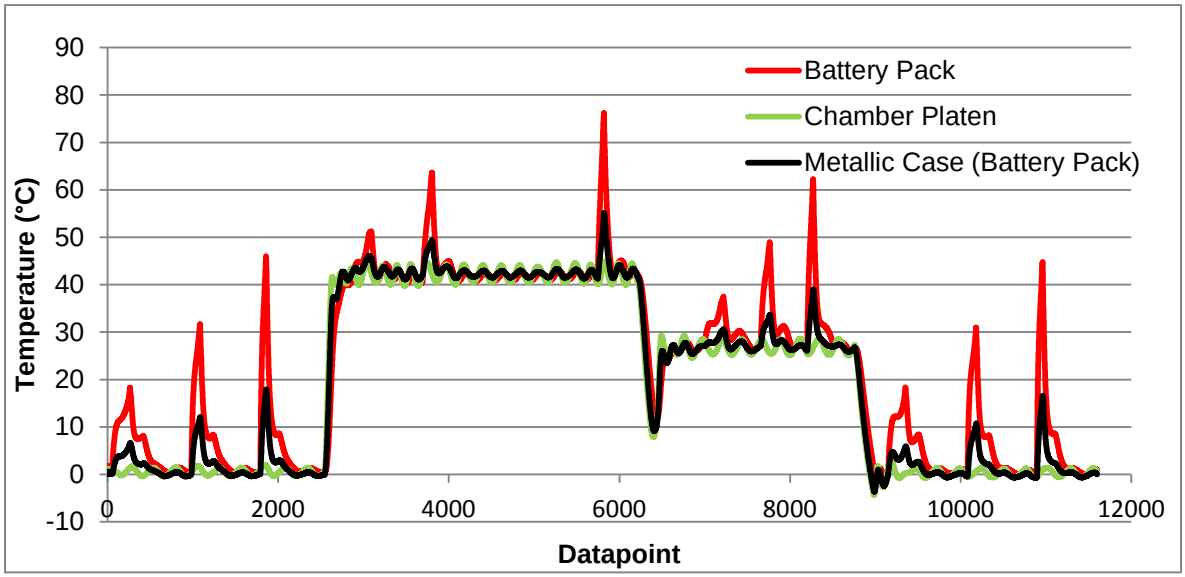

Figure 62: Measured Temperature Data from Thermocouples on a Single Battery Cell in a Battery Pack

Figure 62 shows only the measured temperature data of a single cell in the battery pack, the metallic case housing the pack, and the chamber platen. Similarly to Figure 61, oscillation of the chamber platen temperature is observed. For the battery pack experiment, the metallic case

and chamber platen have good conduction; however, like the single battery cell experiment, the metallic case deviates from the chamber platen during areas of testing where there is a temperature increase in the battery cell. This results in an increase in the metallic case temperature as well. The average deviation in temperature between the Chamber Platen and the single battery cell of the Battery Pack is 4.44 ° C with a maximum deviation of 44.09° C throughout the entire dataset. The average deviation in temperature between the Chamber Platen and Metallic Case of the Battery pack 1.62° C with a maximum deviation of 16.09° C. The average deviation in temperature between the single battery cell of the Battery Pack and Metallic Case is 3.09° C with a maximum deviation of 28.59° C.

Comparing the peak temperature values of the thermocouple shown in Figure 62 and the peak temperature values of the thermistors shown in Figs. 58, 59, and 60, the thermocouple does not match up to thermistor. An example is shown in Figure 62 from datapoint 2500 to 6000, the thermocouple data is shown to peak at approximately 51°, 65° and 75° C, respectively. This portion of the curve relates to the test cases for the battery pack at 40° C. From Figure 60, the experimental data from the thermistor is shown to peak at approximately 45°, 51°, and 61° C. As temperature increases, a larger deviation between the thermocouple and thermistor becomes apparent. Another example is from datapoint 0 to 2000 or 9000 to 11,000 for the 0° C case. The peak values from the thermocouple are 19°, 31° and 45° C. In comparison with Figure 58, the thermistor temperatures peak at 10°, 19° and 22° C.

4.5 Summary

Overall, the modified Thevenin Equivalent Circuit Model incorporating thermal effects is capable of predicting the performance of a 2S2P battery pack in the space environment; however, there are areas that could be improved. The modified HJGC model was able to achieve

an average absolute error of 1.26, 0.76, and 0.61% for the 0°, 25° and 40° C test cases respectively over all three test scenarios: Low, Normal and High current discharges. There are areas that need improvement, specifically the thermal model and charging aspect of the model. Although the model is accurate in predicting the overall performance of a battery pack, the model is inaccurate in regions where the battery pack transitions from an end of discharge state to a charge state. This inaccuracy is observable in the analysis of maximum absolute error for voltage at the transition region between discharge and charge where the error exceeded expected results presented by HJGC [38]. When compared to the results presented by HJGC where the maximum absolute error of the voltage did not exceed 2%, the model for all 3 temperature cases exceeded this limit. For the 0° C test case, the Low, Normal and High current test scenarios had maximum absolute error of 20.56, 21.79, and 21.25 % respectively. For the 25° C test case, the Low, Normal and High current test scenarios had maximum absolute error of 12.87, 15.31, and 19.93 % respectively. For the 40° C test case, the Low, Normal and High current test scenarios had maximum absolute error of 12.47, 13.98, and 14.27 % respectively.

The thermal aspect of the model shows an average absolute error of temperature for battery cells 1 and 4, representing the outer most cells, as 1.2901, 1.1682, and 0.5799% for the 0°, 25°, and 40° C test case respectively. The average absolute error for battery cells 2 and 3, representing the inner most cell, are 1.2921, 1.1659, and 0.6750% for the 0°, 25°, and 40° C test case respectively. Overall, the thermal model is able to accurately predict the temperature of the battery cells; however, the thermal model had difficulty matching the gradual rise in temperature during the initial start of discharge as well in the transition region between discharge and charge. During the transition region, the maximum absolute error for the Low, Normal and High current test scenarios at 0° C are 3.53, 6.20, and 11.05 %, respectively. For the Low, Normal and High

current test scenarios at 25° C, the maximum absolute error are 2.61, 4.23, and 8.81 %, respectively. For the Low, Normal and High current test scenarios at 40° C, the maximum absolute error are 2.13, 4.55, and 9.67 %, respectively.

The analysis between the model and experimental data for both voltage and temperature show that the modified HJGC Battery model using a single RC network does not accurately model a battery pack's performance in the transition region between charge and discharge when compared to expected results presented by HJGC. The inaccuracy is due a combination between the thermal model and estimated parameters in the lookup tables. Because the modified HJGC Battery model is heavily reliant on the lookup tables to generate the model output of a battery pack, any inaccuracy between the *Parameter Estimation Model* and the experiment data when generating the lookup table would result in an inaccurate battery pack model. Hysteresis also plays a role in the accuracy of the charge portion of the model and can be incorporated into the model by adding an additional RC network. For space simulation that requires a high level of accuracy, more modifications to the HJGC model should be investigated in improving the areas of thermal modeling and parameter estimation for multiple RC networks.

V. Conclusions and Recommendations

5.1 Conclusions of Research

This research presented a background on CubeSats, Li-ion batteries, and battery modeling. The proposed model to simulate spacecraft battery behavior is the equivalent circuit based model presented by Huria, Jackey, Gazzari, and Ceraolo (HJGC) [38]. The HJGC model combines multiple equivalent circuit models that represent a single battery cell to form a larger model that represents a single battery pack. The HJGC model was modified through the arrangement of four equivalent circuit models of a battery cell to simulate a battery pack in a 2S2P configuration. Each equivalent circuit model of a battery cell incorporates only one RC network. Experimental data was gathered at temperatures of 0°, 25° and 40° C using pulse discharges on an LG ICR18650C2 battery cell. The experimental data from the battery cell was used to create a lookup table containing the RC parameters using the *Parameter Estimation Model* presented by HJGC. The results of the modified HJGC model was compared to experimental test data of battery cells in a 2S2P configuration. This comparison showed that the model using a single RC network does not accurately model a battery pack's performance in the transition region between charge and discharge when compared to expected results of absolute error not exceeding 2% [38]. During the transition region, the 0° C test case for the Low, Normal and High current test scenarios had maximum absolute error for voltage of 20.56, 21.79, and 21.25 % respectively. For the 25° C test case, the Low, Normal and High current test scenarios had maximum absolute error for voltage of 12.87, 15.31, and 19.93 % respectively. For the 40° C test case, the Low, Normal and High current test scenarios had maximum absolute error for voltage of 12.47, 13.98, and 14.27 % respectively. Inaccuracy of the model at the transition

region is due to a combination between the thermal model and estimated parameters from the lookup tables.

5.2 Significance of Research

Modeling an EPS for CubeSats is an area of research that has not widely been explored. The significance of analyzing the HJGC model provides a step towards developing a model that is capable of simulating an entire complex CubeSat EPS consisting of solar arrays, EPS card, and battery pack. The analysis presented in this research provides recommendations of improvements to a pre-existing battery model that can be further enhanced to provide a more accurate prediction of battery pack behavior for EPS modeling. The findings of this research showed that further research must be conducted in the aspects of battery pack thermal modeling and parameter estimation to provide a more accurate model of a battery pack.

5.3 Recommendations for Action

The limitations of the modified HJGC model were due to the accuracy based primarily on the parameter estimation of the RC elements and the thermal model. The modified HJGC model was also limited in terms of accuracy due to the lack of hysteresis incorporated into the model. A recommendation for action to incorporate the hysteresis effect would be to implement more RC networks into the equivalent circuit model of each battery cell. Additionally, more research on estimating parameters should have been explored earlier during the research to provide a more accurate and less tedious method of RC parameter extraction for an equivalent circuit model using a single RC network. The thermal model did not incorporate heat loss due to convection and radiation and should be an area to explore for further improvement of the modified HJGC model.

In terms of experimental testing, the contact between the metallic case and chamber platen could be improved by replacing the copper mesh with indium or copper foil. The mesh has holes where contact between the case and platen is limited. Indium or copper foil would provide better contact than a mesh. Additionally, 8 to 10 battery cells should be tested to gather more sufficient data on the single battery cell. Not all battery cells are identical, and additional single battery cell tests would develop a statistical argument that the experimental data from the single battery cell used in this research is representative of the cells used in the 2S2P battery pack.

5.4 Recommendations for Future Research

Future research should focus on the areas of improving the methods used to estimate RC parameter, especially for equivalent circuit models that incorporate two or more RC networks. A starting point would be the layered technique presented by HJGC used for parameter estimation of a model containing three RC networks[48]. Alternatively, research on the thermal aspects of a battery cell would provide a basis on developing a more accurate thermal model capable of providing accurate simulation of a battery pack’s temperature.

Appendix 1.0 Test Plans

Li-Ion Battery TVAC Test Plan

James Liu, 2d Lt, USAF

DEPARTMENT OF THE AIR FORCE

AIR UNIVERSITY

AIR FORCE INSTITUTE OF TECHNOLOGY

Wright-Patterson Air Force Base, Ohio

Signature Page

Authored Action Taken	James Liu, 2d Lt, USAF	Date

Table of Contents

List of Tables

1. Introduction

1.1. Purpose

The purpose of this test plan is to lay out the procedure for gathering discharge characteristics of a lithium ion cell and a lithium ion battery pack at various temperatures.

1.2. Scope

This test plan will provide details on testing for a single cell lithium ion battery and a battery pack with 4 cells (2S2P).

The cell and battery pack will be tested at chamber temperatures of 0° C, 25° C and 40° C. Battery temperature will be recorded and monitored using thermocouples.

The single cell and battery pack will be tested simultaneously using two discharge profiles: pulse and constant current.

The pulse test will only be conducted for the single cell using a discharge current of 1C at each temperature. A discharge duty cycle of 360 sec on and 1800 sec (5 time constants) off will be used to discharge the cell to the cutoff voltage of 3.0V. The sole purpose of the pulse test is to collect data on the battery cell to calculate RC-circuit parameters for the used in battery cell modeling.

The constant current discharge test will be conducted for both cells at a rate of 0.5C, 1C and 2C at each temperature.

1.3. Objective

The objective is to gather cell and battery pack discharge data at various operating temperatures. This data will be used to create lookup tables for battery modeling and battery behavior prediction.

2. Resource Requirements

2.1. Facilities

This test shall be performed at the Air Force Institute of Technology, Wright

Patterson AFB, OH.

2.2. Roles and Responsibilities

A Quality Assurance representative shall perform the following:

a. Inspection of the initial test setup and all configuration changes shall be performed.
b. Visual inspection of the test articles at points indicated in this procedure, including visual damage.
c. Review data and accept at completion of this procedure.

A Test director representative shall perform the following:

a. Confirm facilities and test articles are ready to be tested
b. Ensure connections and setup meet all requirements as specified by the interface control document (ICD)
c. Verify that all software and equipment are functional in gathering the required data
d. Review data to ensure all required data has been gathered.

A Test conductor representative shall perform the following:

a. Inspect and verify all test equipment are working prior to TVAC setup
b. Execute test plan procedures to ensure all required data has been gathered.

2.3. Safety Compliance

a. For operations occurring during normal duty days, all accidents and hazardous incidents shall be reported to Chris Sheffield.
b. During non-standard hours, all accidents and incidents shall be reported to Chris Sheffield on the next working day.

2.4. Hazardous Operation

As a safety measure to prevent thermal runaway in Lithium-Ion Batteries during the

40°C test, battery temperature shall be monitored and limited through the BatteryLab

Software to not exceed 80° C. If vibration testing is being performed in the lab, earmuffs must be worn.

2.5. Personnel Requirements

Quality Assurance, Test Director, and Test Conductor shall participate in conducting this test procedure. QA shall primarily support the test configuration verification and test data review and is not required for the complete duration of testing. The test director will ensure equipment is ready to gather data. The test conductor will execute the test procedures and gather the data. A list of the test personnel is provided below in Table 1.

Table 9 Test Personnel

Position	Team Member	Initials
Quality Assurance	Chris Sheffield/Sean Miller	
Test Director	James Liu	
Test Conductor	James Liu	

2.6. Material/Equipment

The materials and equipment required for this test are shown below in Table 10.

Table 10 Test Equipment

Item	Description	Quantity
Computer	Two computers are required to run LabVIEW Software and BatteryLab Software Each computer shall have a minimum of 2 USB connections for the Mouse, Keyboard. Computer connected to the CADEX battery testing system shall have access to CubeNet	2
Test HW/SW	CADEX C8000 Battery Testing System w/ 2 Power Port Cables (http://www.CADEX.com/en/products/c8000-battery-testing-system)	1
Test HW/SW	CubeSat TVAC chamber/ABBESS	1
Battery Cell	1 Lithium-Ion battery cell	1

Battery Pack	4 cell lithium-ion battery pack (2S2P)	1
Type K Thermocouples	Measures surface temperature of battery pack and individual battery cell	5
CADEX C8000 Thermistor	Measures surface temperature of battery pack/cell. Used in conjunction with BatteryLab software to act as a shutoff mechanism for high temperature.	2
Multimeter	Measures voltage of batteries	1
Rolling Cart	Transporting equipment	1
Earmuffs	Protects ears from loud noises	1
TVAC Connectors	<u>Cell</u> • One DB25 connector to connect the CADEX C8000 Battery Tester from outside the chamber to inside the chamber via Channel 1 on the CADEX • One DB25 connector to connect the battery cell from inside the TVAC Chamber to outside the chamber. <u>Pack</u> • One DB25 connector to connect the CADEX C8000 Battery Tester from outside the chamber to inside the chamber via Channel 2 on the CADEX • One DB25 connector to connect the battery pack from inside the TVAC Chamber to outside the chamber. Refer to Battery Testing ICD for further details on TVAC connectors	4
Gloves (pair)	Used to protect test equipment and chamber from contamination.	multiple
Alcohol	Used to clean test articles	1

3. Test Configuration

3.1. Test Setup

This test will take place in the AFIT Space Environmental Chamber Lab.

Battery cell and Battery Pack Setup

The battery pack and battery cell will be placed in two separate metallic casings to hold the pack and cell.

Thermocouples will be secured on the metallic casing, the chamber platen and on the battery cells to monitor temperature differentials between the case, cell and platen temperature. They will be secured on the cell using Kapton tape.

Thermistor will be secured in the middle of the battery pack; it will be secured on top of the battery cell.

Note: Refer to Appendix 2.0 for pictures of Thermocouple and Thermistor placement on the Battery Pack and Cell

Test Setup Checklist:

1. Clean all test articles and connectors using alcohol prior to putting into chamber.
2. Using "Battery Test TVAC ICD" as a reference, connect ***Inside Female DB25 TVAC Connector*** (connector attached to battery pack and cell) to ***Inside Male DB25 TVAC connection port*** inside TVAC Chamber.
3. Using "Battery Test TVAC ICD" as a reference, *connect* ***Outside Female DB25 TVAC Connector*** (connector attached to banana plugs) to ***Outside Male DB25 TVAC connection port*** outside TVAC Chamber.
4. Connect DB25 connected to battery cell to Ch1 Power Port connector from the CADEX C8000.
5. Connect DB25 connected to battery pack to Ch2 Power Port connector from the CADEX C8000.

3.2. Test Results

All pass/fail test results will be recorded on this test procedure. The data that is collected from the CADEX C8000 Battery Tester and thermocouples will be recorded in an electronic file on the computer. This data to be collected is shown below.

Table 11 Data to be Collected

Data Collected	Source:
Temperature of Battery Cell and Pack from Thermocouple Refer to APPENDIX 2.0 for Thermocouple Location	LabVIEW Software

Discharge Current of Battery Cell & Pack	BatteryLab Software
Voltage of Battery Cell & Pack	BatteryLab Software
Temperature of Battery Cell and Pack from Thermistor (through DB25) Refer to APPENDIX 2.0 for Thermistor Location	BatteryLab Software

3.3. Test Software

The CADEX C8000 Battery Testing System has its own software (BatteryLab) that can be used to test both the battery cell and pack. ABBESS control software is used to control the TVAC chamber. LabVIEW software is used to record thermocouple data and chamber pressure.

4. TVAC Initial Set Up

Table 12 Initial Set-Up Procedure

Step	Activity	Initials/Date	QA/Date
1.	Gather all equipment from Table 10 and ensure availability for duration of test		
2.	Ensure that BatteryLab software is working properly on all computers that require the software		
3.	Ensure TVAC & ABBESS software is working properly on all computers that require the software		
4.	Setup/prep the TVAC Chamber Refer to section 3.1 Test Setup		
5.	Insert Battery cell and Battery Pack into the TVAC chamber Refer to TVAC Battery Testing ICD for battery connection Refer to section 3.1 Test Setup		
6.	Record battery cell and pack voltage using CADEX C8000 Battery Testing System to determine offset from wires		

5. Battery Cell & Battery Pack Operational Test

Table 13 Battery Procedure

Step	Activity	Initials/Date	QA/Date
7.	Collect ambient temperature and voltage of battery cell and battery pack using CADEX C8000 and Thermocouple		
8.	Use CADEX C8000 to draw power from Battery Cell and Battery Pack at a rate of 0.5C Use CADEX C8000 to charge Battery Cell and Battery Pack at a max rate of 0.5C		
9.	Ensure Battery Cell is charged to at least 4.3 V Ensure Battery Pack is charged to at least 8.6 V		
10.	<u>Constant Current Discharge at Ambient Temperature</u> Use CADEX C8000 to discharge battery cell and pack at the following discharge rates: 0.5C, 1C and 2C. Discharge until batteries reach cutoff voltage of 3.0 V (cell) and 6.0 V (pack). Charge the battery cell and pack back up to at least 4.3 V and 8.6 V respectively at the end of each discharge at a max rate of 0.5C. Wait for Battery Cell and Pack to settle at equilibrium temperature between each discharge.		
11.	<u>Pulse Discharge at Ambient Temperature</u> Using the CADEX C8000, pulse discharge the battery cell • Discharge rate: 1C (2.70 A at ambient) • Period on: 360 seconds • Period off: 1800 seconds • Set cutoff voltage to 3.0 V Charge Battery cell back up to at least 4.3V at a max rate of 0.5C		
12.	Pump chamber down to vacuum pressure		
13.	Ramp temperature down to 0° C		
14.	Wait for Battery Cell and Pack to settle at 0° C		
15.	Measure initial battery temperature using thermocouple and initial battery voltage using CADEX C8000		
16.	<u>Constant Current Discharge at 0° C</u> Use CADEX C8000 to discharge battery cell and pack at the following discharge rates: 0.5C, 1C and 2C. Discharge until batteries reach cutoff voltage of 3.0 V (cell) and 6.0 V (pack). Charge the battery cell and pack back up to at least 4.3 V and 8.6 V respectively at the end of each discharge at a max rate		

	of 0.5C. Wait for Battery Cell and Pack to settle at equilibrium temperature between each discharge.		
17.	<u>Pulse Discharge at 0° C</u> Using the CADEX C8000, pulse discharge the battery cell • Discharge rate: 1C (2.7 A at 0° C) • Period on: 360 seconds • Period off: 1800 seconds • Set cutoff voltage to 3.0 V Charge Battery cell back up to at least 4.3V at a max rate of 0.5C		
18.	Ramp temperature up to 25° C		
19.	<u>Constant Current Discharge at 25°C</u> Use CADEX C8000 to discharge battery cell and pack at the following discharge rates: 0.5C, 1C and 2C. Discharge until batteries reach cutoff voltage of 3.0 V (cell) and 6.0 V (pack). Charge the battery cell and pack back up to at least 4.3 V and 8.6 V respectively between each discharge at a max rate of 0.5C. Wait for Battery Cell and Pack to settle at equilibrium temperature between each discharge.		
20.	<u>Pulse Discharge at 25° C</u> Using the CADEX C8000, pulse discharge the battery cell • Discharge rate: 1C (2.7 A at 25° C) • Period on: 360 seconds • Period off: 1800 seconds • Set cutoff voltage to 3.0 V Charge Battery cell back up to at least 4.3V at a max rate of 0.5C		
21.	Ramp temperature up to 40° C		
22.	Measure battery pack and cell temperature using thermocouple and battery voltage using CADEX C8000		
23.	<u>Constant Current Discharge at 40°C</u> Use CADEX C8000 to discharge battery cell and pack at the following discharge rates: 0.5C, 1C and 2C. Discharge until batteries reach cutoff voltage of 3.0 V (cell) and 6.0 V (pack). Charge the battery cell and pack back up to at least 4.3 V and 8.6 V respectively between each discharge at a max rate of 0.5C. Wait for Battery Cell and Pack to settle at equilibrium temperature between each discharge.		

24.	<u>Pulse Discharge at 40°C</u> Using the CADEX C8000, pulse discharge the battery cell • Discharge rate: 1C (2.70 A at 40° C) • Period on: 360 seconds • Period off: 1800 seconds • Set cutoff voltage to 3.0 V Charge Battery cell back up to at least 4.3V at a max rate of 0.5C		
25.	Ramp temperature down to ambient temperature		
26.	Pump chamber back to atmospheric pressure		
27.	Record ambient Temperature		
28.	Measure initial battery pack and cell temperature using thermocouple and initial battery voltage using CADEX C8000		
29.	<u>Constant Current Discharge at Ambient Temperature</u> Use CADEX C8000 to discharge battery cell and pack at the following discharge rates: 0.5C, 1C and 2C. Discharge until batteries reach cutoff voltage of 3.0 V (cell) and 6.0 V (pack). Charge the battery cell and pack back up to at least 4.3 V and 8.6 V respectively between each discharge at a max rate of 0.5C. Wait for Battery Cell and Pack to settle at equilibrium temperature between each discharge.		
30.	<u>Pulse Discharge at Ambient Temperature</u> Using the CADEX C8000, pulse discharge the battery cell • Discharge rate: 1C (2.70 A at ambient) • Period on: 360 seconds • Period off: 1800 seconds • Set cutoff voltage to 3.0 V Charge Battery cell back up to at least 4.3V at a max rate of 0.5C		
31.	Collect final temperature and voltage of battery cell and battery pack using CADEX C8000 and Thermocouple		

Appendix 1.0 – Test Log

Item	TIME	EVENT / STATUS	FILENAME
(#)	*(HHMM)*	*(Desc.)*	*(Type-Current-MMDD-Cell or Pack)*
1			
2			
3			
4			
5			
6			
7			
8			
9			
10			
11			
12			
13			

14			
15			
16			
17			
18			
19			
20			
21			
22			
23			
24			
25			
26			
27			
28			
29			

30			
31			
32			
33			
34			

Appendix 2.0 – Test Setup

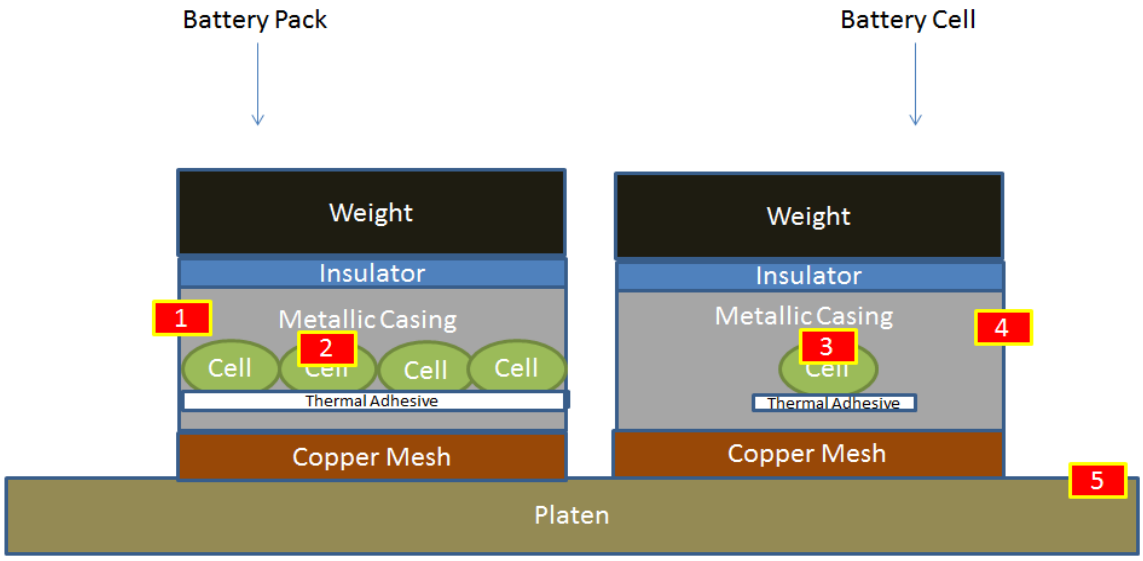

Figure 63: Thermocouple Placement Location 1 through 5

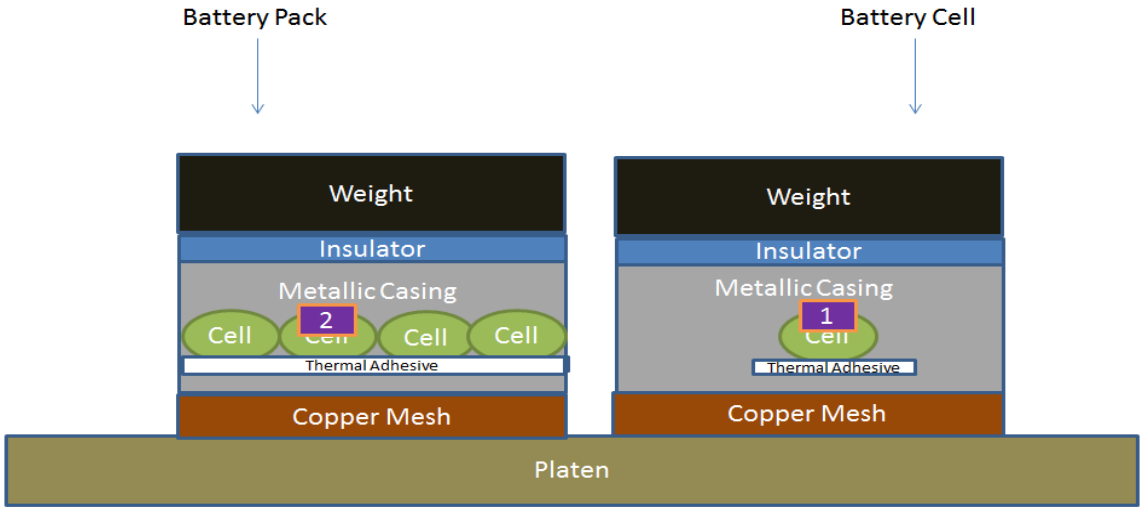

Figure 64: Thermistor Placement Locations 1 and 2

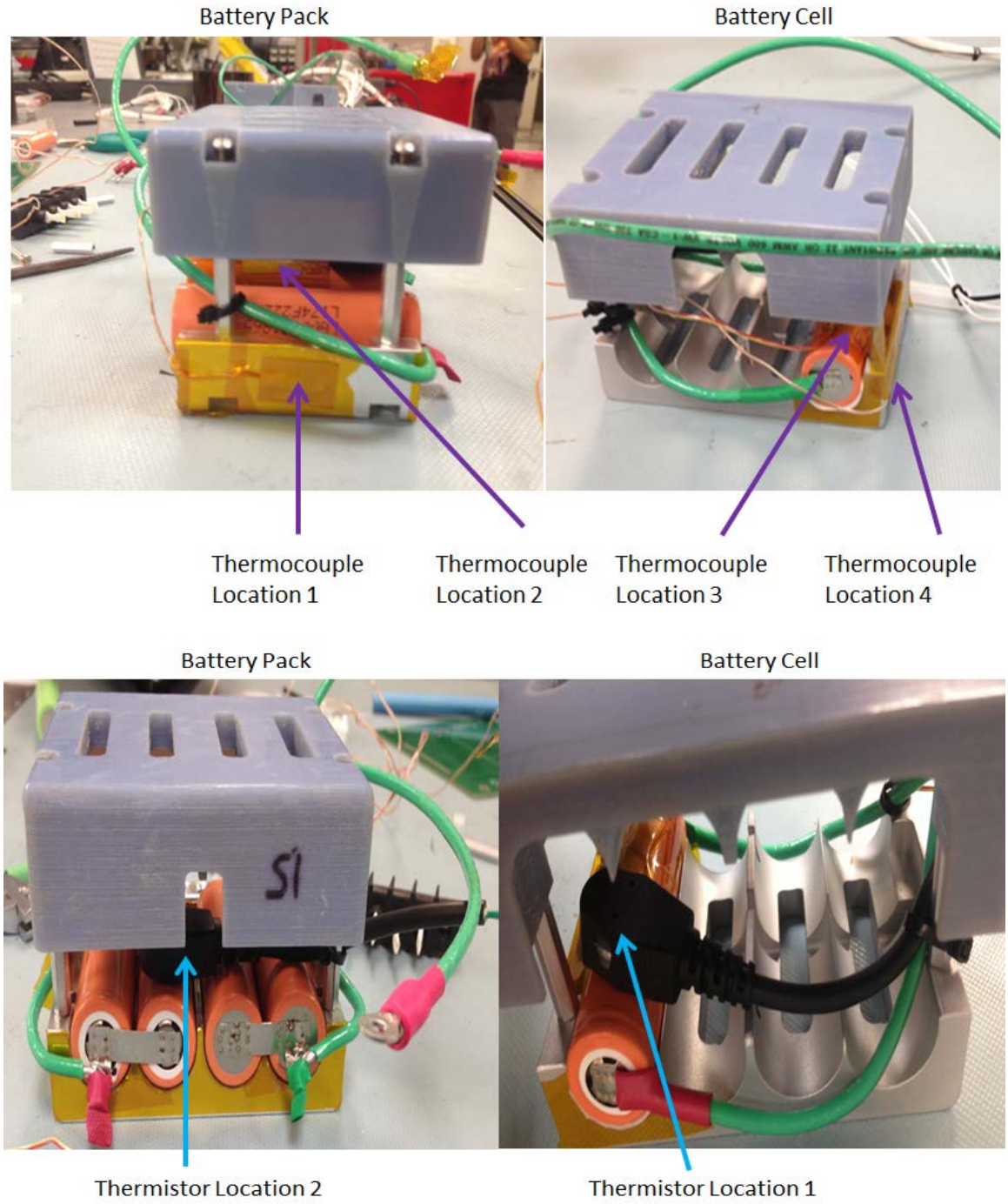

Figure 65: Thermocouple and Thermistor Location

Thermocouple	Location
1	Metallic Case (Pack)
2	Cell (Pack)
3	Single Cell
4	Metallic Case (Cell)
5	Chamber Platen

Bibliography

[1] D. Messier, “Tiny ‘Cubesats’ Gaining Bigger Role in Space.” [Online]. Available: http://www.space.com/29464-cubesats-space-science-missions.html. [Accessed: 20-Jul-2015].

[2] CalPoly, “Cubesat design specification rev. 13,” *CubeSat Program, Calif. Polytech. State …*, vol. 8651, p. 22, 2009.

[3] “Fox-1 Cubesat by AMSAT.” [Online]. Available: http://www.amsat.org/?page_id=1113.

[4] G. L. Plett, “Lesson 1: Battery Boot Camp,” pp. 1–32.

[5] M. Swartwout, “The First One Hundred CubeSats: A Statistical Look.”

[6] Mark Betancourt, “Half of All First-Time CubeSat Projects End in Failure,” *Air & Space Magazine*, 2014. [Online]. Available: http://www.airspacemag.com/daily-planet/cubesats-are-great-even-if-they-die-you-180952745/?no-ist.

[7] C. Clark, “An Advanced Electrical Power System For CubeSats.”

[8] “2015 AFIT 6U EDU CubeSat Bus Interface Control Document (ICD),” WPAFB, 2015.

[9] J. Wertz, *Space Mission Engineering: The New SMAD*. Hawthorne: Microcosm Press, 2011.

[10] “Keywords to understanding Sony Energy Devices.” [Online]. Available: http://www.sonyenergy-devices.co.jp/en/keyword/.

[11] Lighting Global, “Lithium-ion Battery Overview,” *Tech. Notes*, vol. 27, no. 10, pp. 820–821, 1989.

[12] “Saftey Concerns with Li-Ion.” [Online]. Available: http://batteryuniversity.com/learn/article/safety_concerns_with_li_ion.

[13] “Types of Li-Ion.” [Online]. Available: http://batteryuniversity.com/learn/article/types_of_lithium_ion.

[14] M. Safety, D. Sheet, and L. G. C. Limited, “Model ICR18650S3 Lithium-Ion Battery LG CHEMICAL LIMITED 1 . Chemical Product and Company Identification Emergency Overview,” pp. 1–7.

[15] C. J. Orendorff, “The Role of Separators in Lithium-Ion Cell Safety,” *Electrochem. Soc. Interface*, vol. 21, no. 2, pp. 61–65, 2004.

[16] S. Keeping, “A Designer’s Guide to Lithium Battery Charging,” 2012. [Online]. Available: http://www.digikey.com/en/articles/techzone/2012/sep/a-designers-guide-to-lithium-battery-charging.

[17] G. Ning, B. Haran, and B. N. Popov, “Capacity fade study of lithium-ion batteries cycled at high discharge rates,” *J. Power Sources*, vol. 117, no. 1–2, pp. 160–169, 2003.

[18] B. Mckissock, P. Loyselle, and E. Vogel, “Guidelines on Lithium-ion Battery Use in Space Applications,” no. May, 2009.

[19] K. Sun and Q. Shu, “Overview of the types of battery models,” *Proc. 30th Chinese Control Conf.*, pp. 3644–3648, 2011.

[20] a Shafiei, a Momeni, and S. S. Williamson, “Battery modeling approaches and management techniques for Plug-in Hybrid Electric Vehicles,” *Veh. Power Propuls. Conf. (VPPC), 2011 IEEE*, pp. 1–5, 2011.

[21] M. Doyle, T. F. Fuller, and J. Newman, “Modeling of galvanostatic charge and discharge of the lithium/polymer/insertion cell,” *J. Electrochem. Soc.*, vol. 140, no. 6, pp. 1526–1533, 1993.

[22] P. Weicker, *A Systems Approach to Lithium-Ion Battery Management*. Artech House, 2014.

[23] J. C. Forman, S. J. Moura, J. L. Stein, and H. K. Fathy, “Genetic identification and fisher identifiability analysis of the Doyle-Fuller-Newman model from experimental cycling of a LiFePO 4 cell,” *J. Power Sources*, vol. 210, pp. 263–275, 2012.

[24] J. Newman, “FORTRAN Programs for the Simulation of Electrochemical Systems,” 1998. [Online]. Available: http://www.cchem.berkeley.edu/jsngrp/fortran.html. [Accessed: 01-Jan-2016].

[25] M. Jongerden and B. Haverkort, “Battery modeling,” *Thecnical Rep. Fac. Electr. Eng. Math. Comput. Sci.*, p. 18, 2008.

[26] V. Ramadesigan, P. W. C. Northrop, S. De, S. Santhanagopalan, R. D. Braatz, and V. R. Subramanian, “Modeling and Simulation of Lithium-Ion Batteries from a Systems Engineering Perspective,” *J. Electrochem. Soc.*, vol. 159, no. 3, pp. R31–R45, 2012.

[27] D. N. Rakhmatov and S. B. K. Vrudhula, “An analytical high-level battery model for use in energy management of portable electronic systems,” *2001 IEEE/ACM Int. Conf. Comput. Des.*, pp. 488–493, 2001.

[28] C.-F. Chiasserini and R. R. Rao, “Energy efficient battery management,” *IEEE J.*

Sel. Areas Commun., vol. 19, no. 7, pp. 1235–1245, 2001.

[29] A. Hentunen, T. Lehmuspelto, and J. Suomela, "Time-Domain Parameter Extraction Method for Thévenin-Equivalent Circuit Battery Models," *IEEE Trans. Energy Convers.*, vol. 29, no. 3, pp. 558–566, 2014.

[30] G. L. Plett, "Lesson 2: Equivalent-Circuit Cell Models," 2014.

[31] W. Luo, C. Lv, L. Wang, and C. Liu, "Study on impedance model of Li-ion battery," *Proc. 2011 6th IEEE Conf. Ind. Electron. Appl. ICIEA 2011*, pp. 1943–1947, 2011.

[32] Chris Beasley, "Basics of Electrochemical Impedance Spectroscopy," 2015. [Online]. Available: https://www.gamry.com/application-notes/EIS/basics-of-electrochemical-impedance-spectroscopy/. [Accessed: 01-Jan-2016].

[33] S. Gold, "A PSPICE macromodel for lithium-ion batteries," *Twelfth Annu. Batter. Conf. Appl. Adv.*, pp. 215–222, 1997.

[34] R. A. Dougal, L. Gao, and S. Liu, "Dynamic lithium-ion battery model for system simulation," *IEEE Trans. Components Packag. Technol.*, vol. 25, no. 3, pp. 495–505, 2002.

[35] M. Chen and G. a. Rincón-Mora, "Accurate electrical battery model capable of predicting runtime and I-V performance," *IEEE Trans. Energy Convers.*, vol. 21, no. 2, pp. 504–511, 2006.

[36] O. Erdinc, B. Vural, and M. Uzunoglu, "A dynamic lithium-ion battery model considering the effects of temperature and capacity fading," *2009 Int. Conf. Clean Electr. Power, ICCEP 2009*, pp. 383–386, 2009.

[37] C. Fleischer, W. Waag, H. M. Heyn, and D. U. Sauer, “On-line adaptive battery impedance parameter and state estimation considering physical principles in reduced order equivalent circuit battery models: Part 1. Requirements, critical review of methods and modeling,” *J. Power Sources*, vol. 260, pp. 276–291, 2014.

[38] T. Huria, M. Ceraolo, J. Gazzarri, and R. Jackey, “High fidelity electrical model with thermal dependence for characterization and simulation of high power lithium battery cells,” *2012 IEEE Int. Electr. Veh. Conf. IEVC 2012*, pp. 1–8, 2012.

[39] U. Test and P. Guide, “Energy Systems Test Area (ESTA) Battery Test Operations User Test Planning Guide.”

[40] “Mathworks Products: SIMSCAPE Overview.” [Online]. Available: http://www.mathworks.com/products/simscape/index.html. [Accessed: 01-Jul-2015].

[41] W. P. Afb, “ABBESS INSTRUMENTS AND SYSTEMS , INC . Thermal Vacuum Solar Simulation System for,” no. 508.

[42] Cadex Electronics Inc., *C8000 Battery Testing System User Manual (V2 . x).* 2010.

[43] Cadex Electronics Inc., “CADEX C8000 Technical Specfications.”

[44] L. P. R. Cell, “Product specification for LG ICR18650C2,” 2009.

[45] 3M, “VHB ™ Tape Specialty Tapes Technical Data,” vol. 25, no. October, pp. 1–9, 2014.

[46] R. Jackey, “Lithium Battery Model, Simscape Language and Simulink Design Optimization.” [Online]. Available:

https://www.mathworks.com/matlabcentral/fileexchange/36019-lithium-battery-model--simscape-language-and-simulink-design-optimization.

[47] “Mathworks: Parameter Estimation.” [Online]. Available: http://www.mathworks.com/discovery/parameter-estimation.html?refresh=true.

[48] R. Jackey, M. Saginaw, P. Sanghvi, J. Gazzarri, T. Huria, and M. Ceraolo, “Battery Model Parameter Estimation Using a Layered Technique : An Example Using a Lithium Iron Phosphate Cell,” *MathWorks*, pp. 1–14, 2013.

REPORT DOCUMENTATION PAGE

Form Approved
OMB No. 0704-0188

PLEASE DO NOT RETURN YOUR FORM TO THE ABOVE ADDRESS.

1. REPORT DATE *(DD-MM-YYYY)*	2. REPORT TYPE	3. DATES COVERED *(From - To)*
24-03-2016	Master's Thesis	September 2014 - March 2016

4. TITLE AND SUBTITLE

Analysis of a Modified Equivalent Circuit Model for Lithium-Ion Battery Modules in CubeSats

5a. CONTRACT NUMBER

5b. GRANT NUMBER

5c. PROGRAM ELEMENT NUMBER

6. AUTHOR(S)

Liu, James J., 2d Lt,USAF

5d. PROJECT NUMBER

5e. TASK NUMBER

5f. WORK UNIT NUMBER

7. PERFORMING ORGANIZATION NAME(S) AND ADDRESS(ES)

Air Force Institute of Technology
Graduate School of Engineering and Management (AFIT/EN)
2950 Hobson Way
Wright-Patterson AFB OH 45433-7765

8. PERFORMING ORGANIZATION REPORT NUMBER

AFIT-ENY-MS-16-M-224

9. SPONSORING/MONITORING AGENCY NAME(S) AND ADDRESS(ES)

Intentionally Left Blank

10. SPONSOR/MONITOR'S ACRONYM(S)

11. SPONSOR/MONITOR'S REPORT NUMBER(S)

12. DISTRIBUTION/AVAILABILITY STATEMENT

Distribution Statement A. Approved for Public Release;Distribution Unlimited

13. SUPPLEMENTARY NOTES

14. ABSTRACT

Failure of the electrical power system (EPS) to meet mission requirements is a common problem in nano-size satellites commonly referred to as CubeSats. The motivation for this research stems from the desired prevention of EPS failure through a process of testing and space qualification of components. Utilizing models to predict the behavior of an EPS before it is designed, built, and tested for space can provide critical insight in areas of limitation in performance and survivability. Experimental test data is collected under a simulated space environment through the use of a Thermal Vacuum Chamber (TVAC). Data collected from battery testing in the space environment is used to validate a modified Thevenin Equivalent Circuit model. The experimental test data and battery model are compared and evaluated resulting in a promising model that can reasonably predict performance of a battery pack in a two-series two-parallel configuration.

15. SUBJECT TERMS

CubeSat Lithium-Ion Battery Equivalent Circuit Model

16. SECURITY CLASSIFICATION OF:			17. LIMITATION OF ABSTRACT	18. NUMBER OF PAGES	19a. NAME OF RESPONSIBLE PERSON
a. REPORT	b. ABSTRACT	c. THIS PAGE			Dr. Eric Swenson, Eric.Swenson@AFIT.edu, AFIT/
U	U	U	UU	138	19b. TELEPHONE NUMBER *(Include area code)* (937)255-3636 x7479

Reset

Standard Form 298 (Rev. 8/98)
Prescribed by ANSI Std. Z39.18